

Hydrophobic Modification of Starch

by

Ryan Amos

A thesis

presented to the University of Waterloo

in fulfillment of the

thesis requirement for the degree of

Doctor of Philosophy

in

Chemistry

Waterloo, Ontario, Canada, 2019

©Ryan Amos 2019

Examining Committee Membership

The following served on the Examining Committee for this thesis. The decision of the Examining Committee is by majority vote.

External Examiner

NAME: Harald Stöver

Title: Professor McMaster University

Supervisor(s)

NAME: Mario Gauthier

Title: Professor Chemistry

Internal Member

NAME: Jean Duhamel

Title: Professor Chemistry

Internal Member

NAME: Juewen Liu

Title: Professor Chemistry

Internal-external Member

NAME: Leonardo Simon

Title: Professor Chemical Engineering

AUTHOR'S DECLARATION

This thesis consists of material all of which I authored or co-authored: see Statement of Contributions included in the thesis. This is a true copy of the thesis, including any required final revisions, as accepted by my examiners.

I understand that my thesis may be made electronically available to the public.

Statement of Contributions

Chapter 3 of this Thesis, entitled “Hydrophobic Modification of Starch”, was developed by myself and my supervisor Dr. Mario Gauthier. I completed all experimental work, characterization, analysis, and wrote the chapter with regular consultation with my supervisor.

Chapter 4, entitled “Castor Oil-Isocyanate Prepolymers as Cross-linkers for Starch”, was developed by myself, my supervisor, and Dr. Julien Mesnager formerly of EcoSynthetix. I completed all experimental work, characterization, analysis, and wrote the chapter with regular consultation with my supervisor.

Chapter 5, entitled “Maleation of Linseed and Soybean Oils”, was developed by myself, my supervisor, and Dr. Julien Mesnager. Michael Kuska of EcoSynthetix completed pilot plant scale reactions in an open glass reactor. I completed the characterization of the products he synthesized. I completed all remaining experimental work, characterization, analysis, and wrote the chapter with regular consultation with my supervisor.

Chapter 6, entitled “Production of “Cyclic Anhydride-Modified Starches”, was developed by myself, my supervisor, and Dr. Julien Mesnager. Reactive extrusion was completed at EcoSynthetix by Julien Mesnager and Michael Kuska. I purified the reactive extrusion products and characterized them. I completed all remaining experimental work, characterization, analysis, and wrote the chapter with regular consultation with my supervisor.

Abstract

Starch is a very common polysaccharide with multiple applications in the industry, but the range of physical properties exhibited by that material is relatively limited due to its strongly hydrophilic character. The work reported in this Thesis mainly concerns the development of synthetic methods for the chemical modification of starch, either in the nanoparticle or cooked forms, with different reactive hydrophobic reagents, under conditions including solution, slurry, melt mixing and reactive extrusion, so as to introduce amphiphilic character in the materials.

Starch nanoparticles (SNPs) were modified with hexanoic and propionic acid anhydrides in the presence of pyridine and 4-dimethylaminopyridine (DMAP) in dimethyl sulfoxide (DMSO) as solvent. A reaction efficiency (RE) of 100% was achieved over the entire degree of substitution (DS) range tested for both anhydrides and SNPs of different sizes. The integrity of the products was maintained, as the reaction conditions used did not lead to fragmentation of the starch and the addition of hydrophobic microdomains did not influence the D_h of the SNPs.

Polyurethane prepolymers (PUPs) were synthesized from castor oil and toluene diisocyanate (TDI) without solvent at an OH:NCO ratio of 1:2. Full conversion of the hydroxyl groups was achieved, even at this low OH:NCO ratio. The castor oil PUPs were used to cross-link and add hydrophobic microdomains in thermoplastic starch (TPS) without organic solvents or catalysts in a melt mixer. The reactions proceeded with high overall RE, which would make further purification of the products unnecessary for most applications. The reaction between the starch hydroxyl and the isocyanate groups formed no by-products, with 100% atom economy.

The maleation of raw linseed oil and soybean oil was completed in a benchtop pressure

reactor, while reactions with soybean oil were also completed using a benchtop open glass reactor or a pilot plant scale open glass reactor. In contrast to soybean oil, the maleation of linseed oil led to extensive cross-linking. Soybean oil products were synthesized containing up to 2.6 anhydride units on average per triglyceride. Gel permeation chromatography (GPC) analysis indicated that the sealed reactor approach led to significant oligomerization, while products from both open reactor methods were predominantly isolated triglycerides. A procedure was developed to determine the weight fraction of unreacted triglycerides in the maleated oil.

Hydrophobic starch esters were successfully prepared by reacting cooked starch with different cyclic anhydrides including octenyl succinic anhydride (OSA), dodecenyl succinic anhydride (DDSA), a maleated fatty acid (TENAX 2010), phthalic anhydride (PA), trimellitic anhydride (TMA), and maleated soybean oils (MSOs) in slurry reactions and in a melt mixer. Finally, hydrophobic modification by reactive extrusion was completed using DDSA, TENAX 2010, and MSO. For reactions in the dispersed phase, the RE was above 80% regardless of the anhydride loading, except for samples with high loadings of DDSA and maleated soybean oil. Reactions completed in a melt mixer with a base had a higher RE than reactions without base for all anhydride loadings. For reactive extrusion, the RE increased with the hydrophobicity of the anhydride. Reactive extrusion proved to be most advantageous to produce hydrophobically modified starch in an environmentally friendly and scalable way, with REs high enough to make purification of the products unnecessary for most applications.

The results obtained show that the hydrophobic modification of starch can be achieved efficiently, using a wide range of hydrophobic reagents and reaction conditions.

Acknowledgements

I would like to thank my supervisor Prof. Mario Gauthier for providing this opportunity, along with all the help, support, guidance, knowledge, expertise and motivation for the duration of my research at the University of Waterloo.

I would like to thank my advisory committee members, Prof. Jean Duhamel, Prof. Juewen Liu, and Prof. Leonardo Simon, for their advice and support.

I would like to thank Dr. Julien Mesnager and Dr. Niels Smeets, formerly of EcoSynthetix, for all their help through the years, as well as Dr. Steven Bloembergen, Michael Kuska, Dr. Ian McLennan, and everyone else involved in the collaboration with the University of Waterloo and EcoSynthetix.

I would like to thank all the past and present members of the Gauthier and Duhamel research laboratories for making my time at Waterloo such a pleasure.

I would like to thank the Natural Sciences and Engineering Research Council (NSERC) and EcoSynthetix for funding.

Finally, I would like to thank my family and friends for their unconditional support of my studies.

Dedication

I would like to dedicate this dissertation to the loving memory of Helen May Amos (1918-2017).

“When I was a little kid, I was really scared of the dark. But then I sort of came to see that dark just means the absence of photons in the visible wavelength, 400-700 nanometers. Then I thought, well that’s really silly to be afraid of a lack of photons. Then I wasn’t afraid of the dark anymore after that.”

-Elon Musk

Table of Contents

Examining Committee Membership	ii
AUTHOR'S DECLARATION	iii
Statement of Contributions	iv
Abstract	v
Acknowledgements.....	vii
Dedication	viii
List of Figures	xv
List of Tables	xx
List of Schemes.....	xxiii
List of Abbreviations and Symbols	xxvi
Chapter 1 Foreword	1
1.1 Opening Remarks	1
1.2 Research Objectives and Thesis Outline	2
Chapter 2 Starch and Vegetable Oils	4
2.1 Introduction	4
2.2 Starch Structure	7
2.2.1 Amylose and Amylopectin	7
2.2.2 Starch Granules	11
2.2.3 Starch Gelatinization	12
2.2.4 Starch Nanoparticles (SNPs) and Starch Nanocrystals (SNCs)	15

2.3 Chemical Modification of Starch	16
2.3.1 Starch Esterification	19
2.3.2 Starch Etherification.....	25
2.3.3 Starch Oxidation.....	31
2.3.4 Reaction of Starch with Cross-linking Agents	33
2.4 Vegetable Oils	38
2.4.1 Vegetable Oil Structure	38
2.4.2 Chemical Modification of Vegetable Oils.....	40
2.5 Conclusions	45
Chapter 3 Hydrophobic Modification of Starch Nanoparticles	47
3.1 Abstract	47
3.2 Introduction	48
3.3 Experimental Section	51
3.3.1 Materials	51
3.3.2 Synthesis of Water-dispersible HM-SNPs	52
3.3.3 Synthesis of High DS HM-SNPs	52
3.3.4 ¹ H NMR Analysis	53
3.3.5 Gel Permeation Chromatography (GPC) Analysis	53
3.4 Results and Discussion.....	54
3.4.1 Preparation of Starch Esters	54
3.4.2 Macromolecular Characterization of Starch Esters.....	60

3.5 Conclusions	67
Chapter 4 Castor Oil–Isocyanate Prepolymers as Cross-linkers for Starch	69
4.1 Abstract	69
4.2 Introduction	70
4.3 Experimental Section	74
4.3.1 Materials	74
4.3.2 Synthesis of Castor Oil PUPs	75
4.3.3 Determination of %NCO in Castor Oil PUP	75
4.3.4 Modification of Starch with Castor Oil PUP in a Melt Mixer	76
4.3.5 ¹ H NMR Analysis	77
4.3.6 Gel Permeation Chromatography (GPC) Analysis	77
4.4 Results and Discussion	78
4.4.1 Synthesis of Castor Oil PUPs	78
4.4.2 Modification of Starch with Castor Oil PUPs	87
4.4.3 Molecular Weight and Size of Castor Oil PUP-modified Starch	95
4.5 Conclusions	100
Chapter 5 Maleation of Linseed and Soybean Oils	102
5.1 Abstract	102
5.2 Introduction	103
5.3 Experimental Section	107
5.3.1 Materials	107

5.3.2 Maleation of Linseed Oil in a Sealed High Pressure Reactor	108
5.3.3 Maleation of Soybean Oil in a Sealed High Pressure Reactor	108
5.3.4 Maleation of Soybean Oil in an Open Glass Benchtop Reactor	108
5.3.5 Maleation of Soybean Oil on a Pilot Plant Scale	109
5.3.6 Soap Number Determination (ASTM D94-07).....	109
5.3.7 ¹ H NMR Analysis	110
5.3.8 Gel Permeation Chromatography (GPC) Analysis	110
5.3.9 Quantification of Unreacted Triglycerides.....	111
5.4 Results and Discussion.....	111
5.4.1 Maleation of Linseed Oil.....	111
5.4.2 Maleation of Soybean oil	117
5.4.3 Quantification of Unreacted Triglycerides.....	126
5.4.4 Scaled-up Maleation Reaction.....	130
5.5 Conclusions	132
Chapter 6 Production of Cyclic Anhydride-Modified Starches.....	135
6.1 Abstract	135
6.2 Introduction	136
6.3 Experimental Section	140
6.3.1 Materials.....	140
6.3.2 Modification of Dispersed Starch with Cyclic Anhydrides (Benchtop Procedure).....	141
6.3.3 Modification of Starch in a Melt Mixer	141

6.3.4 Modification of Starch with Cyclic Anhydrides in a Pilot Plant Scale Twin Screw Extruder	142
6.3.5 ¹ H NMR Analysis	143
6.3.6 Gel Permeation Chromatography (GPC) Analysis	143
6.4 Results and Discussion.....	145
6.4.1 Reaction of Starch with OSA and DDSA in Dispersions and in the Melt Mixer	147
6.4.2 Reaction of Starch with Phthalic Anhydride (PA) and 1,2,4-Benzenetri-carboxylic Acid Anhydride (TMA) in Dispersions and in the Melt Mixer	158
6.4.3 Reaction of Starch with Maleated Vegetable Oil in Dispersions and in the Melt Mixer	165
6.4.4 Starch Modification by Reactive Extrusion	176
6.5 Conclusions	181
Chapter 7 Concluding Remarks and Suggestions for Future Work.....	184
7.1 Original Contributions to Knowledge.....	184
7.2 Suggestions for Future Work	188
7.2.1 Measurement of Physical Properties of Synthesized Starch Products	188
7.2.2 Controlled Oligomerization of Maleated Vegetable Oil	189
7.2.3 Reactive Extrusion of Starch with Vegetable Oil-based Modifying Agents.....	191
7.2.4 Synthesis of Novel Drug Delivery Vehicles derived from Bio-based Materials .	192
References.....	194
Chapter 1	194

Chapter 2	194
Chapter 3	202
Chapter 4	204
Chapter 5	207
Chapter 6	209
Chapter 7	212

List of Figures

Figure 2.1. Chemical structure of (A) cellulose, (B) starch, (C) chitin, and (D) chitosan.....	5
Figure 2.2. Chemical structure of (A) amylose and (B) amylopectin.....	8
Figure 2.3. Structure of amylopectin.	10
Figure 2.4. Structure of (A) a starch granule, (B) large and small blocklets, (C) crystalline and amorphous lamellae, and (D) an amylopectin chain.....	12
Figure 2.5. Chemical structure of a TG and commonly found FAs.	39
Figure 3.1. ¹ H NMR spectra for (top) C6(0.1)-SNP-1 and (bottom) C3(0.1)-SNP-1.	56
Figure 3.2. Effect of varying the anhydride loading for (top) C6-SNP-1 (✕), C3-SNP-1 (◆) and (bottom) C6-SNP-2 (✕), C3-SNP-2 (◆).	59
Figure 3.3. RI peak area (after baseline subtraction) for C6(1)-SNP-1 (top) and C3(1)-SNP-1 (bottom) as a function of concentration. The dashed line is for a linear fit not forced through the origin.....	63
Figure 3.4. GPC baseline-subtracted RI elution curves of (a) SNP-1, (b) C6(0.05)-SNP-1, (c) C6(0.1)-SNP-1, (d) C3(0.05)-SNP-1, and (e) C3(0.1)-SNP-1. The position of each curve was adjusted on the vertical scale for clarity.	66
Figure 4.1. Structure of a triglyceride and common fatty acids.	72
Figure 4.2. ¹ H NMR spectra for (A) methanol-blocked 2,4-TDI, (B) castor oil and, and (C) the methanol-blocked castor oil PUP synthesized with DBTDL.	81

Figure 4.3. GPC elution curves from the RI detector for methanol-blocked castor oil PUP synthesized with (a) DBTDL, (b) K-KAT 348, and (c) without catalyst, as well as for (d) castor oil, (e) methanol-blocked TDI, and (f) oleic acid. The curves were normalized relatively to the maximum response and shifted vertically for clarity. 85

Figure 4.4. RI detector response calibration curve for methanol-blocked TDI. 86

Figure 4.5. Typical torque curves for starch with water (—) and for starch reactions with (A) DBTDL-catalyzed PUP at weight loadings of 1.65 (— —), 4.84 (- - -) and 6.73 wt% (— . -); starch reactions with (B) K-KAT 348-catalyzed PUP at weight loadings of 1.62 (— —), 4.94 (- - -) and 6.86 wt% (— . -); starch reactions with (C) PUP without catalyst at weight loadings of 1.99 (— —), 5.05 (- - -) and 7.10 wt% (— . -). 91

Figure 4.6. Typical temperature curves for starch with water (—) and for starch reactions with PUP without catalyst at weight loadings of 1.99 (— —), 5.05 (- - -) and 7.10 wt% (— . -). 92

Figure 4.7. ¹H NMR spectra for the reaction between DBTDL-catalyzed PUP and starch at 4.84 wt% PUP loading, (top) before and (bottom) after purification. 93

Figure 4.8. Reaction efficiency for starch and castor oil PUPs in a melt mixer catalyzed with (A) DBTDL, (B) K-KAT 348, and (C) without catalyst. 94

Figure 5.1. Structure of triglyceride and common fatty acids. 104

Figure 5.2. (A) Ene reaction mechanism between an ene and an enophile. (B) Ene reaction between a non-conjugated double bond (ene) with an allylic hydrogen and maleic anhydride (enophile).....	106
Figure 5.3. ¹ H NMR spectra for (A) raw linseed oil and (B) maleated linseed oil synthesized with 4.5 eq. of MA in a sealed reactor with 5 wt% toluene added.	114
Figure 5.4. ¹ H NMR for (A) raw soybean oil and (B) maleated soybean oil synthesized with 4.5 eq. of MA in a sealed reactor.	119
Figure 5.5. GPC elution curves for maleated soybean oil from a sealed reactor with an average of (a) 2.1, (b) 1.7, (c) 1.1 MA/TG, (d) soybean oil heated at 200 °C for 2 h in a sealed reactor without MA, (e) oleic acid, and (f) soybean oil substrate.	125
Figure 5.6. GPC elution curves for maleated soybean oil from an open glass reactor with an average of (a) 2.6, (b) 1.8, (c) 1.0 MA/ TG and (d) soybean oil substrate.	126
Figure 5.7. ¹ H NMR spectra for (A) maleated soybean oil from a sealed reactor with an average of 2.1 MA/TG, (B) hexanes-soluble fraction, (C) THF-soluble fraction, and (D) GPC traces for (a) maleated soybean oil from a sealed reactor with an average of 2.14 MA/TG, (b) hexanes-soluble fraction, (c) THF-soluble fraction, and (d) soybean oil.	129
Figure 5.8. GPC elution curves for maleated soybean oil synthesized in a pilot scale glass reactor with an average of (a) 2.3, (b) 2.0, (c) 1.1 MA/TG, and (d) soybean oil. .	132

Figure 6.1. Chemical structure of (A) amylose and (B) amylopectin.....	137
Figure 6.2. Chemical structure of (A) OSA, (B) DDSA, (C) phthalic anhydride, (D) 1,2,4-benzenetricarboxylic acid anhydride, (E) TENAX 2010, and (F) maleated soybean oil with one equivalent of maleic anhydride (many isomers possible).....	147
Figure 6.3. ¹ H NMR spectra for OSA-modified starch in DMSO- <i>d</i> ₆ (top) prior to purification and (bottom) after purification with acetone.	149
Figure 6.4. Modification of starch with (A) OSA and (B) DDSA. Conversion at different weight loadings for (▲) gelatinized starch dispersions, (□) melt mixer reactions without base, and (■) melt mixer reactions with base.	151
Figure 6.5. Typical torque variation at 90 °C and 40 rpm for starch with water (—) and starch with water and OSA (- - -)......	153
Figure 6.6. GPC elution curves for the baseline-subtracted normalized RI detector response for (a) unmodified gelatinized starch, gelatinized starch modified with (b) 5 wt% OSA, (c) 10 wt% OSA, (d) 5 wt% DDSA, and (e) 10 wt% DDSA in dispersed phase reactions. The position of each curve was shifted on the vertical axis for clarity.	156
Figure 6.7. GPC elution curves with RI (—) and LALS (- - -) detector responses for starch modified in a melt mixer under identical conditions, leading to LALS detector saturation (top; 5 wt% DDSA without base) and no saturation (bottom; 10 wt% OSA with base).....	159

Figure 6.8. GPC elution curves with baseline-subtracted normalized RI detector response for starch modified in the melt mixer: (a) unmodified starch, and starch modified with (b) 5 wt% OSA, (c) 10 wt% OSA, (d) 5 wt% DDSA, and (e) 10 wt% DDSA without base; starch modified with (f) 5 wt% OSA, (g) 10 wt% OSA, (h) 5 wt% DDSA, and (i) 10 wt% DDSA with base. The position of each curve was shifted on the vertical axis for clarity. 160

Figure 6.9. Modification of starch with (A) PA and (B) TMA. Reaction efficiency at different weight loadings for (▲) dispersed starch, (□) melt mixer reactions without base, (■) melt mixer reactions with 1.1 eq. of NaOH, and (x) melt mixer reactions with 2.2 eq. NaOH. 162

Figure 6.10. Modification of starch with (A) TENAX 2010, (B) MSO-1.1, (C) MSO-2.2, and (D) MSO-2.3. Conversion at different weight loadings for (▲) dispersed starch and melt mixer reactions (□) without and (■) with base. 168

Figure 6.11. Typical torque curves at 90 °C and 60 rpm for starch with water (———), and for starch, water and MSO-2.0 without base (— . . .) and with base (- - -). 171

Figure 6.12. Modification of starch in a pilot plant twin screw extruder (□) without base and (■) with 1.1 eq. of NaOH and (A) DDSA, (B) TENAX 2010, and (C) MSO-1.1. 178

List of Tables

Table 2.1. Starch composition and physical characteristics of starch granules from commonly cultivated sources.....	9
Table 2.2. FA composition of common vegetable oils.....	39
Table 3.1. Characteristics of SNPs and HMSNPs determined by GPC analysis.	67
Table 4.1. Chemical characteristics of castor oil PUPs.	82
Table 4.2. Molecular weight and hydrodynamic diameter (D_h) of PUP-modified starch samples determined from GPC analysis.....	98
Table 5.1. Soap numbers and MA incorporation in Alder-Ene reaction with linseed oil, using 4.5 MA/TG at 230 °C for 4 h.....	116
Table 5.2. Soap numbers and MA incorporation in ene reaction with linseed oil, using 4.5 eq. MA and 50 wt% toluene in a sealed reactor.....	117
Table 5.3. Soap numbers and MA incorporation in ene reaction with soybean oil, using 4.5 eq. MA in a sealed reactor.	121
Table 5.4. Soap numbers and MA incorporation in ene reaction with soybean oil in sealed and open glass reactors at 200 °C.....	122

Table 5.5. Gravimetric study of unreacted triglycerides in maleated soybean oil prepared in a sealed reactor, with an average $n = 2.1$ MA/TG, after column chromatography on silica gel.	128
Table 5.6. Gravimetric study of unreacted triglycerides in maleated soybean oil prepared in a sealed reactor, with an average $n = 1.1$ MA/TG, after column chromatography on silica gel.	130
Table 5.7. MA incorporation, unreacted MA and unreacted triglycerides in the ene reaction with soybean oil in a pilot plant scale open glass reactor.	131
Table 6.1. Absolute molecular weight averages determined by GPC analysis of starch modified in the dispersed phase with OSA and DDSA.	157
Table 6.2. Absolute molecular weight averages determined by GPC analysis of starch modified with PA and TMA in the dispersed phase.	163
Table 6.3. Absolute molecular weight averages determined by GPC for starch modified with PA and TMA in a melt mixer.	164
Table 6.4. Maleated soybean oil products synthesized in Chapter 5, used for the modification of starch.....	167
Table 6.5. Absolute molecular weight averages of starch modified with TENAX and maleated soybean oil in the dispersed phase.	172

Table 6.6. Absolute molecular weight averages and hydrodynamic diameter of starch modified with TENAX and maleated soybean oil in the melt mixer.....	173
Table 6.7. Absolute molecular weight averages and D_h for starch modified with DDSA, TENAX, and maleated soybean oil by reactive extrusion.....	180

List of Schemes

- Scheme 2.1. Reaction of starch with (A) acid halide (X represents a halogen atom), (B) linear anhydride, and (C) alkenyl succinic (cyclic) anhydride. The ester group is drawn at the C2 position of the GPy unit, however the reaction is possible at C2, C3, or C6. 22
- Scheme 2.2. Reaction of starch with (A) alkenyl oxides and (B) alkyl halides. The ether bond is drawn at the C2 position of GPy unit, however the reaction is also possible at C3 or C6. 26
- Scheme 2. 3. Oxidation of (A) secondary and (B) primary hydroxyls of starch. 33
- Scheme 2.4. Modification of starch with (A) POCl₃, (B) STMP, and (C) EPI. For simplicity, modification is shown at the C2 position of the first GPy unit, and at the C6 position of the subsequent GPy units, however the reaction is possible at either C2, C3, or C6 for each GPy unit. 36
- Scheme 2.5. Reaction of starch with an aldehyde forming hemiacetal and acetal functionalities. The modification is drawn at the C2 position of the first GPy unit and the C6 position of the second GPy unit for simplicity, however the reaction is possible at either C2, C3, or C6 for each GPy unit..... 37
- Scheme 2.6. Oxidation of linolenic acid residue resulting in a cross-link between fatty acids. 41
- Scheme 2.7. Reaction of (A) oleic acid residue with acetic acid and H₂O₂, (B) epoxidized oleic acid residue with methanol and HBF₄, and (C) oleic acid residue with MA. The

reaction with methanol is shown at C10 of the FA residue for simplicity, but reaction at C9 is also possible.....	43
Scheme 2.8. Transesterification of a triglyceride with three moles of methanol. The reaction is shown to occur at the second position initially, but it can take place at either position.....	45
 Scheme 3.1. Reaction of starch with OSA. The ester is shown at C2 for simplicity, but the reaction can occur with a hydroxyl group at either C2, C3 or C6 on the GPy units.	49
Scheme 3.2. Reaction of starch with an alkyl carboxylic acid anhydride. For hexanoic anhydride $n = 4$ and for propionic anhydride $n = 1$. The ester is shown at C6 for simplicity, but the reaction can also occur with a hydroxyl group at C2 or C3 on the GPy units.....	55
 Scheme 4.1. Reaction of a polyol with a diisocyanate to form a PUP.	71
Scheme 4.2. Reaction of castor oil with 2,4-TDI. The reaction can also happen at position 6 for 2,6-TDI present in the technical grade product (many isomers possible).	80
Scheme 4.3. Reaction of starch with castor oil PUP (many isomers possible). The reaction is drawn at the 2 position of the GPy units for simplicity, but reaction at the 2, 3 and 6 positions is possible.	90

Scheme 6.1. Reaction of starch with OSA. The ester is drawn in the C2 position, but esterification is possible at C2, C3 or C6. 149

List of Abbreviations and Symbols

%NCO	Weight percent of isocyanate groups in the sample
$\left(\frac{dn}{dc}\right)$	Specific refractive index increment
[O]	Oxidizing agent
$[\eta]$	Intrinsic viscosity
^{13}C NMR	Carbon-13 nuclear magnetic resonance spectroscopy
^1H NMR	Proton nuclear magnetic resonance spectroscopy
α	Mark-Houwink exponent value
η_0	Viscosity of pure solvent
λ	Wavelength
ϕ	Volume fraction
A_2	Second virial coefficient
ACS	American Chemical Society
ASA	Alkenyl succinic anhydride
BO	1,2-Butene oxide
c	Concentration
CHPTAC	3-Chloro-2-hydroxypropyltrimethyl ammonium chloride
\mathbb{D}	Polydispersity
DBTDL	Dibutyltin dilaurate
DDSA	Dodeceny succinic anhydride
D_h	Hydrodynamic diameter
DIEA	<i>N,N</i> -Diisopropylethylamine
DMAP	4-Dimethylaminopyridine

DMSO	Dimethyl sulfoxide
DP	Degree of polymerization
DS	Degree of substitution
EPI	Epichlorohydrin (1-chloro-2,3-epoxypropane)
Eq.	Equation
eq.	Equivalent
FA	Fatty acid
FDA	Food and Drug Administration
FTIR	Fourier transform infrared
GMAC	2,3-Epoxypropyltrimethylammonium chloride
GPC	Gel permeation chromatography
GPy	Glucopyranose
h	Hour
HMDI	Hexamethylene diisocyanate
HM-SNP	Hydrophobically modified starch nanoparticle
HPLC	High pressure liquid chromatography
I.D.	Inner diameter
IPDI	Isophorone diisocyanate
K	Optical constant in light scattering
kDa	Kilodalton
K-KAT 348	Bismuth 2-ethylhexanoate
LALS	Low angle light scattering
LS	Light scattering
M	Molar concentration (mol/L)
MA	Maleic anhydride

MA/TG	Average number of maleic anhydride units per triglyceride
MCA	Monochloroacetic acid
MDa	Megadalton
MDI	Methylene diisocyanate
min	Minutes
mmol	Millimole
M_n	Number-average molecular weight
mol	Mole
M_p	Peak molecular weight
MS	Molar degree of substitution
MSO-x	Maleated soybean oil with an average of x anhydride units per triglyceride
MW	Molecular weight
M_w	Weight-average molecular weight
MWCO	Molecular weight cut-off
M_x	Mass of compound x
N_A	Avogadro's number
n_o	Refractive index of the solvent
OH:NCO	Mole ratio of hydroxyl to isocyanate groups
OSA	Octenyl succinic anhydride
PA	Phthalic anhydride
PO	Propylene oxide
ppm	Part per million
PS	Polystyrene
PU	Polyurethane
PUP	Polyurethane prepolymer

P _θ	Particle scattering factor
RE	Reaction efficiency
RI	Refractive index
R _θ	Rayleigh ratio
SEM	Scanning electron microscope
SMCA	Sodium monochloroacetate
SN	Soap number
SNP	Starch nanoparticle
STMP	Sodium trimetaphosphate
TDI	Toluene diisocyanate
TEA	Triethylamine
TEMPO	2,2,6,6-Tetramethyl-1-piperidine-1-oxyl radical
TFA	Trifluoroacetic acid
TG	Triglyceride
THF	Tetrahydrofuran
TMA	Trimellitic anhydride, 1,2,4-benzenetricarboxylic acid anhydride
TPS	Thermoplastic starch
wrt	With respect to
wt%	Weight percent

Chapter 1

Foreword

1.1 Opening Remarks

Starch is a natural biopolymer which is renewable, biodegradable, readily available, and cost-effective.¹ These attributes make it attractive not only for food, but also as a feedstock to replace petroleum-based materials in industrial applications.² Native starch has several drawbacks as direct replacement for petroleum-based materials such as sensitivity to water and poor mechanical properties.³ To overcome these issues and to tune its physical properties, starch is commonly modified industrially.⁴ Traditionally, the modification of native starch has been completed in stirred batch or continuous reactors.⁵ A significant obstacle to the modification of granular starch is that the highly ordered starch granules physically sequester glucopyranose (GPy) units in their interior.⁶

Gelatinization is an irreversible process resulting in the destruction of the granule structure and the release of the starch polymer chains.⁷ In either single or twin screw extruders, starch can be heated with a plasticizer, which in combination with the mechanical treatment causes gelatinization and yields thermoplasticized starch (TPS).⁵ After the mechanical treatment, TPS has undergone significant fragmentation producing starch particles with a diameter on the nanometer scale. Modification of the gelatinized starch or TPS during processing in a single step should result in a higher reaction efficiency (RE), since all GPy units are accessible to react, in contrast to native (granular) starch.

1.2 Research Objectives and Thesis Outline

The hydrophobic modification of starch is the main focus of the research described in this Dissertation. Starch was first hydrophobically modified while dispersed in an organic solvent or in water. A torque rheometer, commonly referred to as a melt mixer, was then used to mimic the high shear environment of an extruder and modify TPS in a single procedure. Finally, starch modification was completed in a pilot plant scale twin screw extruder, to demonstrate that the chemistry and procedures developed are efficient on an industrial scale. Vegetable oils were also modified to serve as hydrophobic reactive modifiers for starch.

This Dissertation comprises 7 chapters. Following this brief foreword, a literature review (Chapter 2) is presented which provides background information subdivided into three sections on starch structure, the chemical modification of starch, and a brief discussion of the structure and modification of vegetable oils. Chapter 3 reports on the modification of starch nanoparticles (SNPs) with either hexanoic or propionic anhydride, while still retaining their ability to disperse in water. Chapter 4 reports on the synthesis of polyurethane prepolymers (PUPs) from castor oil and toluene 2,4-diisocyanate (TDI) in the absence of organic solvents. The castor oil PUPs were used to introduce hydrophobic domains and cross-links in starch in a melt mixer. Chapter 5 reports on the maleation of linseed and soybean oils. The soybean oil reactions were carried out from benchtop to pilot plant scales. Chapter 6 reports on the modification of starch with octenylsuccinic anhydride (OSA), dodecenylsuccinic anhydride (DDSA), a maleated fatty acid (TENAX 2010), phthalic anhydride (PA), 1,2,4-benzenetricarboxylic acid anhydride (trimellitic

anhydride, TMA), and with three maleated soybean oil samples synthesized as described in Chapter 5. For each anhydride, reactions were completed on gelatinized starch dispersed in water and in a melt mixer, with and without a base. DDSA, TENAX 2010, and maleated soybean oil were also reacted with starch in a pilot plant scale twin screw extruder.

The Dissertation is concluded (Chapter 7) with a general summary of the results obtained, the original contributions to knowledge arising from the research, and suggestions for further work.

In agreement with the University of Waterloo Thesis guidelines, Chapters 3-6 are written in the format of individual papers to be submitted for publication in scientific journals. Included within each chapter is an abstract, an introductory section providing background related to the specific topic considered, an experimental section detailing the materials and methods used, a results and discussion section, and finally a summary of conclusions drawn from the work.

Chapter 2

Starch and Vegetable Oils

2.1 Introduction

Due to the increasing world population and depleting petroleum supplies, there is greater need to develop sustainable materials to meet market demands.¹ Organic polymers including polyethylene, polypropylene, polystyrene, and poly(vinyl chloride) have traditionally been inexpensive materials for applications in packaging, construction, automobiles, furniture, and toys.² A material is typically selected based on its expected performance, durability and cost,³ but its ability to degrade or to be recycled often is not considered.⁴ While some of the synthetic materials can be recycled with appropriate infrastructure, these are often incinerated and produce carbon dioxide, or end up in landfills and oceans without significant degradation.³ To mitigate some of these issues, scientists are searching alternatives including biodegradable polymers such as polylactide, poly(butylene succinate), and poly(3-hydroxybutyrate) for packaging, films, and agriculture.³

One option to decrease the reliance on petroleum products is to use renewable materials as a carbon source.⁵ The polysaccharides cellulose, starch, and chitin are the most abundant biopolymers on the planet.^{6,7} For these biopolymers to be put into industrial practice, they must meet or exceed the properties of petroleum-based materials in terms of performance, durability, and cost.³ While native biopolymers are unlikely to meet these requirements, the modification

of biopolymers through physical or chemical means can serve to tailor their properties for desired applications.⁶ Cellulose is the most abundant biopolymer on the planet.⁸ It is a structural biopolymer forming stiff rod-like structures, found in the cell wall of plants.⁹ It has a linear chain structure composed of glucopyranose (GPy) units connected through β -1,4 glycosidic linkages (Figure 2.1(A)) forming highly crystalline domains.² Multiple hydroxyl groups form hydrogen bonds with other cellulose chains, to yield microfibrils with a high tensile strength.¹⁰ Due to this tight hydrogen-bonded network structure, cellulose does not dissolve in common organic solvents.⁸ Cellulose, making up approximately 90% of cotton and 40-50% of wood, finds uses in the food, paper, textiles, adhesives, and coatings industries.¹⁰

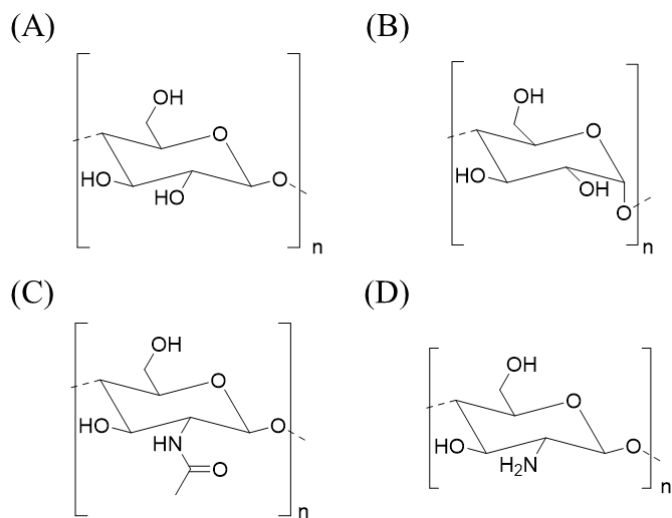


Figure 2.1. Chemical structure of (A) cellulose, (B) starch, (C) chitin, and (D) chitosan.

Starch is the second most abundant biopolymer and is the topic of this Thesis.¹¹ Similarly to cellulose starch is synthesized by plants, but it is used for energy storage.¹² Starch is commonly extracted from cereals (e.g. corn and wheat), tubers (e.g. potatoes), and roots (e.g. tapioca).¹³ Starch is composed of GPy units connected through α -1,4 linkages (Figure 2.1(B)), with branching introduced through α -1,6 linkages.¹¹ A more detailed analysis of the chain structure of starch will be provided in Section 2.2. Besides the food industry, starch has found uses in the paper, adhesives, and construction industries.¹⁴

Chitin, the third most common biopolymer, is a structural biopolymer found in the shell of crustaceans.¹⁵ Unlike cellulose and starch, chitin also contains nitrogen since it is composed of 2-acetamido-2-deoxy- β -D-glucose units connected through β -1,4 glycosidic linkages (Figure 2.1(C)).⁷ It has the same structure as cellulose, except that the hydroxyl group on the C2 carbon is replaced with an acetylamido functional group. As a result, chitin microfibrils have a stronger hydrogen-bonded network than cellulose.¹⁵ Chitin is commercially deacetylated with a base to produce chitosan (Figure 2.1(D)),^{16,17} which typically has 60-100% of the repeat units in the free amine form and is dispersible in water below pH 6.0.^{7,16} Chitin and chitosan do not find the same level of industrial use as cellulose and starch, but they are employed in agriculture, as sorbents for filtration, and in the biomedical area.⁷

2.2 Starch Structure

2.2.1 Amylose and Amylopectin

Starch is composed predominately of two different macromolecules, amylose and amylopectin (Figure 2.2), as well as trace amounts of cell-wall fragments, proteins, amino acids, nucleic acids, and lipids.¹³ Amylose is a predominantly linear polymer containing more than 99% α -1,4 glycosidic linkages, the remainder being α -1,6 glycosidic linkages, and has a molecular weight on the order of 10^5 - 10^6 g/mol.¹⁸ Amylopectin contains approximately 95-99% α -1,4 glycosidic linkages, the remainder being α -1,6 glycosidic linkages, and has a molecular weight on the order of 10^7 - 10^9 g/mol.¹² The composition, molecular size, shape, structure and polydispersity of amylose and amylopectin depend on the plant species from which they are derived (Table 2.1).^{12,19,20} In water, amylose adopts a single left-handed helix conformation in the presence of complexing agents such as lipids, emulsifiers, or alcohols.¹² In the absence of complexing agents, amylose forms left-handed parallel double helices.¹⁸ The 3D structure of the double helix has been elucidated by X-ray diffraction and other techniques.²¹ There are 2 common types of 3D arrangements for the double helices known as the A- and B-types.¹⁸ Both types form a “6-fold structure” with a crystal repeat unit of approximately 1.05 nm.¹³ The A-type helices form a tight monoclinic lattice, with a total of four water molecules located between the helices in each unit cell.¹² The B-type helices are more expanded and form a hexagonal lattice with 36 water molecules in the unit cell.²⁰ Half of the water molecules are located between the double helices, while the remaining molecules are located in the center cavity of the hexagon.¹²

The B-type starch crystal structure is common under cool wet conditions such as in starches found in tubers and roots (in the ground), as well as in high amylose starches, while the A-type starch crystal structure is more common under warm dry conditions (above the ground), such as in cereal starches.²⁰ Furthermore, longer helical chains favor the formation of the B-type crystal structure while shorter chains form the A-type structure.¹² A C-type starch crystal structure is also known, however it was shown to be a combination of A- and B-type structures rather than a new distinct crystalline form.²¹

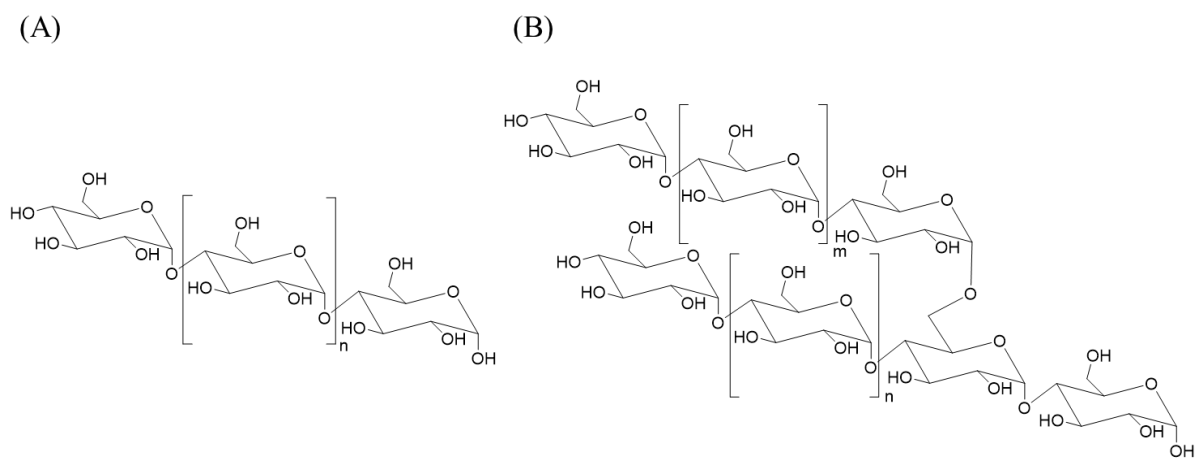


Figure 2.2. Chemical structure of (A) amylose and (B) amylopectin.

Table 2.1. Starch composition and physical characteristics of starch granules from commonly cultivated sources.

Starch	Type	Amylose (%)	Amylopectin (%)	Granule shape	Granule size (µm)
Maize ²⁰	Cereal	28	72	Spherical	2-30
Amylomaize ²⁰	Cereal	60-73	27-40	Irregular	2-30
Waxy maize ²⁰	Cereal	< 1	> 99	Spherical	2-30
Wheat ²⁰	Cereal	25-29	71-75	Lenticular, spherical	15-35, 2-10
Rice ¹²	Cereal	20-25	75-80	Polyhedral	3-8
Potato ¹⁹	Tuber	21	79	Lenticular	5-100
Tapioca ²²	Root	17	83	Lenticular, spherical	4-35

Due to the branched structure of amylopectin, GPy segments are characterized as either A-, B- or C-chains (Figure 2.3).²⁰ There is generally a single C-chain per amylopectin molecule, with a high degree of polymerization (DP), carrying other chains as branches and GPy units with a hydroxyl group on the C1 carbon, known as the reducing end.¹¹ The A-chains are shortest and are bound to amylopectin through α -1,6 glycosidic linkages. These do not carry any additional branches and do not have a reducing end.¹³ The B-chains are similarly connected to amylopectin through α -1,6 glycosidic linkages but carry other branches, their DP is variable, and like the A-chains, they do not have a reducing end.¹⁸ Similarly to amylose, the amylopectin segments form double helices with either amylose or other amylopectin chain segments.²¹ A molecule of amylopectin can form multiple double helices and either A-, B-, or C-type crystalline structures in solution.¹³ As with amylose, short segments favor the formation of A-type structures, while

intermediate length segments form C-type structures transitioning to B-type structures for longer segments.¹² Amylopectin with a higher proportion of A-type structures frequently has smaller crystalline domains, in contrast to B-type structures which have a smaller number of larger crystalline domains.¹³ Increasing the amylose content with respect to amylopectin in solution favors the formation of B-type structures.¹⁹ Amylopectin with a higher proportion of A-type structures has a higher crystallinity as compared to amylopectin with a higher proportion of B-type structures.²¹ Cereal starches have a higher proportion of A-type structures, while tuber and root starches have a higher proportion of B-type structures, and legume starches are enriched in C-type structures.¹³

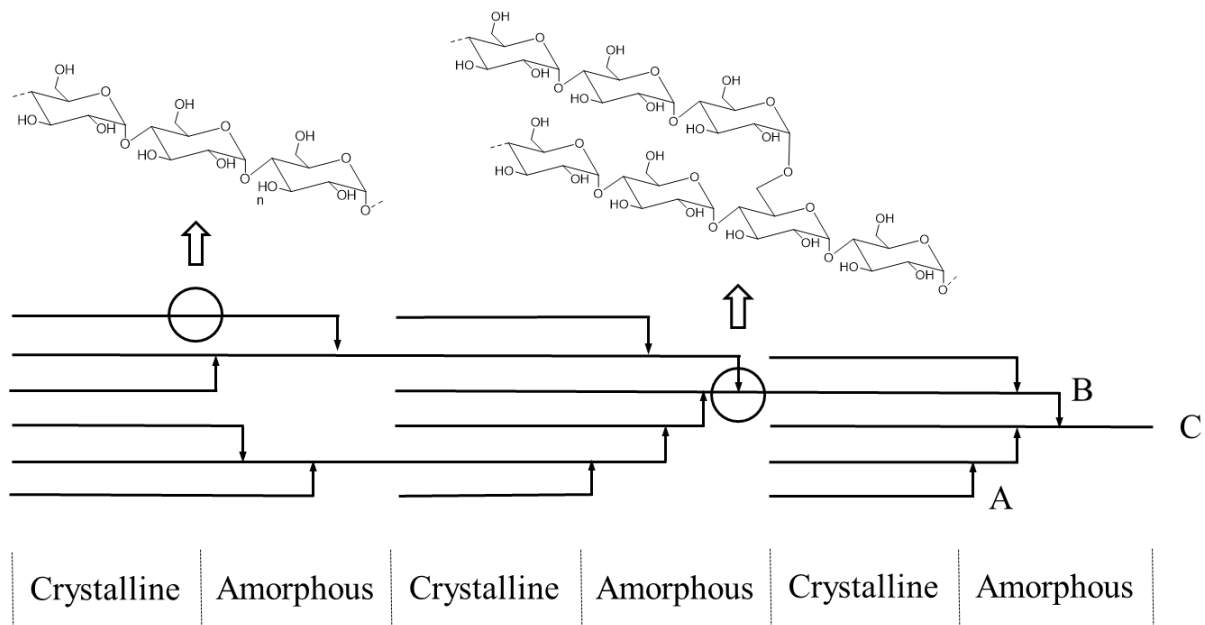


Figure 2.3. Structure of amylopectin.

2.2.2 Starch Granules

Amylose and amylopectin are found in starch granules which, as stated previously, vary in diameter and shape among different plant species.^{12,19,20} Starch granules from all plants have a similar complex multiscale structure; the center of starch granules is composed of an amorphous region known as the hilum (Figure 2.4).¹⁸ From the hilum, concentric growth rings are superimposed outward which are composed of alternating semi-crystalline and amorphous regions.²³ Scanning electron microscopy analysis of starch granules revealed that the semi-crystalline and amorphous rings are composed of large and small ellipsoid structures known as blockets.¹³ The large blockets have a diameter between 20-50 nm and are composed of semi-crystalline layers. These semi-crystalline layers consist of alternating crystalline and amorphous lamellae.^{24,25} One crystalline lamella and one amorphous lamella have a combined thickness of 9-11 nm regardless of the plant species.¹⁹ Amylopectin chains are embedded in both the crystalline and amorphous lamellae.¹¹ The reducing end of amylopectin is oriented toward the hilum, while the (non-reducing) chain ends are oriented toward the surface of the granule.²⁰ The helical linear segments of amylopectin compose the crystalline lamellae, while the branched regions are incorporated in the amorphous lamellae.²³ The small blockets have a diameter around 25 nm and are composed predominately of amorphous chains.²⁴ One large and one small blocket compose a semi-crystalline growth ring.²⁶ In contrast to amylopectin, the location of amylose is not universal and changes in each plant species.²⁷ Amylose has indeed been found at higher concentrations in the amorphous regions, in bundles between amylopectin segments, or

interspersed with amylopectin segments throughout crystalline and amorphous regions of the granule.²⁷

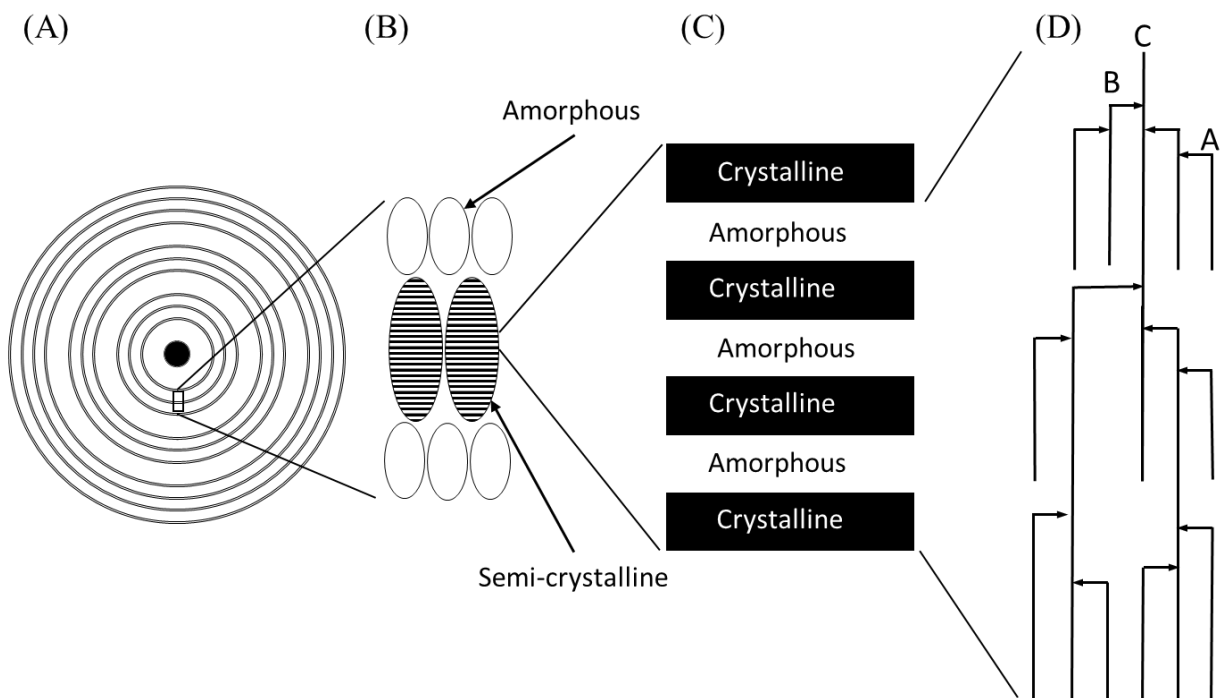


Figure 2.4. Structure of (A) a starch granule, (B) large and small blockets, (C) crystalline and amorphous lamellae, and (D) an amylopectin chain.

2.2.3 Starch Gelatinization

Starch gelatinization is an irreversible process which results in the destruction of the ordered architecture of starch granules and releases individual starch chains.²⁸ The process requires heat and a solvent (plasticizer) such as water, and while mechanical treatment is not

necessary, it can accelerate the process.²⁹ In the absence of mechanical treatment (shearless conditions), gelatinization begins with water diffusing into the granules, resulting in increased starch chain mobility in the amorphous regions.²⁴ Without heat, the starch granule structure remains stable in solution, as it is held together by both van der Waals forces and hydrogen bonding.²⁵ The starch chains in the amorphous regions can reversibly rearrange, resulting in new intermolecular interactions.²¹ Upon heating above the minimum gelatinization temperature, the crystalline regions of the granules begin to melt, which allows water to diffuse into the helical starch segments.³⁰ The double helices within the amylopectin structure begin to dissociate from the ordered intermolecular hydrogen-bonded network, which leads to starch chains dispersing in solution and the loss of the granule structure.^{31,32} The new material, commonly referred to as thermoplastic starch (TPS), exhibits physical properties characteristic of thermoplastic polymers.²⁵ The minimum temperature required for gelatinization depends on many factors including, for example, the ratio of amylopectin to amylose, the water content, the pH, as well as the presence of and the concentration of salts.³²

With mechanical treatment (high shear), the amount of solvent (plasticizer) required for gelatinization is significantly decreased because shear forces physically tear the granules apart.³³ Water is a common plasticizer for starch, however other polyhydric compounds such as glycerol or sorbitol can also plasticize starch effectively.²⁵ Single and twin screw extruders have been used to gelatinize starch in continuous processes from small benchtop to industrial scales.³⁴ Extruders are designed to achieve good mixing of viscous materials and can produce the high

shear required for starch gelatinization.¹⁴ In contrast to shearless conditions, starch crystallinity is lost under high shear due to mechanical forces rather than granule swelling.³⁵ A mechanistic study on the twin screw extrusion of starch by Gilbert and coworkers³⁶ revealed that starch fragmentation preferentially effects larger molecules, based on GPC analysis of the extrusion products. The fragmentation of starch occurs through shear scission, and not through a combination of cross-linking, branching, or end group reactions as in the extrusion of polyolefins. Amylopectin is more susceptible to chain scission because of its branched structure, since its short chain segments make it more resistant to deformation under high shear as compared to amylose, despite its higher molecular weight. Chain scission occurs preferentially at the center of the molecule, resulting in a monomodal distribution of products of intermediate size. Using extruders as chemical reactors, commonly referred to as reactive extrusion, has become common, and examples of starch reactive extrusion will be discussed in Section 2.3.¹⁴

While single and twin screw extruders are efficient mixing devices, it can be difficult to obtain information using small amounts of material by reactive extrusion.³⁷ Torque rheometers incorporating a twin-roller mixer, also known as melt mixers, have been used in batch processes to mimic a high shear environment and obtain TPS on a smaller scale than extruders.³⁸ A torque rheometer allows the constant measurement of torque, which enables the quantification of the specific mechanical energy (SME) by integrating the torque with respect to time.³⁹ This technique allows the quantification of the SME required to gelatinize starch under controlled

conditions including a specific starch type, mixing speed, time, temperature, plasticizer type(s), and weight loading of plasticizer(s), among others.³⁸

After gelatinization, the starch chains begin to associate with each other in a process called retrogradation.³² This process is primarily driven by random coil amylose chains forming new double helices, and to a lesser extent A-chains in amylopectin forming double helices.³³ These double helices act as nucleation sites favoring the formation of new crystalline domains by other starch chains.⁴⁰ Over time, water is expelled and the new crystalline domains form the B-type structures discussed previously.³² Starches with higher amylose contents form stronger films with a stabilized 3D hydrogen bonded network, while waxy starches form soft gels without a network.³³ Consequently, the amylose content of starch must be considered for starch-based film-forming applications.

2.2.4 Starch Nanoparticles (SNPs) and Starch Nanocrystals (SNCs)

Nanoparticles derived from starch have previously been referred to as starch nanoparticles (SNPs), starch crystallites, starch nanocrystals (SNCs), microcrystalline starch, and hydrolyzed starch, but there are no universal definitions allowing these terms to be distinguished.⁴¹ It has thus been suggested by Dufresne and coworkers¹³ to use the terminology SNCs to describe nano-sized starch products having a higher degree of crystallinity than the native starch from which they are prepared. The term SNPs would be used to describe nano-sized starch products having a degree of crystallinity comparable to or lower than the native starch from which they are prepared. An example of SNCs would be the products which

Dufresne and coworkers⁴² prepared by exposing granular waxy maize starch to 2.2 M HCl for 15 days, to induce the controlled degradation of the amorphous regions, before purification by centrifugation. The purified SNCs were dispersible in water using a homogenizer, but were obtained in low yield as they had to be purified before use.¹³ In contrast, SNPs produced through mechanical treatment, for example in a twin screw extruder, are obtained in yields as high as 100% and may not require purification.¹⁴ For example, Deng and coworkers⁴³ reported that SNPs prepared by processing maize starch in a twin screw extruder with 22 wt% water and 23 wt% glycerol (as plasticizers), at a maximum barrel temperature of 90 °C and 300 rpm, had a lower crystallinity level than the native starch feedstock, based on wide angle X-ray diffraction analysis of the samples.

2.3 Chemical Modification of Starch

The chemical modification of starch is typically regulated by the intrinsic reactivity of the individual GPy units in the starch backbone.¹⁴ As stated previously, GPy units typically contain one primary hydroxyl group at the C6 position, and secondary hydroxyl groups at the C2 and C3 positions.⁴⁴ Common techniques used to characterize modified starch will be discussed before specific esterification (Section 2.3.1), etherification (Section 2.3.2), oxidation (Section 2.3.3), and cross-linking (Section 2.3.4) reactions of starch, including reactive extrusion techniques. The synthesis of vinyl graft copolymers of starch, which was previously reviewed,⁴⁵ will not be considered.

Chemically modified starches are often characterized by their degree of substitution (DS), defined as the average number of hydroxyl groups modified on each GPy unit.^{46,47} The theoretical maximum DS is 3, since the GPy units on starch have on average 3 hydroxyl groups.⁴⁸ For each GPy unit with an α -1,6 linkage, which contains only 2 hydroxyl groups, there is a chain end containing 4 hydroxyl groups. Starch can also be modified with polymerizable groups, such as propylene oxide (PO), and characterized in terms of molar degree of substitution (MS),⁴⁹ defined as the average number of polymerizable monomer groups per GPy unit.⁵⁰ In contrast to the DS, the MS can exceed 3 for modified starch products.⁵¹ It is also possible to characterize modified starch products with both DS and MS values. In that case the DS indicates the average number of polymeric chains per GPy unit, and the MS the average number of monomer units per GPy unit, with $MS \geq DS$ for starch graft copolymers.⁵⁰

The DS of modified starch products is commonly measured by at least one of four techniques, namely titration, ¹H NMR spectroscopy, elemental analysis, or Fourier transform infrared (FTIR) spectroscopy.⁴⁴ In the titration (also referred to as saponification) methods, the modified starch is suspended in an alkaline solution to hydrolyze the modifying groups. The excess alkali is then back-titrated with a standardized acid solution. The amount of base consumed in the modified product is compared with a blank value obtained by the same procedure using unmodified starch.⁵²

¹H NMR analysis is often used to quantify the DS or MS of modified starch,⁵³ by comparison of the intensity for the proton on the anomeric (C1) carbon with the protons on the

modifying groups.⁵⁴ For accurate quantification, the modifying group should have at least one proton producing a signal that does not overlap with the protons from starch. For example, the substitution level of starch modified with sodium trimetaphosphate (STMP) cannot be quantified by ¹H NMR analysis.⁵³ Advanced NMR techniques, such as heteronuclear single quantum coherence ¹H-¹³C NMR, have been used to determine specifically which hydroxyl groups in the GPy units reacted.⁵⁵

Elemental analysis may also be used to determine the DS or MS of modified starch.⁵⁶ Since native starch contains 44.4% carbon, the carbon density of modified starch will vary with the type of modification used and the DS or MS of the sample.⁵⁷ Starch modifications involving atoms other than carbon, hydrogen, or oxygen are easily quantified.⁵⁸ In addition, FTIR analysis can be used to confirm the modification of starch with specific functional groups.⁵⁹ For example, starch esters produce a new band at 1749 cm⁻¹, while starch urethane products yield peaks at 1644, 1710 and 1732 cm⁻¹.^{60,61} The intensity of the peaks is linearly related to the DS or MS, however DS or MS determinations below 0.30 are typically not reliable.⁴⁴

The characteristics of starch are sensitive to variations during the growth season such as exposure to sunlight, temperature, water uptake, or the method of starch isolation, among others. As a result, parameters such as the molecular weight of amylopectin molecules can vary by more than one order of magnitude. It is therefore essential to include parameters such as the M_w of the unmodified starch when reporting new modifications methods, to determine in which way the

characteristics of the new product(s) are related to the starch starting material or result from the modification procedure.^{18,32}

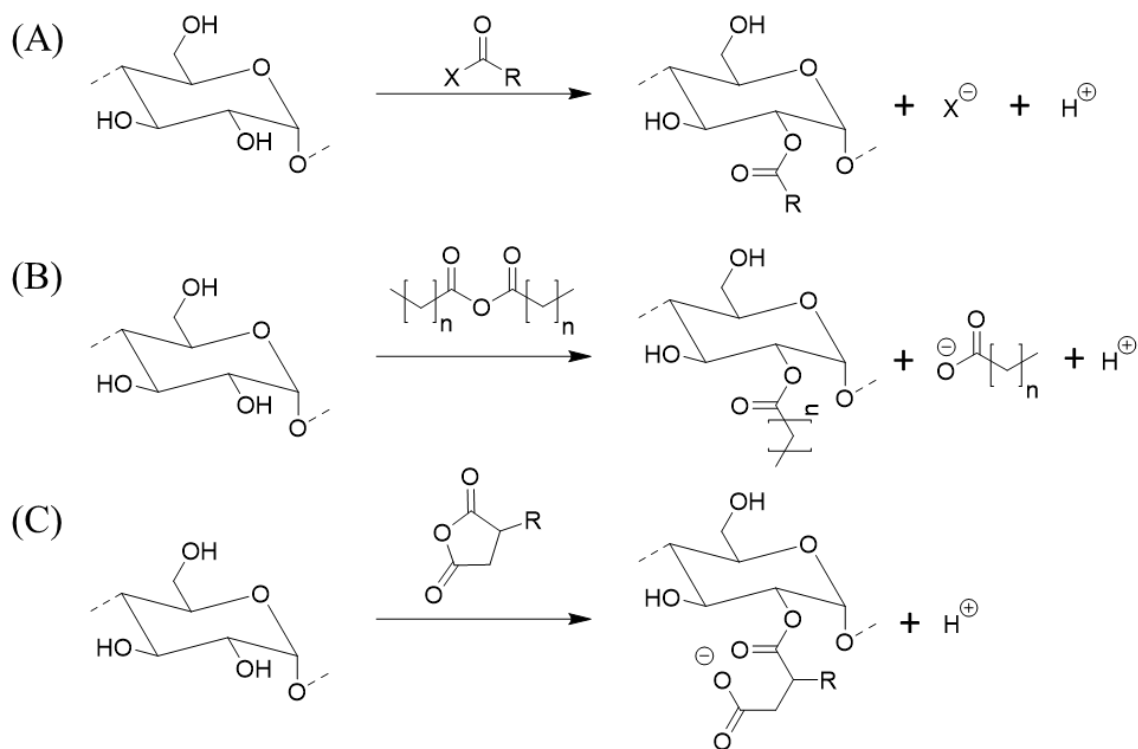
2.3.1 Starch Esterification

Starch esters have found uses as emulsifiers, in encapsulation, films, coatings, and as adhesives, among others, with hydrophobicity of the product increasing directly with the DS.⁴⁴ The esterification of starch is usually carried out to disrupt the crystallinity of the starch chains, or to manipulate the hydrophilic-hydrophobic balance of starch.⁶² Esterification reactions can be completed using acid halides (Scheme 2.1(A)), linear anhydrides (Scheme 2.1(B)), and cyclic anhydrides (Scheme 2.1(C)).¹⁴ In solution, the reaction between starch and acid halides proceeds by nucleophilic attack of a starch hydroxyl group at the carbonyl carbon of the acid halide.⁶³ Upon carbonyl group reformation, a halide anion and an acidic proton are produced along with the starch ester. A stoichiometric amount of base is typically added before the acid chloride, to prevent the acid-catalyzed hydrolysis of starch.⁶⁴ Fowler and coworkers⁶⁰ reported the modification of different gelatinized maize starches (with amylose contents of 1, 50, and 70%) with 6 eq. NaOH wrt to acid chloride and 1 eq. of either 4-dimethylaminopyridine (DMAP), triethylamine (TEA), pyridine, *N,N*-diisopropylethylamine (DIEA) wrt acid chloride, or no added organic base. The reaction was completed at room temperature in 1 h with 0.5 eq. of either acetyl, butyryl, octanoyl, or octadecanoyl (stearoyl) chloride. The acetyl, butryl, and octadecanoyl chlorides did not yield any starch esters under these conditions, illustrating the importance of selecting a suitable reagent and solvent. The authors theorized that the water-

miscible acetyl and butyryl chlorides underwent rapid hydrolysis in the strongly alkaline conditions of the reaction medium, while octadecanoyl chloride was not miscible with the starch mixture, which prevented the reaction. Reactions completed with octanoyl chloride had RE of 36, 54 and 46% for starch samples containing 1, 50 and 70% amylose, respectively. The DS of the products was determined by elemental analysis. The authors concluded there was little depolymerization of the products, because the viscosity of the gelatinized 70% amylose starch and the esterified products was comparable, between 40-51 cP in DMSO at 4.5 wt% concentration. The authors did not report viscosity results for the 1 and 50% amylose starches. In a similar fashion, Namazi and Dadkhah⁶⁵ reported the modification of pregelatinized (H_2SO_4 , 3.16 M) waxy maize starch with 6 eq. NaOH wrt acid chloride at room temperature over 20 minutes, followed by drop-wise addition of octanoyl, nonanoyl, or decanoyl chloride. Using 0.5 eq. of acid chloride led to RE values of 54, 59, and 41% for octanoyl, nonanoyl and decanoyl chloride, respectively. The DS was measured by elemental analysis, and the diameter of the unmodified and modified particles was determined to be between 70-100 nm by transmission electron microscopy (TEM). While water is a convenient solvent for the esterification reaction, it competes with the starch hydroxyl groups for the reaction with the acid chloride and its polarity prevents the preparation of hydrophobic products, unlike organic solvents less polar than water.⁶⁴ With that limitation in mind, Panayiotou and coworkers⁵⁶ achieved the modification of granular potato starch (19% amylose) and amylo maize starch (70% amylose) at 105 °C in pyridine as solvent for 3 hours, with varying amounts of either octanoyl, dodecanoyl, or octadecanoyl

chloride. The starch was gelatinized *in situ* due to heating. They were able to achieve a RE of 59% when using 4.55 eq. for each of the 3 acid chlorides tested, corresponding to a DS of 2.7 by elemental analysis.

The reaction between starch and linear anhydrides typically requires a catalyst, or a base to neutralize the acid formed.⁴⁷ Similarly to acid chlorides, starch esterification has been completed with linear anhydrides in either water or polar organic solvents.⁵⁶ Hanna and coworkers⁴⁷ reported the modification of granular amylo maize starch with acetic anhydride (2-6.4 eq) acting as both anhydride source and solvent. The reaction was completed at 123 °C with NaOH (added as a 50 wt% solution, in amounts varying from 0.61 to 1.4 eq. with respect to starch), and the reaction time was varied from 0.5 to 4 h. By this method, a RE of 65% was achieved for the modified product after 4 h, with a DS reaching 1.3 by titration. Increasing the number of equivalents of acetic anhydride up to 6.4 per GPy unit in the reaction resulted in decreased REs. The authors did not report any molecular weight-related data (e.g. viscosity) for the modified products. Mullen and Pascu⁶⁶ also modified different types of gelatinized starches (corn, wheat, rice, potato and tapioca) in pyridine at 115 °C, with 3-3.5 eq. of either acetic, propionic, or butyric anhydride for 1 h. RE values between 86-100% were achieved for the products with DS = 3 as measured by titration. The intrinsic viscosity $[\eta]$ of the products synthesized from potato starch was 32-38 $\frac{\text{dL}}{\text{g}}$ for the acylated derivatives in excess pyridine at 25 °C, which led the authors to conclude that there was a minor decrease in molecular weight for



Scheme 2.1. Reaction of starch with (A) acid halide (X represents a halogen atom), (B) linear anhydride, and (C) alkenyl succinic (cyclic) anhydride. The ester group is drawn at the C2 position of the GPy unit, however the reaction is possible at C2, C3, or C6.

the modified products. The esters prepared from acetic anhydride had the largest decrease, followed by the propionic and butyric anhydrides. Unfortunately, the authors did not report the $[\eta]$ of the unmodified potato starch gelatinized in pyridine for comparison.

The reaction of starch with cyclic anhydrides proceeds in a similar manner to linear anhydrides, but the conjugate acid formed in the reaction is covalently bound to the ester group.

As a result, the reaction between starch and cyclic anhydrides does not produce any small molecule by-products. Gross and coworkers⁶⁷ reported a comprehensive study on the reactivity of alkenyl succinic anhydrides (ASAs) with granular waxy maize starch. Using dodecenyl succinic anhydride (DDSA), individual reaction parameters were optimized. It was found that the concentration of starch in the suspension did not have a large effect on the RE: A maximum RE of 50% was achieved at 45 wt% starch content, while at the highest starch loading of 65 wt% the RE dropped to 40%. The DS was measured by titration. A pH range of 8.5-9.0, maintained by addition of NaOH (as a 2 wt% solution), achieved the highest RE of 64% at 45 wt% starch loading. While the reaction was completed at different temperatures, 23-28 °C was found optimal with a RE of 63-64%. Below 20 °C the RE dropped to less than 40%, which was attributed to the inhibited diffusion of DDSA into the starch granules, while it was hypothesized that at temperatures above 30 °C, RE values below 55% were due to an increased rate of anhydride hydrolysis. The RE was dependent on the DDSA loading, as for reactions under optimal conditions a RE of 80% was achieved at a DDSA loading of 5 wt%, but the RE dropped to 18% at increased DDSA loadings. The duration of the reaction also influenced the RE, reaching 98% after 24 or 48 h but dropping to 33% after 72 h, presumably due to ester hydrolysis. Finally, using ASAs with alkyl groups containing either 8 (octenyl succinic anhydride, OSA), 12 (DDSA), 16 (hexadecenyl succinic anhydride), or 18 (octadecenyl succinic anhydride, ODSA) carbons atoms, the RE decreased from 78% for OSA to 30% for ODSA under the optimal conditions stated above. The authors did not report any molecular weight or size data for the

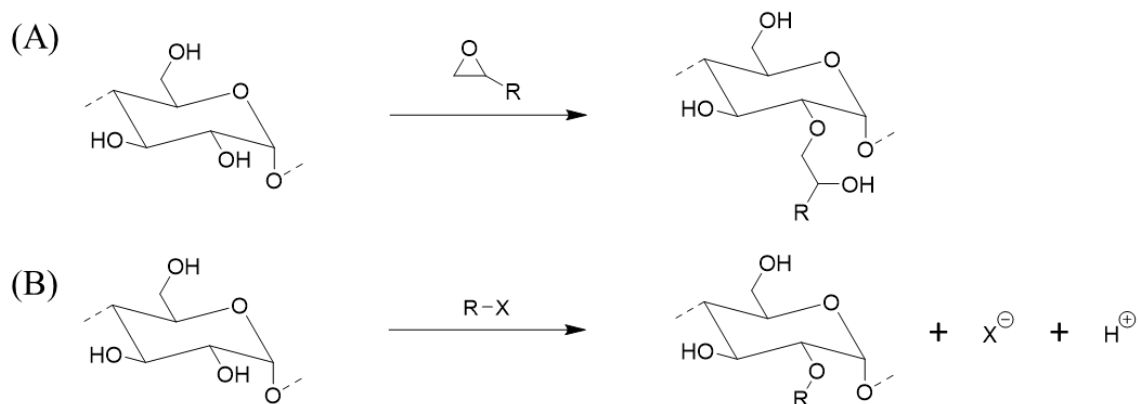
modified products. Miao and coworkers⁶⁸ compared the reactivity of OSA with granular waxy maize starch and gelatinized sugary-1 maize starch. Starch modified with up to 3 wt% OSA is approved by the Food and Drug administration (FDA) for consumption.⁴⁸ It was found that gelatinized starch had a higher RE than granular starch for all OSA loadings tested between 0.5-3.0 wt% (at 0.5 wt% intervals), when using 30 wt% starch in water and maintaining a pH of 8.5 through the addition of NaOH (0.3 wt% solution) and 35 °C for 8 h. The DS of the products was determined by titration. GPC analysis of the OSA starch products revealed that there was no significant change in molecular weight ($2.1\text{-}2.4 \times 10^7$ g/mol) or radius of gyration ($R_g = 36\text{-}40$ nm) for the gelatinized starch reaction products. In comparison, when the granular starch reaction products were gelatinized after the reaction for GPC analysis, the molecular weight decreased from 22×10^7 to 10×10^7 g/mol for increasing OSA loadings, but there was no change in R_g (175 nm).

Reactive extrusion is commonly used to prepare modified starch in large scale continuous processes.¹⁴ Miladinov and Hanna⁶⁹ reported the modification of amylo maize starch with acetic, propionic, heptanoic, and hexadecanoyl (palmitic) anhydrides in a single screw extruder. The optimized conditions were 20 wt% water as plasticizer, 0.01 eq. excess NaOH wrt the anhydride, a maximum barrel temperature of 140 °C, and 140 rpm. There was no significant difference in reactivity among the anhydrides. The highest RE achieved was 85% for a DS of 0.085 using acetic anhydride, while the lowest RE reported was 71% for a DS of 0.071 using hexadecanoyl anhydride. The DS of the modified products was determined by titration. The authors did not

report the molecular weight or size of the products in solution. Wu and coworkers⁷⁰ reported the modification of maize starch with DDSA in a twin screw extruder. The optimized conditions were 30 wt% water, 0.7 eq. NaOH wrt to DDSA, a maximum barrel temperature of 120 °C, and 110 rpm. The highest RE achieved was 78% for a DS of 0.014, as determined by titration. The authors did not report the molecular weight and size of the modified products.

2.3.2 Starch Etherification

Starch ethers have found uses as flocculants, in paper making, and as coatings.⁷¹ Starch ethers are typically prepared by the reaction of a hydroxyl group in starch with either an epoxide (Scheme 2.2(A)) or an alkyl halide (Scheme 2.2(B)).⁷² The reaction of starch with alkenyl oxides proceeds through nucleophilic attack of a starch hydroxyl group on the epoxide ring, resulting in the formation of an ether linkage and a new hydroxyl group.⁵⁰ Similarly to cyclic anhydrides, no small molecule by-products are produced in the substitution reaction.¹⁴ In some cases the alkenyl oxide is formed *in situ*, such as in the reaction of 3-chloro-2-hydroxypropyltrimethyl ammonium chloride (CHPTAC), which is first converted to 2,3-epoxypropyltrimethylammonium chloride (GMAC) in the presence of a base.⁷³ The base thus promotes intramolecular ring closing by nucleophilic substitution of the chloride, which yields an epoxide ring. A halide anion by-product forms, which eventually must be removed through purification. Reactions completed between starch and alkenyl oxides are best characterized in terms of MS, because the newly introduced hydroxyl group can induce polymerization by reacting with another alkenyl oxide molecule.⁵⁰



Scheme 2.2. Reaction of starch with (A) alkenyl oxides and (B) alkyl halides. The ether bond is drawn at the C2 position of GPy unit, however the reaction is also possible at C3 or C6.

Reactions between starch and alkyl halides proceed through nucleophilic substitution of the halide by a starch hydroxyl group. In contrast to epoxides, the reactions with alkyl halides produce halide anions which must be removed by purification, and a proton which must be neutralized to prevent the acid-catalyzed hydrolysis of starch. Starch etherification reactions can be classified into three types of modifications, namely for the production of cationic, anionic, and non-ionic starch ethers.⁷² Amphoteric starch ethers have also been prepared by dual modification with cationic and anionic reagents.⁶ The reagents used to produce cationic starch ethers typically contain a quaternary nitrogen.⁷³ Heinze and coworkers⁵⁸ thus reported the synthesis of cationic starch ethers from granular maize, amylomaize, waxy maize, potato, and wheat starches and CHPTAC or GMAC. The reactions were completed either in an ethanol-water mixture (4:1) with 1.1 eq. NaOH (8.5 wt%) wrt CHPTAC at 60 °C for 6 h, in water with

0.1 eq. NaOH (0.5 wt%) at 60 °C for 6 h, or in DMSO with 0.1 eq. NaOH (0.5 wt%) at 60 °C for 24 h. The reactions with CHPTAC had to be completed in an ethanol-water medium. The highest RE achieved was 46-47% for amylo maize and potato starches, namely the starch samples with the highest amylose contents, while the highest RE for waxy maize starch under the same conditions was only 5%. The MS of the modified products was determined by elemental analysis. For reactions completed in water with GMAC, the highest RE achieved was 76% with an MS of 0.38 using waxy maize starch, which had given the lowest RE in an ethanol-water mixture. There was no difference in RE for high and medium amylose content starches. The highest RE achieved in an organic solvent (DMSO) with GMAC was 57%, again for waxy maize, but for a MS of 0.58. There was no difference in RE between the high and medium amylose content starches. The molecular weight of the modified starch products prepared in water decreased with respect to the starting material, from 7.6×10^7 g/mol for maize starch to 3.5×10^7 g/mol after modification with GMAC to a MS of 1. No molecular weights were reported for the remaining products. Interestingly, the decrease in molecular weight did not appear to be correlated with the MS.

The reagent most commonly used to prepare anionic starch ethers is monochloroacetic acid (MCA) or its sodium salt (SMCA).⁷⁴ The reaction between starch and MCA can be completed in water using NaOH as base for low DS values, but the reaction is typically carried out in a mixture of organic solvent and water for moderate and higher DS.⁷⁵ Hydrolysis of the alkyl halide competes with the etherification reaction, however a small amount of water is

required to swell the starch granules, so the water content must be controlled.⁷⁶ Heinze and coworkers⁷⁷ reported the synthesis of carboxymethyl starch (CMS) by reacting low (<1%, amioca), medium (25%, wheat), and high (70%, Hylon VII) amylose content starch samples with SMCA under heterogeneous reaction conditions. The reactions were completed in 2-propanol at 55 °C for 5 h, using 0.95 eq. of NaOH wrt SMCA (15 wt%). By this method, the high and medium amylose content starches reached a maximum RE of 82.4% and a DS of 1.40, while the low amylose content starch had a maximum RE of 75.9% and a DS of 1.29. The DS of the modified products was measured by ¹H NMR spectroscopy. DMSO was also investigated as a solvent to achieve homogeneous reaction conditions at 80 °C for 2 h, using 2 eq. NaOH wrt SMCA. The modified starch gelatinized *in situ* under these conditions, and the highest RE achieved across all starch sources was 15.1%. The authors did not report any molecular weight or size data for the modified starch products.

Non-ionic starch ethers have been prepared in water to introduce hydrophobic domains, or other functionalities such as terminal alkenes for polymerization.⁵⁷ Pal and coworkers⁷⁵ reported the optimization of the reaction of propylene oxide (PO) with granular maize and waxy amaranth starches at low substitution levels. The optimized conditions involved suspending granular starch and 1.1 eq. NaOH wrt PO in water at 40 °C for 20 h, with slow PO addition while stirring in a sealed reactor. The DS of the modified products was determined spectrophotometrically after converting the hydroxypropyl groups to propionaldehyde, followed by reaction with ninhydrin. A calibration curve, created with propylene glycol in lieu of

hydroxypropyl groups, was used to convert absorbance readings to concentrations. RE values up to 27% for maize starch and 24% for amaranth starch were achieved for MS of 0.025 and 0.022, respectively. The authors did not report the size of the modified starch products in solution. Taylor and coworkers⁷⁵ reported the modification of SNPs with 1,2-butene oxide (BO) at higher substitution levels. The optimized conditions involved dispersing SNPs in water at pH 13.0, adjusted through NaOH (40 wt%) addition, followed by BO addition and heating to 40 °C for 24 h. The MS of the modified products was determined by ¹H NMR analysis. A RE up to 52% was achieved for the product with an MS of 1.29. The authors measured the size of the products in solution by DLS and reported no significant change in D_n for measurements at 15 °C. Rahman and coworkers⁷⁵ reported the modification of granular maize starch with allyl chloride under heterogenous conditions with water and dichloromethane. The latter was used because allyl chloride is not miscible with water. The granular maize starch was gelatinized before the reaction by heating to 100 °C for 1 h, and after cooling to room temperature dichloromethane was added to achieve a 1:2 ratio of dichloromethane to water. Cetyltrimethylammonium bromide (0.1 mol%) was used as a phase transfer catalyst, along with excess pyridine. The allyl chloride was added drop-wise and the reaction was stirred for 24 h before characterization by ¹H NMR and elemental analysis. A RE of 47% was achieved for the product with a DS of 0.32. The authors did not report any molecular weight or size data for the modified starch products.

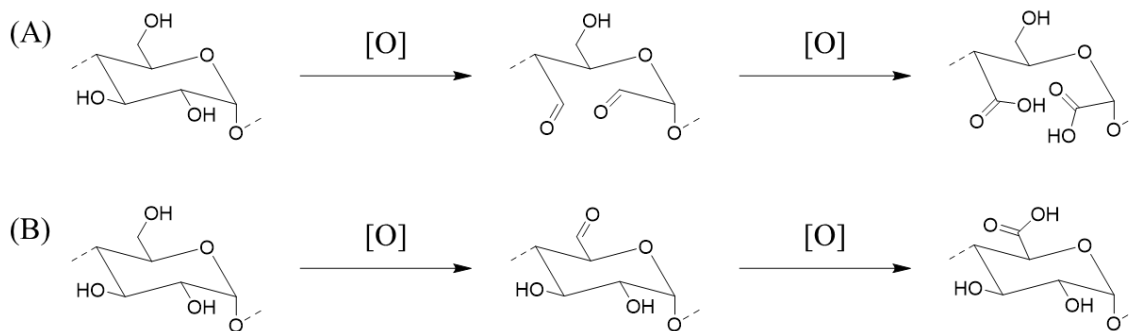
Gimmler and Meuser⁷⁸ modified potato starch in a twin screw extruder with either GMAC or SMCA. The optimized conditions were an MS of 0.03, 21.5 wt% water as plasticizer,

no base, a maximum barrel temperature of 153 °C and a rotation speed of 320 rpm for GMAC, as compared with a DS of 0.3, 22 wt% water as plasticizer, a maximum barrel temperature of 110 °C and a rotation speed of 324 rpm for SMCA, with 1 eq. NaOH wrt SCMA. Under the optimized conditions, the highest REs achieved were 98% and 85% for GMAC and SMCA, respectively. The DS of the modified products was measured by titration. The authors did not report the size of the modified starch products in solution. Bhandari and Hanna⁷⁹ modified maize starch in a twin screw extruder with SMCA. Starch, SMCA, and 1:1 water:ethanol as plasticizer were combined in different ratios in a planetary mixer before being fed into a twin screw extruder, along with 0.74 eq. NaOH wrt SCMA, at a maximum barrel temperature of 85 °C and 70 rpm. Two reaction conditions achieved the highest RE of 42%, using 12.5 wt% aqueous ethanol as plasticizer and either 2.73 or 3.62 eq. of SMCA, corresponding to DS of 1.15 and 1.54, respectively. The DS of the modified starch was measured by titration. The authors did not report the size of the modified products in solution. De Graaf and Janssen⁵¹ reported the modification of potato starch with PO in a twin screw extruder. The optimized conditions were 40 wt% water as plasticizer, 0.4 eq. NaOH wrt PO as base, a maximum barrel temperature of 110 °C, and 215 rpm. The highest RE achieved was approximately 95%, corresponding to a measured MS of 0.25. The reported DS was determined by quantifying the amount of free propylene glycol (hydrolysis product of PO) in the sample by gas chromatography. The authors did not measure the size of the modified starch products in solution.

2.3.3 Starch Oxidation

Oxidized starch has found applications in food as well as paper, textiles, and building materials.⁸⁰ It is produced by the reaction of starch with an oxidizing agent.¹⁴ Depending on the oxidizing agent used, the secondary hydroxyl groups at C2 or C3 (Scheme 2.3(A)), as well as the primary hydroxyl at C6 (Scheme 2.3(B)) can be oxidized to aldehydes or carboxylic acids.⁸¹ Oxidation at C2 or C3 results in opening of the GPy ring.⁵⁹ The oxidation procedure often leads to degradation of the starch granules, resulting in low viscosity products.⁷² Common oxidizing agents for starch include NaOCl, KMnO₄, K₂S₂O₈ or H₂O₂, but NaOCl is used to produce oxidized starch on an industrial scale.⁵⁹ Kuakpetoon and Wang⁸⁰ investigated the oxidation of granular maize, rice, and potato starches with NaOCl. Starch was dispersed in water adjusted to pH 9.5 with NaOH (8 wt%) before drop-wise addition of either 0.8 or 2.0 wt% NaOCl wrt starch. The pH was maintained at 9.5 by addition of H₂SO₄ (2 M) during the NaOCl addition, and by addition of NaOH (8 wt%) afterwards, and the reaction was allowed to stir for a total of 50 min. The DS of the modified products was measured by titration. The oxidation of potato starch was most efficient at both weight loadings, followed by rice and then maize starch. Oxidized starch underwent significant degradation, as an increase in elution volume in GPC analysis was observed. Not surprisingly, there was a greater increase in elution volume for the 2.0 wt% modified samples compared to the 0.8 wt% modified samples for each starch type, but the authors did not provide the corresponding average molecular weights for their products. A drawback of using NaOCl to oxidize starch is the production of chlorine by-products, which are

harmful to the environment.⁷² To avoid using NaOCl, Wang and coworkers⁸⁰ reported the oxidation of maize, pea, and sweet potato starch with H₂O₂ and a catalytic amount of CuSO₄. Starch was gelatinized by dispersing the starch in water and heating to 80 °C for 0.5 h. The optimized reaction conditions were a temperature of 55 °C, a duration of 11 h, and a CuSO₄ concentration of 0.5 mol% wrt GPy units. The highest RE achieved was 39% while using 0.5 eq. of H₂O₂. The [η] of the modified products decreased from 37 to 18 $\frac{\text{dL}}{\text{g}}$ as the DS increased from 0.19 to 0.55. The authors did not report further information on the size of the products in solution. Kim and coworkers⁸¹ reported the oxidation of granular maize starch with a catalytic amount of 2,2,6,6-tetramethyl-1-piperidine-1-oxyl radical (TEMPO) and NaOCl to oxidize selectively the primary hydroxyl group on C6. Starch was suspended at 35 °C in water at pH 8.5, and 0.01 eq. of TEMPO was added to the reaction, followed by slow addition of 2.2 eq. of NaOCl. The pH of the reaction was maintained at 8.5, initially by addition of HCl (4.0 M), followed by NaOH (2 wt%). The reaction was quenched with ethanol after 1 eq. of NaOH was consumed at pH 8.5. The DS of the products was measured by titration, while selectivity of the oxidation was confirmed by ¹³C NMR. The maximum RE achieved was 96%, corresponding to a DS of 0.96. The authors did not report the size of the oxidized starch products in solution.



Scheme 2. 3. Oxidation of (A) secondary and (B) primary hydroxyls of starch.

Wing and Willet⁸² reported the oxidation of waxy maize, maize, and amylo maize starch in a twin screw extruder using H_2O_2 , FeSO_4 , and CuSO_4 as catalyst. The optimized conditions were 40 wt% water as plasticizer, a maximum barrel temperature of 110 °C, and 110 rpm at reagent concentrations of 7.4, 0.08, and 0.05 wt% H_2O_2 , Fe^{2+} , and Cu^{2+} , respectively. The authors did not report the DS of the oxidized starches. The modified waxy maize starch products underwent significant degradation, as the viscosity of a 5 wt% solution in water decreased from 4.0 Pa·s for waxy maize starch extruded without peroxide, to 1.2 for the product modified with the highest H_2O_2 content. The authors did not report the viscosity of the regular maize used nor the amylo maize products.

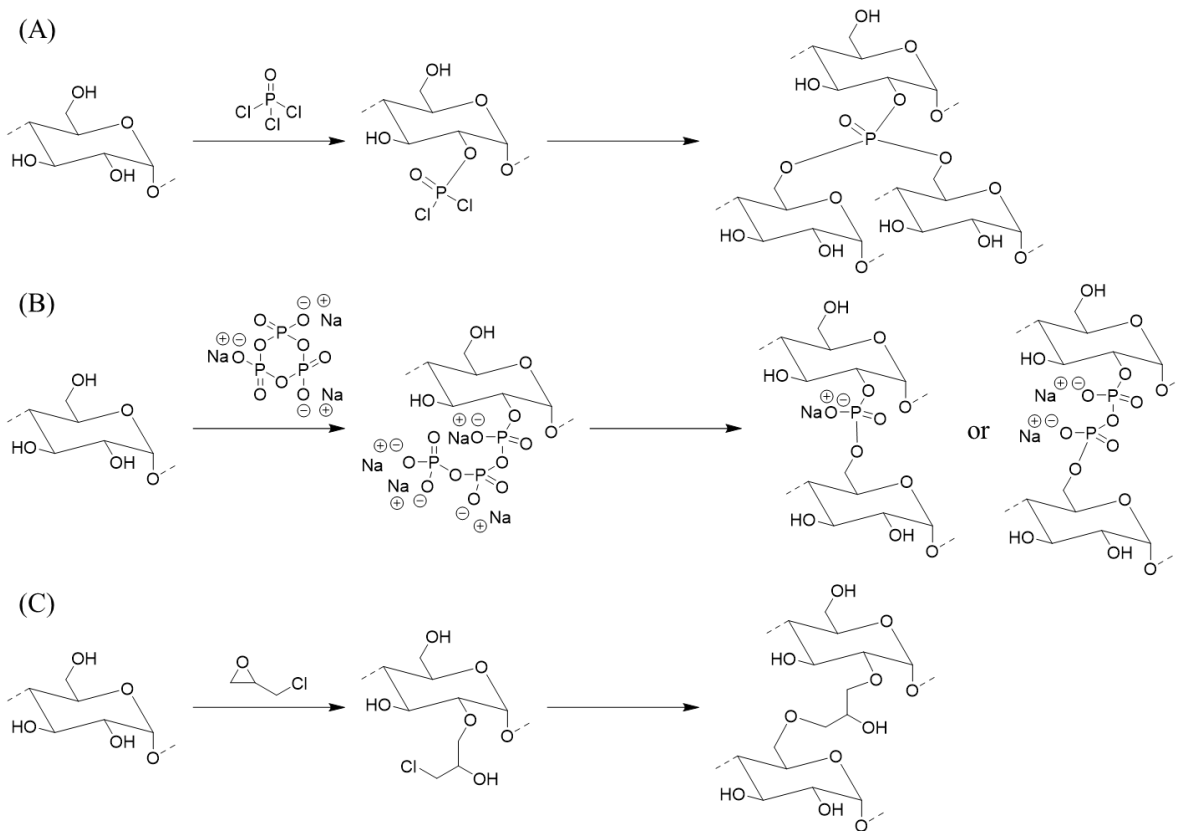
2.3.4 Reaction of Starch with Cross-linking Agents

The cross-linking of granular starch is typically completed to decrease the viscosity and swelling of starch in solution, while also increasing the gelatinization temperature, shear

stability, and freeze-thaw stability for food applications.⁷¹ Hirsch and Kokini⁸³ studied the cross-linking of granular waxy maize starch with phosphorous oxychloride (POCl_3), sodium trimetaphosphate (STMP), and epichlorohydrin (EPI). The formation of phosphoesters between the hydroxyl groups in starch and POCl_3 proceeds in a manner similar to the reaction with acid halides, discussed in Section 2.3.1, except that POCl_3 can react with up to three hydroxyl groups to form a phosphotriester (Scheme 2.4(A)) while acid halides can only react with one hydroxyl group. As a result, the reaction with one eq. of POCl_3 produces 3 eq. of HCl. The formation of phosphodiester between STMP and the hydroxyl groups of starch (Scheme 2.4(B)) proceeds in a manner similar to the reactions with cyclic anhydrides, by nucleophilic attack of a starch hydroxyl moiety at one of the phosphate groups. The cyclic structure of the triphosphate reagent is lost after reaction of the first hydroxyl group producing starch tripolyphosphate. Cross-linking occurs by reaction of a second hydroxyl on a different GPy unit with the polyphosphate group. Either mono- or diphosphoric acids are produced as byproducts. The reaction between starch and EPI can proceed by etherification, as discussed in Section 2.3.2, through either the epoxide or the chloride functionality (Scheme 2.4(C)). If the epoxide reacts first, the resulting secondary hydroxyl from EPI can undergo intramolecular ring closing forming a new epoxide functional group. A hydroxyl group on another GPy unit may then react with the newly formed epoxide. If nucleophilic substitution of the chloride occurs first, the epoxide remains intact and is able to react with a hydroxyl group on a second GPy unit. HCl is produced regardless of which functional group reacts first. The EPI reactions were completed by dispersing starch (40 wt%)

in water with 0.5 wt% NaCl with respect to starch, and NaOH for a final pH of 12. For reactions with STMP, 0.1 wt% CaCl₂ was added to minimize granule swelling, and NaOH for a final pH of 12. The reactions with POCl₃ were stirred for 35 min at 25 °C, while reactions with STMP were stirred for 5 h at 30 °C, and NaOH was added for a final pH of 12. The EPI reactions were completed in a heated tumbler with continuous end-over-end agitation for 17 h at 40 °C, and the concentration of cross-linker was varied from 0.005-0.02 wt%. The low levels of cross-linker used did not result in a drop in pH, and the authors were also unable to determine DS (and RE) under these conditions. They nevertheless concluded that increasing the cross-linker content decreased the water swellability of the products and the viscosity in water at 5.5 wt%. The size of the modified starch products in solution was not reported.

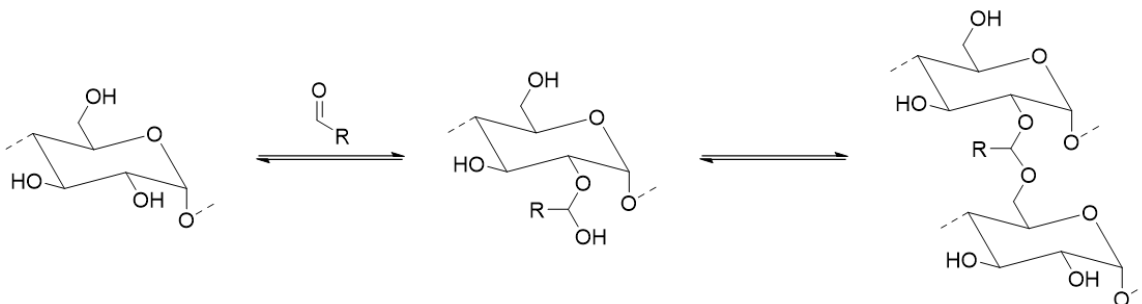
Deng and coworkers⁴³ reported a detailed mechanistic study of the cross-linking of starch with a model cross-linker, glyoxal (C₂H₂O₂), in a twin screw extruder. Aldehydes form reversible hemiacetals with hydroxyl groups, and hemiacetals can react further to form acetals (Scheme 2.5). Each aldehyde is capable of reacting with two hydroxyl groups so glyoxal, as a dialdehyde, is capable of forming reversible acetal linkages with up to four GPy units.⁸⁴ The



Scheme 2.4. Modification of starch with (A) POCl_3 , (B) STMP, and (C) EPI. For simplicity, modification is shown at the C2 position of the first GPy unit, and at the C6 position of the subsequent GPy units, however the reaction is possible at either C2, C3, or C6 for each GPy unit.

authors observed a decrease in size of the starch products as the recorded torque increased in the extruder, which is consistent with previous findings of Gilbert and coworkers.³⁶ To measure the

effect of increasing the cross-linker content, the operating conditions were set at 22 wt% water and 23 wt% glycerol as plasticizers, a barrel temperature of 90 °C, and 300 rpm. Interestingly, upon addition of cross-linker the torque and temperature increased, even though the D_h of the resulting products decreased from 550 nm without cross-linker to 225 nm for 3 wt% cross-linker. While an increase in temperature typically reduces the torque, this effect was not observed when the cross-linker was added. The authors concluded that in a high shear environment, the introduction of a starch cross-linker led to the formation of a cross-linked starch network. The formation of a network resulted in an increase in torque, which led to a rise in temperature. The increased temperature further softened the starch, making it more susceptible to chain scission, while the higher torque led to further shear-induced chain scission, which ultimately resulted in starch derivatives with a lower D_h .



Scheme 2.5. Reaction of starch with an aldehyde forming hemiacetal and acetal functionalities.

The modification is drawn at the C2 position of the first GPy unit and the C6 position of the second GPy unit for simplicity, however the reaction is possible at either C2, C3, or C6 for each GPy unit.

2.4 Vegetable Oils

2.4.1 Vegetable Oil Structure

Vegetable oils are renewable, biodegradable, readily available and cost-effective.⁸⁵ They are produced by plants and are extracted from plant seeds.⁸⁶ Unlike starch, vegetable oils are very hydrophobic and typically liquid at room temperature.⁸⁷ Vegetable oils are composed of triglyceride molecules (TGs, Figure 2.5) which contain a glyceryl backbone forming three ester bonds with various fatty acids (FAs).⁸⁸ The composition of the FAs changes among the different plant species (Table 2.2).⁸⁹ The FAs differ in terms of length and unsaturation level. Saturated FAs, as the name suggests, do not contain any carbon-carbon double bonds and are most commonly palmitic and stearic acids.⁹⁰ Unsaturated FAs contain at least one carbon-carbon double bond and are most commonly oleic and linoleic acids, containing 18 carbons with one and two double bonds, respectively.⁹¹ Some less common FAs, such as ricinoleic acid, also contain other functional groups.⁹²

The physical and chemical properties of vegetable oils depend on their FA composition.⁸⁶ The oils are commonly grouped into one of three categories based on their degree of unsaturation, using the iodine number to quantify the degree of unsaturation.⁹⁴ The iodine number is the amount of iodine (in mg) that reacts with 100 g of oil, ultimately forming diiodoalkane moieties from the carbon-carbon double bonds.⁹⁵ Non-drying oils do not harden

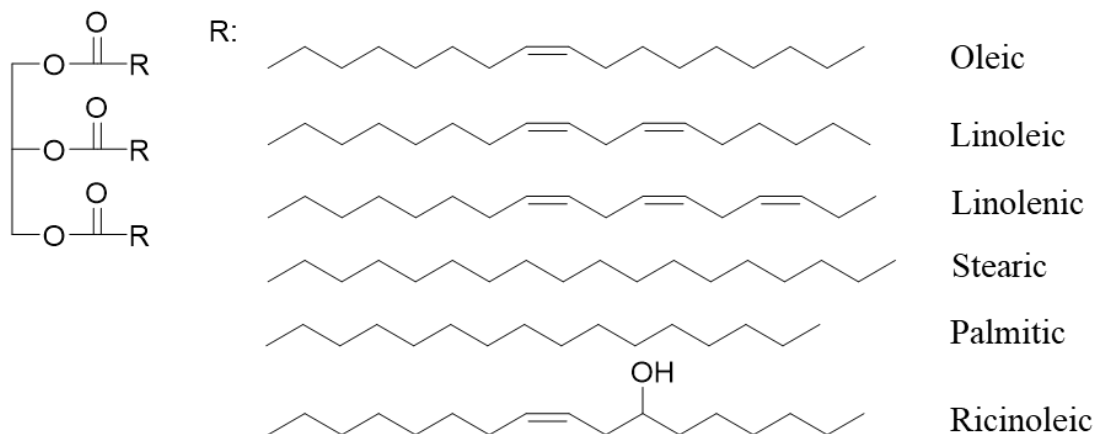


Figure 2.5. Chemical structure of a TG and commonly found FAs.

Table 2.2. FA composition of common vegetable oils.

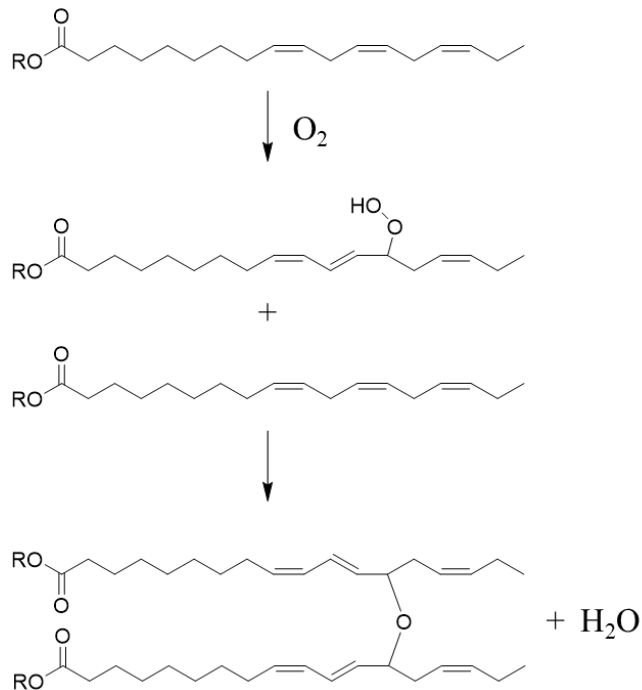
Oil	Palmitic	Stearic	Oleic	Linoleic	Linolenic	Ricinoleic
Palm ⁸⁷	42.8	4.2	40.5	10.1	2.4	0
Soybean ⁸⁹	10.1	4.3	22.3	53.7	8.1	0
Canola ⁹³	4.1	1.9	56.1	21.0	7.9	0
Sunflower ⁸⁹	5.2	3.7	33.7	56.5	0	0
Olive ⁹⁰	13.7	2.5	71.1	10.0	0.6	0
Corn ⁸⁹	11.6	2.5	38.7	44.7	1.4	0
Castor ⁹²	1	2	1	4	1	87

when exposed to oxygen in the air, and have a low degree of unsaturation corresponding to an iodine number of less than 125. Drying oils, on the other, form a hard solid layer when exposed to oxygen in the air, and have a high degree of unsaturation with an iodine number above 140.⁹⁶

Semi-drying oils partially harden when exposed to oxygen in the air, and have a moderate degree of unsaturation with an iodine number between 125 and 140.⁹⁴

2.4.2 Chemical Modification of Vegetable Oils

The chemical modification of vegetable oils generally focuses on the carbon-carbon double bonds in FAs, as opposed to the ester groups.⁸⁶ Drying oils have found uses as coatings because oxygen in the air spontaneously reacts with the unsaturation sites (Scheme 2.6), in a process referred to as auto-oxidation or curing.⁹¹ Oxidation begins with oxygen (O_2) adding to a carbon-carbon double bond, which results in the migration of the double bond by one carbon.⁹⁷ The hydroperoxide formed reacts with a double bond on a different FA.⁸⁷ If the FAs are on different TGs, a cross-linked network results and water is produced as a by-product.⁹⁷ The hydroperoxide can also decompose into an alkoxy radical which can initiate the polymerization of carbon-carbon double bonds on other FAs.⁹⁶ The oxidation process can be accelerated by the addition of catalysts known as driers.⁹⁵ Depending on the activity of the added drier it is classified into one of three categories, namely primary, secondary, or auxiliary.⁹⁵ Primary driers, including for example Co^{2+} , Mn^{2+} and Fe^{3+} , reduce the activation energy for hydroperoxide decomposition.⁹⁶ Secondary driers, including Pb^{2+} , Zr^{4+} and Al^{3+} , act during the polymerization step.⁹⁵ Finally, auxiliary driers, including Ca^{2+} , Li^+ , and Zn^{2+} , among others, modify the activity of primary driers.⁹⁶

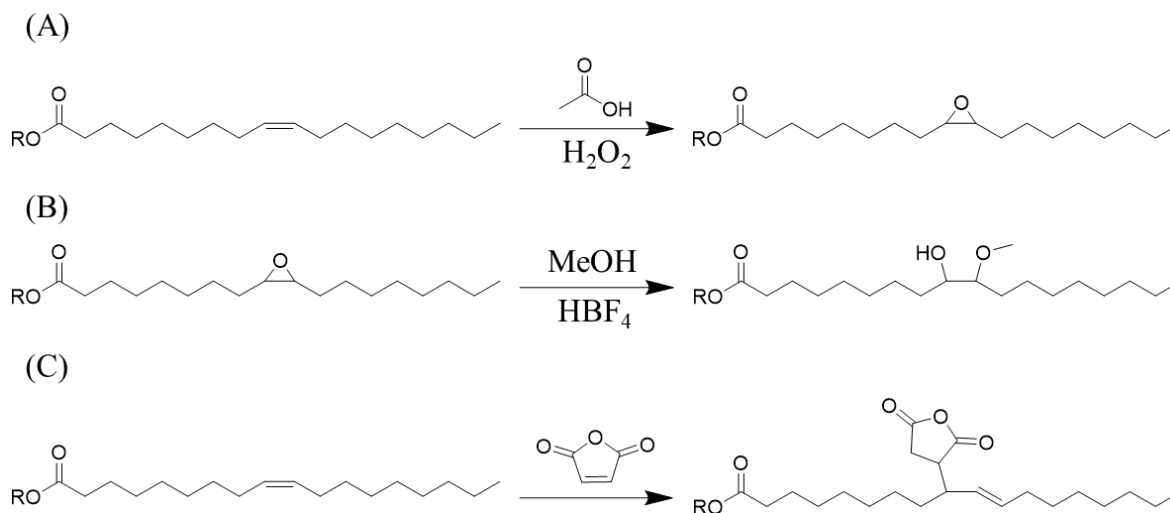


Scheme 2.6. Oxidation of linolenic acid residue resulting in a cross-link between fatty acids.

For industrial applications, vegetable oils have been modified to replace petroleum-based materials.⁸⁵ For example, the introduction of hydroxyl groups yields polyols for the production of polyurethanes (PU).⁸⁶ Different vegetable oils have been converted to epoxides by targeting the carbon-carbon double bonds in the FAs, followed by a ring-opening reaction with an alcohol.⁸⁵ Petrović and coworkers⁹⁵ used this reaction path for canola, corn, linseed, soybean, and sunflower oils. Epoxidation was completed by treating the individual oils with 0.5 eq. of glacial acetic acid and 1.5 eq. of H₂O₂ wrt the carbon-carbon double bonds for 12 h at 80 °C, using toluene as solvent (Scheme 2.7(A)). Acetic acid is converted into peracetic acid by reaction

with H_2O_2 *in situ*, and the peracid reacts through a concerted mechanism in a Prilezhaev reaction with the carbon-carbon double bonds in the FA, forming an epoxide functional group and reforming acetic acid.⁹⁸ Excess H_2O_2 is required to ensure a high RE, while less than 1 eq. of acetic acid is required because it is recycled. The RE of all the epoxidation reactions was between 91-94%. Ring opening (Scheme 2.7(B)) was completed by boiling the epoxidized oils in methanol with tetrafluoroboric acid (HBF_4). The RE was lowest for sunflower oil (75.5%), with an average of 3.47 hydroxyls per TG, and highest for canola oil (83.7%), with an average of 3.3 hydroxyls per TG. Interestingly, linseed oil had a RE of 82.7%, with an average of 5.2 hydroxyls per TG, indicating that the average number of hydroxyls per TG was not the primary factor determining the RE. The resulting vegetable oil polyols were able to form PUs upon reaction with 4,4-diphenylmethane diisocyanate (MDI).

Rosenau and coworkers⁹⁹ reported the maleation of canola, linseed, soybean, and high oleic acid sunflower oil with maleic anhydride (MA, Scheme 2.7(B)). The reaction proceeds through an “ene” (also called Alder-ene) reaction, resulting in a new carbon-carbon single bond between the anhydride ring and the FA. This involves an allylic proton transfer from the FA to the anhydride ring, as well as a shift of the double bond by one carbon.⁹⁴ There are no by-products from the reaction. The optimized reaction conditions consisted in heating the selected oil to 180-220 °C before the addition of MA and stirring under inert atmosphere for 6-8 h. Excess MA was then distilled off under reduced pressure at a temperature of 120-140 °C. Using canola



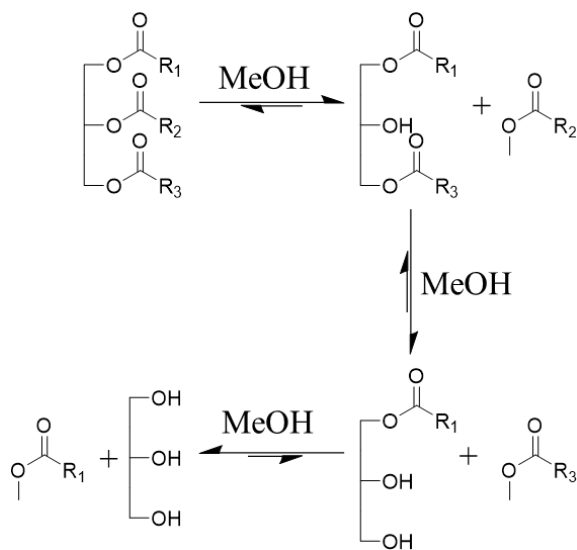
Scheme 2.7. Reaction of (A) oleic acid residue with acetic acid and H_2O_2 , (B) epoxidized oleic acid residue with methanol and HBF_4 , and (C) oleic acid residue with MA. The reaction with methanol is shown at C10 of the FA residue for simplicity, but reaction at C9 is also possible.

oil, a RE of 60% was achieved with respect to MA, for an average of 1.2 MA units incorporated per TG (MA/TG). For linseed oil a RE of 66.7% was achieved for 2.0 MA/TG, for soybean oil a RE of 50% was achieved for both 0.5 and 1.0 MA/TG, and for high oleic acid sunflower oil a RE of 40% was achieved for 1.2 MA/TG.

In the context of vegetable oils, transesterification is the reaction between an alcohol and the glyceryl backbone esters.⁸⁵ A base, acid, or enzyme is commonly used as catalyst for the reaction.¹⁰⁰ Common base catalysts include NaOH, KOH, carbonates and alkoxides, while acid catalysts include sulfuric, sulfonic and hydrochloric acids.¹⁰¹ Lipases have also been used as

catalysts.¹⁰⁰ FA esters of vegetable oil have been investigated as alternatives to diesel fuels.¹⁰⁰ Methanol is the most common alcohol because of its low cost. Polar catalysts are more soluble in it than in longer alkyl chain alcohols, and it reacts with the ester group faster than other alcohols.¹⁰² Since there are three ester groups per TG molecule, 3 eq. of alcohol are required for complete transesterification and a glycerol molecule is formed for each TG that has undergone complete transesterification.⁸⁵ Wang and coworkers¹⁰³ reported the transesterification of soybean oil with methanol using solid CaO and trace amounts of water (less than 2.8 wt%) as catalysts. Solid CaO acts as a base to promote the nucleophilic attack of the TG ester by methanol (Scheme 2.8). Upon reformation of the carbonyl a diglyceride is formed, along with one FA methyl ester (FAME). The reaction is reversible, so an excess of methanol favors the formation of FAMEs. Diglycerides react to give monoglycerides and a FAME, while monoglycerides react to give glycerol and a FAME. The optimal reaction conditions were a 12:1 mole ratio of methanol to soybean oil, 8 wt% CaO, 2.03 wt% water, and heating to 65 °C for 3 h. After that time, heat was removed and excess methanol was removed under reduced pressure. The product was then centrifuged, which produced 3 distinct layers: a top FAME layer, a middle glycerol layer, and a bottom layer consisting in a mixture of CaO and glycerol. More than 99.9% of the glycerol was removed by centrifugation. One advantage of using CaO was its recovery with a simple water rinse, to be used in subsequent reactions. The recovery yield of the reaction was 97%. Water was not required but increased the reaction rate. If the water content exceeded 2.83

wt% hydrolysis of the TG occurred, resulting in the formation of free FAs. Since free FAs act as surfactants in the separation step, their formation needs to be minimized in the reaction.



Scheme 2.8. Transesterification of a triglyceride with three moles of methanol. The reaction is shown to occur at the second position initially, but it can take place at either position.

2.5 Conclusions

In this chapter the complex structure of starch and its chemical modification, as well as the structure and the chemical modification of vegetable oils were surveyed. While starch and vegetable oils have long been part of the human diet, the chemical modification of these feedstocks offers alternatives to petroleum-based materials. Modified starches have already found industrial uses as adhesives, coatings, in mulches, cosmetics, surfactants, and flocculants.²² An understanding of the underlying chemistry is essential to develop naturally

sourced products which can meet or exceed the performance, durability, and cost of petroleum-based materials.⁴ The main goal of the research described in this Thesis was primarily the hydrophobic modification of SNPs or waxy maize starch, as well as the synthesis of new hydrophobic starch modifiers derived from vegetable oils.

Chapter 3

Hydrophobic Modification of Starch Nanoparticles

3.1 Abstract

Hydrophobically modified starch has been used in a wide range of applications for decades. Interest in new hydrophobic biodegradable materials is growing to minimize dependence on petroleum products and negative environmental impacts. While starch nanoparticles (SNPs) are intrinsically hydrophilic, their hydrophilic-lipophilic balance can be tuned through esterification with hydrophobic compounds. One significant challenge in starch modification is maintaining the integrity of the starch backbone, due to hydrolytic degradation in relation to changes in pH or temperature. The synthesis of SNPs hydrophobically modified with alkyl carboxylic acid anhydrides (HM-SNPs) was investigated using SNPs of two different sizes in DMSO as solvent with pyridine and 4-dimethylaminopyridine (DMAP) as catalyst at room temperature. The degree of substitution (DS) was controlled to ensure that the synthesized HM-SNPs remained water-dispersible. ^1H NMR analysis confirmed the full conversion of the anhydrides in the reactions. Analysis of the HM-SNPs on a multi-detector gel permeation chromatography (GPC) system revealed no substantial changes in molecular weight nor hydrodynamic diameter (D_h). These new hydrophobically modified products may be interesting for applications as drug delivery vehicles, thickeners, stabilizers, compatibilizers, or food ingredients.

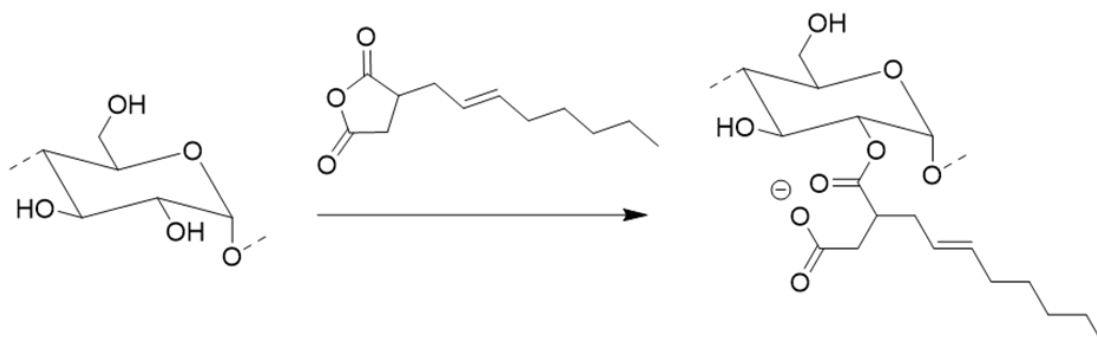
3.2 Introduction

Petroleum-based products are generally considered advantageous due to their widespread availability, low cost, and properties tailorable to a multitude of applications.^{1,2} Unfortunately, most petrochemical products ultimately accumulate in landfills or the environment, and continue to complicate waste disposal and to contaminate different ecosystems.³ To address these issues, there is great impetus to use renewable biopolymers as readily available and cost-effective materials.⁴ Biopolymers such as cellulose⁵ or starch⁶ can be modified physically, chemically, or through a combination of both, to achieve mechanical performance equivalent to petrochemicals.

Starch, the second most abundant biopolymer, is produced by plants mainly for energy storage. Starch is primarily composed of two polysaccharides, amylose and amylopectin.⁷ Amylose is a predominantly linear polymer in which glucopyranose (GPy) units are connected through α -1,4 linkages, while amylopectin also includes branching points introduced through α -1,6 linkages.⁸ Amylopectin is a much larger molecule than amylose, as it can contain more than 100,000 GPy units. The relative amounts of amylose and amylopectin vary with the plant species; corn (maize) starch typically contains 28% amylose, potato starch 21%, and tapioca 17%.⁹ Some plant strains are enriched in either amylose or amylopectin, such as amylo maize containing > 50% amylose or waxy maize starch containing < 1% amylose.¹⁰

Starch is a hydrophilic polymer that can form brittle films. To overcome this obstacle, researchers have modified starch with different reagents. The hydroxyl groups on the GPy residues are most commonly targeted, albeit other chemical modifications are also possible.¹¹

The use of octenyl succinic anhydride (OSA) for the hydrophobic modification of starch (Scheme 3.1) has been extensively studied.^{12,13} The reaction with OSA introduces a hydrophobic moiety without producing any small molecule by-products. The resulting material has found uses as emulsifier in dressings, sauces, and baby food, with hydrophobicity of the products increasing directly with the DS.¹⁴ Presently, OSA-modified starch is approved for use in food applications at contents of up to 3 wt%.¹⁵ Besides alkenylsuccinic anhydrides (ASAs), starch has been modified with epoxides, alkyl halides, and graft polymers to name but a few examples.¹²



Scheme 3.1. Reaction of starch with OSA. The ester is shown at C2 for simplicity, but the reaction can occur with a hydroxyl group at either C2, C3 or C6 on the GPy units.

The reaction of starch with ASAs introduces two new functional groups onto starch: a hydrophobic alkyl tail and a hydrophilic carboxylate group. The presence of the hydrophilic carboxylate functionality on each alkyl tail disfavors the formation of large hydrophobic domains.¹⁶ Due to this dual contribution, ASAs are not ideal as modifiers to study the influence

of the hydrophobic microdomains on the starch properties. Starch esters derived from linear acid chlorides or anhydrides would be more suitable for that purpose.

The synthesis of starch esters has a long history, as Mullen and Pacsu¹⁷ reported the synthesis of acetyl (C2), propyl (C3), and butyl (C4) starch esters more than 75 years ago. They found that the molar mass of alkyl acid anhydrides affected their reactivity towards starch, smaller anhydrides reacting faster than larger anhydrides. They also highlighted the need to ensure that the starch derivatives did not degrade during the reactions. While multi-detector GPC analysis equipment was unavailable at that time, they measured the intrinsic viscosity of their products to monitor degradation during the reactions. Starch esters are typically prepared simply by heating the anhydride (or acid chloride) and starch without a base,¹ or else in the presence of a base such as pyridine,¹⁸ 4-dimethylaminopyridine (DMAP),¹⁹ or NaOH.²⁰

The current study is concerned with the synthesis and characterization of hydrophobically modified starch nanoparticles (HM-SNPs). The samples were obtained by reacting either hexanoic or propionic anhydride with the SNPs, to generate C6- and C3-SNPs with degrees of substitution (DS) ranging from 0 up to 0.15 or 0.30, respectively, so as to maintain good water dispersibility. These materials will be further investigated to measure the effects of the hydrophobic modification on their solution properties. The materials synthesized have potential applications as drug delivery carriers, associative thickeners, colloidal stabilizers, compatibilizers and food ingredients, to name but a few possibilities.²¹

3.3 Experimental Section

3.3.1 Materials

Organic solvents including dimethyl sulfoxide (DMSO, ACS reagent, $\geq 99.9\%$), deuterated DMSO (99.9 % atom), acetone (HPLC, $\geq 99.9\%$), and trifluoroacetic acid (Reagent plus, 99 %) were purchased from Sigma Aldrich. EcoSynthetix (Burlington, ON) supplied two research grade SNP samples, namely SNP-1 and SNP-2, with weight-average hydrodynamic diameters (D_h) of 54 and 14.2 nm, respectively, as determined by GPC measurements in DMSO with 0.05 M LiBr at 50 °C. Dialysis tubing with 1 kDa and 12-14 kDa molecular weight cut-off (MWCO) was purchased from Spectrum Laboratories Inc. (Shewsbury, MA). Before chemical modification was carried out, the SNP-2 sample was dialyzed against water to remove chemical residues left from their preparation. Aqueous SNP dispersions were prepared by adding the dry SNP to Milli-Q water at a 20 g/L concentration and shaking the mixture in an Innova 4000 incubator shaker (New Brunswick Scientific, Edison, NJ) at 60 °C for 16 h. The homogenous dispersions were removed from the shaker and allowed to cool to room temperature before dialysis in 1 kDa MWCO membranes immersed in Milli-Q water for 5 days. The Milli-Q water was replaced every day. After 5 days, the SNP dispersions were transferred to vials and lyophilized for 3 days. The white powders obtained were stored in clear vials. All the chemicals were used as received from the suppliers unless indicated otherwise.

3.3.2 Synthesis of Water-dispersible HM-SNPs

The research grade SNP-1 and SNP-2 particles were modified with hexanoic or propionic anhydride to yield CN(x)-SNP-Y particles, where N represents the number of carbons for the propionic (3) or hexanoic (6) ester modifications, x is the degree of substitution (DS) achieved, and Y equals 1 or 2 for SNP-1 or SNP-2, respectively. The preparation of sample C6(0.1)-SNP-1 is described in detail hereafter as an example. SNP-1 (1.25 g, 7.7 mmol glucopyranose units) was stirred for 6 h in 20 mL of DMSO at room temperature until a clear homogenous dispersion was obtained. DMAP (0.0071 g, 0.058 mmol) and pyridine (1 mL, 12 mmol) were added to the dispersion before hexanoic anhydride (0.166 g, 0.77 mmol). The amounts of hexanoic or propionic anhydride, DMAP and pyridine were varied to control the DS. The dispersion was stirred overnight and precipitated in acetone. The solid product, recovered by suction filtration, was purified further by Soxhlet extraction with acetone for 2 days, to remove residual DMAP and pyridine. The collected solid was dried in a vacuum oven at 80 °C and characterized by ¹H NMR (300 MHz, DMSO) and GPC analysis.

3.3.3 Synthesis of High DS HM-SNPs

Research grade SNP-1 particles were modified with hexanoic or propionic anhydride. The preparation of sample C6(1)-SNP-1 is described in detail hereafter as an example. Research grade SNP-1 (4.0 g, 24.8 mmol GPy units) was stirred for 6 h in 32 g of DMSO at room temperature to obtain a clear homogenous dispersion. DMAP (0.138 g, 1.1 mmol) and pyridine

(9.0 mL, 112 mmol) were added to the dispersion before hexanoic anhydride (5.31 g, 24.8 mmol). The amounts of hexanoic anhydride, DMAP, and pyridine were varied to control the DS. The dispersion was stirred overnight. The product was purified by dialysis against ethanol for 24 h, followed by dialysis against water for 48 h. The dialysate was changed twice daily to remove DMSO, by-products, DMAP and pyridine. The collected solid was dried in a vacuum oven at 80 °C and characterized by ¹H NMR spectroscopy (300 MHz, DMSO). The moisture content was measured on a CEM Smart 5 microwave moisture analyzer using the manufacturer-installed program before GPC analysis.

3.3.4 ¹H NMR Analysis

The DS was determined by the procedure of Gilbert and co-workers.²² ¹H nuclear magnetic resonance (NMR) spectroscopy analysis was performed on a Bruker 300 MHz spectrometer. The concentration of all the samples was 15–30 mg/mL in dimethyl sulfoxide-d₆ with 6 drops of trifluoroacetic acid (TFA). The chemical shifts reported are relative to the residual solvent proton signal at 2.50 ppm.

3.3.5 Gel Permeation Chromatography (GPC) Analysis

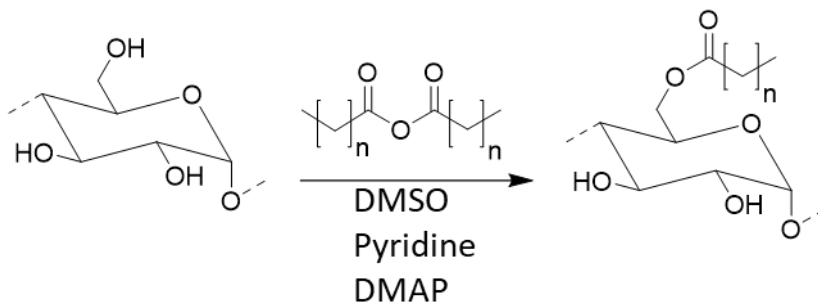
Analytical gel permeation chromatography (GPC) measurements for the starch samples were performed before and after modification on a Malvern GPCmax instrument equipped with a TDA 305 triple detector array, one guard column and one 300 mm × 8.0 mm I.D. PolyAnalytik SuperesTM column having a theoretical linear PS molar mass range of up to 200 MDa. A flow

rate of 0.6 mL/min was used with 0.05 M LiBr in DMSO as the mobile phase at 50 °C. Samples were prepared at a concentration of 2 mg/mL in 0.05 M LiBr in DMSO and filtered through a 0.2 µm nylon filter.

3.4 Results and Discussion

3.4.1 Preparation of Starch Esters

The esterification of the SNPs (Scheme 3.1) was completed in DMSO as a polar aprotic solvent to disperse the starch. The viscous SNP dispersions were clear for the SNP-1 reactions and had a light brown colour for SNP-2. Excess pyridine and a catalytic amount of DMAP (5 mol% with respect to the anhydride) were added before the anhydride. Under these conditions, DMAP reacts with the anhydride to produce conjugate carboxylate- and acyl-DMAP ions. A hydroxyl group from starch (either the primary hydroxyl at C6 or one of the secondary hydroxyls at C2 or C3) then reacts with the acyl-DMAP conjugate. Simultaneously, DMAP deprotonates the hydroxyl group acting as nucleophile. When the starch ester is formed, DMAP is regenerated and is free to react with another anhydride. The reaction should proceed until all the anhydride is consumed. After 24 h the reaction product was precipitated in acetone and further purified by Soxhlet extraction for 48 h, to ensure the complete removal of pyridine and DMAP.



Scheme 3.2. Reaction of starch with an alkyl carboxylic acid anhydride. For hexanoic anhydride $n = 4$ and for propionic anhydride $n = 1$. The ester is shown at C6 for simplicity, but the reaction can also occur with a hydroxyl group at C2 or C3 on the GPy units.

The esterification of the starch was confirmed by ^1H NMR analysis of the purified products (Figure 3.1). For example, the ^1H NMR spectrum for C6(0.1)-SNP-1 contains signals corresponding to the GPy backbone for the protons on C2 and C4 overlapping at 3.34 ppm, while the protons on C3, C5, and C6 overlap at 3.65 ppm. The hydroxyl protons usually overlap with the proton on the anomeric carbon C1, which results in inaccurate integration in the determination of the DS. To avoid this issue TFA was added to the NMR tube before analysis, which resulted in the hydroxyl and water protons (and any other labile protons present) shifting downfield. After the addition of TFA, the proton on the anomeric carbon was well-resolved from the other backbone protons at 5.11 ppm. The signals for the protons on the hydrophobic tail appear upfield from the starch backbone protons. For the hexanoyl group, the signals for the methylene protons α and β to the ester bond are at 2.32 and 1.54 ppm, respectively. The four

protons from the two other methylene groups are at 1.28 ppm, and the methyl protons appear at 0.87 ppm. The DS of the sample was calculated by comparing the integration for the lone proton on the anomeric carbon to either of the peaks corresponding to methylene groups or the methyl group. It should be noted that for high DS samples, the peak at 2.32 ppm may overlap with the solvent peak and should not be used for DS calculations. For the sample shown in Figure 3.1, the DS was 0.10. The reaction efficiency (RE) for this procedure was therefore 100%.

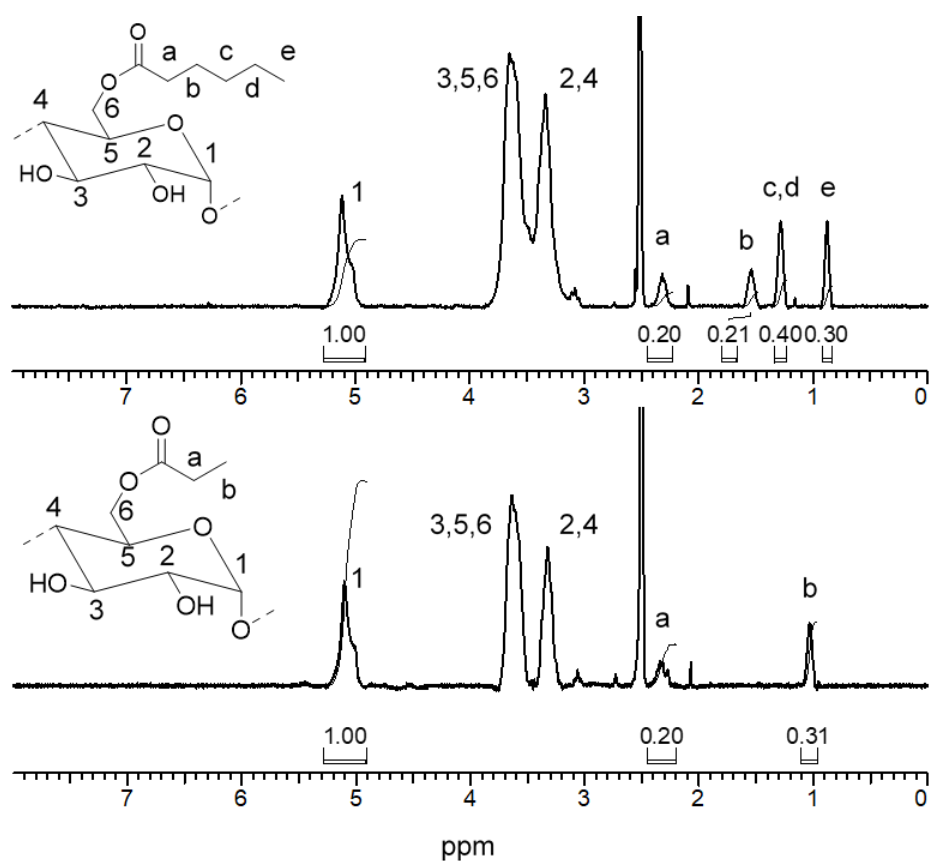


Figure 3.1. ¹H NMR spectra for (top) C6(0.1)-SNP-1 and (bottom) C3(0.1)-SNP-1.

Similarly, the ^1H NMR spectrum for sample C3(0.1)-SNP-1 contained the characteristic starch proton signals at 5.10, 3.32, and 3.64 ppm, but also peaks for a methylene group at 2.34 ppm and a methyl group resonance at 1.03 ppm. The DS, determined in the same manner described above, was also 0.1, corresponding likewise to a RE of 100%. Our finding of 100% REs is consistent with those of Mullen and Pacsu,¹⁷ who reported the synthesis of gelatinized starch triesters from acetic, propionic, and butyric anhydrides using 3-3.5 moles of anhydride with respect to GPy units, corresponding to RE values of 85.7-100%, measured by titration of the hydrolyzed esters. Pyridine served as solvent in that case, rather than in stoichiometric amount as in the current investigation, and the reaction temperature was set to 100-115 °C. The higher temperature required was likely necessary due to the absence of DMSO and DMAP in the reaction. The new protocol used in the current investigation also proceeded to completion but without heat, which should help prevent hydrolytic degradation; however Mullen and Pacsu reported a modest increase in molecular weight based on viscometry measurements in pyridine.

Using the procedure described, both SNP-1 and SNP-2 were modified to different DS values with hexanoic and propionic anhydrides (Figure 3.2). For both the C6-SNP-Y and C3-SNP-Y sample series, REs of 100% were achieved in all cases, but the DS was limited to 0.15 for C6-SNP-Y to maintain good water dispersibility. There was no noticeable change in reactivity when using SNP-2 vs. SNP-1 and either anhydride. This indicates that the conditions (solvent and catalyst system) selected provided excellent control over the reaction. The REs obtained in this investigation are higher than in earlier reports, with the exception of Mullen and

Pacsu. For example, Matharu and coworkers² reported a RE of 98.1% for starch and propionic anhydride for a DS of 1.82. They synthesized esters with DS values between 0.38 and 2.54. The reaction was performed by heating the reaction to 90 °C in toluene, in the presence of 5 mol% DMAP with respect to starch (rather than with respect to the anhydride, as done herein). No other base was used in the reaction. Sun and Sun¹⁹ achieved RE values of up to 50.7% using succinic anhydride for a DS of 1.52. In this case the reaction was catalyzed by DMAP and pyridine, but *N,N*-dimethylacetamide with LiCl served as solvent and the reaction was heated to 105 °C. Hanna and coworkers²⁰ reported a RE of approximately 65% for a target DS of 2.0 using acetic anhydride. No solvent was used, and the reaction was carried out by heating to 123 °C and adding 50 wt% NaOH solution up to 34 wt% with respect to the starch in the reaction. Increasing the number of equivalents of anhydride to 3.0 or 4.0 in the reaction resulted in a RE decrease. Montgomery and coworkers²³ suggested using trifluoroacetic anhydride as a catalyst, to form starch triesters using a carboxylic acid in place of anhydride, by mild heating of 65-70 °C. Unfortunately, more than 2 moles of trifluoroacetic anhydride, a very toxic reagent, were required per starch hydroxyl group to do this. The highest RE reported was 37.1% for acetic acid, while the hexanoyl triester was synthesized with a RE of 24.9%. Foresti and coworkers²⁴ reported the synthesis of starch esters with DS between 0.05-1.59 with a RE of up to 6.3%, by heating a large excess of propionic acid with starch to 130 °C in the presence of 2 moles of L-tartaric acid with respect to the GPy units.

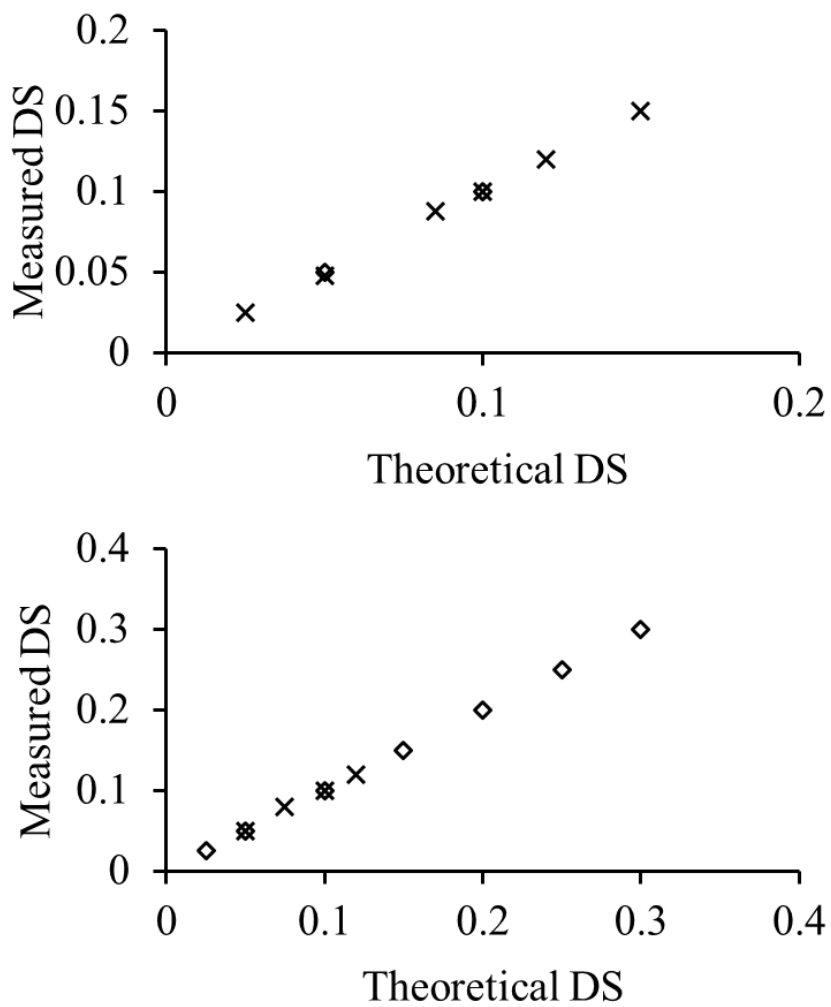


Figure 3.2. Effect of varying the anhydride loading for (top) C6-SNP-1 (x), C3-SNP-1 (◇) and (bottom) C6-SNP-2 (x), C3-SNP-2 (◇).

3.4.2 Macromolecular Characterization of Starch Esters

There are very few reports on molecular weight distribution analysis for starch esters synthesized using alkyl carboxylic acid derivatives (e.g. anhydrides), whereas studies on esters obtained from cyclic anhydrides such as OSA are more prevalent, yet still uncommon.²⁵ To determine how the molecular weight distribution and the molecular size distribution may have been affected by the reaction with anhydrides under the reaction conditions selected, multi-detector GPC analysis was used. This included a light scattering detector, to determine the absolute molecular weight of the samples based on the Zimm equation

$$\frac{Kc}{R_{\theta}} = \left(\frac{1}{M_w} + 2A_2c \right) \left(\frac{1}{P_{\theta}} \right) \quad (1)$$

where K is an optical constant, c is the sample concentration, R_{θ} is the Rayleigh ratio, M_w is the absolute weight-average molecular weight, A_2 is the second virial coefficient, and P_{θ} is the particle scattering function. In the GPC measurements, the sample eluting from the column is dilute, such that the concentration approaches 0 and the $2A_2c$ term in Eq. 1 can be neglected. The light scattering detector used measured the light scattering intensity at 90° and at 7° . At a measurement angle of 7° the P_{θ} term approaches 1, so Eq.1 simplifies to Eq. 2. The term K is defined in Eq. 3,

$$\frac{Kc}{R_{\theta}} = \frac{1}{M_w} \quad (2)$$

$$K = \left(\frac{2\pi^2 n_0^2}{\lambda_0^4 N_A} \right) \left(\frac{dn}{dc} \right)^2 \quad (3)$$

where n_0 is the refractive index of the mobile phase, λ_0 the wavelength of the incident laser beam, N_A is Avogadro's number and $\left(\frac{dn}{dc}\right)$ is the specific refractive index value for the sample.

The $\left(\frac{dn}{dc}\right)$ value for unmodified starch in DMSO is 0.066 mL/g,²⁶ but it needs to be determined for the modified SNP samples before the Zimm equation can be used for accurate molecular weight and molecular weight distribution measurements. Treating the modified SNPs as a copolymer of starch and a hydrophobically modified starch ester, the $\left(\frac{dn}{dc}\right)$ of the modified SNPs can be approximated as the sum of the products of the weight fractions and $\left(\frac{dn}{dc}\right)$ for the individual components, defined by Eq. 4 for the C6 derivatives, and Eq. 5 for C3 compounds,²⁷

$$\begin{aligned} \left(\frac{dn}{dc}\right)_{C6(x)} &= \left(\frac{dn}{dc}\right)_{St} \left(\frac{162.139(1-x)}{162.139(1-x)+260.281x} \right) + \\ &\left(\frac{dn}{dc}\right)_{C6(1)} \left(\frac{260.281x}{162.139(1-x)+260.281x} \right) \end{aligned} \quad (4)$$

$$\begin{aligned} \left(\frac{dn}{dc}\right)_{C3(x)} &= \left(\frac{dn}{dc}\right)_{St} \left(\frac{162.14(1-x)}{162.14(1-x)+218.20x} \right) + \\ &\left(\frac{dn}{dc}\right)_{C3(1)} \left(\frac{218.20x}{162.14(1-x)+218.20x} \right) \end{aligned} \quad (5)$$

where x is the DS of the sample and $\left(\frac{dn}{dc}\right)_{st}$ is 0.066 mL/g. The 162.14 term represents the molar mass of the glucopyranose units in the sample, while the terms 260.28 and 218.20 represent the molar masses of the hexanoyl and propionyl ester-functionalized glucopyranose fragments, respectively. To determine the $\left(\frac{dn}{dc}\right)_{C6(1)}$ and $\left(\frac{dn}{dc}\right)_{C3(1)}$ values, new samples with a higher DS than previously described, C6(1)-SNP-1 and C3(1)-SNP-1, were synthesized. Measurement of the $\left(\frac{dn}{dc}\right)$ values for these samples was completed by chromatographic analysis, because the batch method using a differential refractometer was found not to produce reliable results due to the very hygroscopic nature of starch, LiBr, and DMSO.²⁸ To this end, the RI detector response was plotted against the unmodified SNP concentration (Figure 3.3) and a straight line was fitted to the data points. The slope of the line depends on the RI detector response, the injected volume, and $\left(\frac{dn}{dc}\right)$. The detector response factor, when applied to the analysis of the modified SNP samples, yielded the corresponding $\left(\frac{dn}{dc}\right)$ values for the C6(1)-SNP-1 and C3(1)-SNP-1 samples found to equal 0.0305 ± 0.0008 mL/g and 0.0403 ± 0.0008 mL/g, respectively. It should be noted that these values are specific to a temperature of 50 °C, a mobile phase of 0.05 M LiBr in DMSO, and $DS \leq 1$. The $\left(\frac{dn}{dc}\right)$ values for the modified samples are lower than for unmodified starch, indicating that the modified SNPs scatter less light than unmodified starch. Substituting the $\left(\frac{dn}{dc}\right)$ values in Eqs. 4 and 5 gives Eqs. 6 and 7, yielding the $\left(\frac{dn}{dc}\right)$ of any C6 or C3 starch ester, respectively, where x is the $DS \leq 1$.

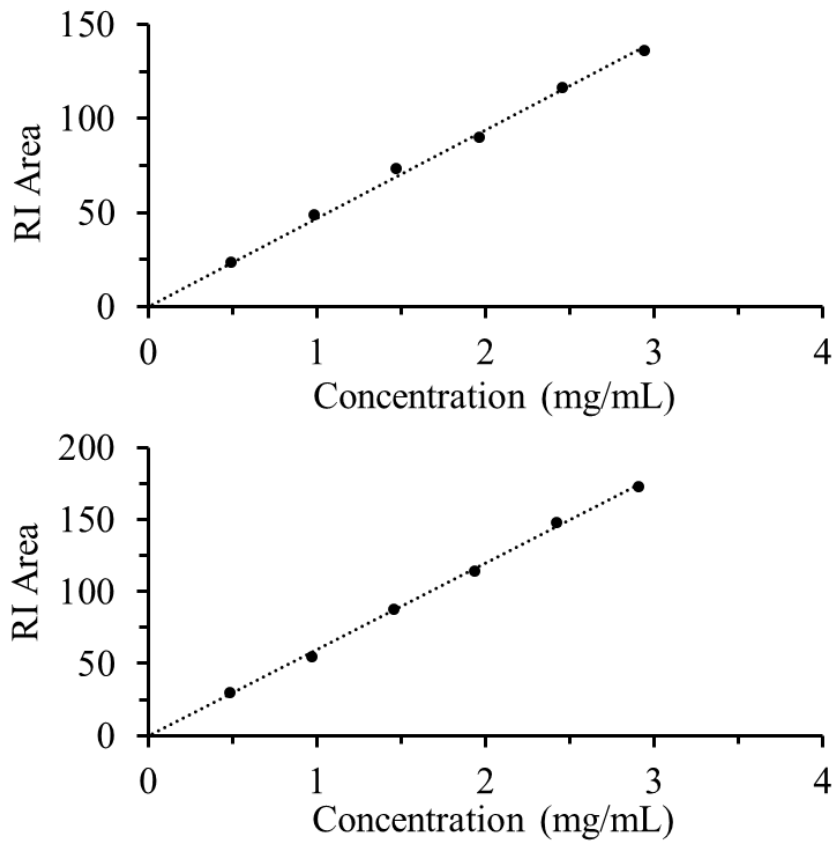


Figure 3.3. RI peak area (after baseline subtraction) for C6(1)-SNP-1 (top) and C3(1)-SNP-1 (bottom) as a function of concentration. The dashed line is for a linear fit not forced through the origin.

$$\left(\frac{dn}{dc}\right)_{C6(x)} = 0.066 \left(\frac{162.14(1-x)}{162.14(1-x)+260.28x}\right) + 0.0305 \left(\frac{260.28x}{162.14(1-x)+260.28x}\right) \quad (6)$$

$$\left(\frac{dn}{dc}\right)_{C3(x)} = 0.066 \left(\frac{162.14(1-x)}{162.14(1-x)+218.20x}\right) + 0.0403 \left(\frac{218.20x}{162.14(1-x)+218.20x}\right) \quad (7)$$

The GPC elution curves obtained for the unmodified SNP-1 and all the HM-SNP-1 samples (Figure 3.4) indicate that all were monomodal and had nearly identical retention volumes. No shoulders or new peaks, corresponding to backbone fragmentation or cross-linking, could be noticed, indicating that there was no significant change in R_h distribution for the HM-SNPs. Due to the highly branched nature of amylopectin, the retention volume or R_h is not solely dependent on the molecular weight as for linear polymers. SNP-1 had $M_w = 5.4 \times 10^6$ g/mol (Table 3.1) and $D_h = 54$ nm. As expected, C6(0.05)-SNP-1 and C6(0.1)-SNP-1 only displayed minor (less than 15%) differences in M_w as compared to unmodified SNP-1, and a D_h difference of less than 4 nm. The absolute molecular weight of the samples, calculated using the $\left(\frac{dn}{dc}\right)$ values of Eq. 6, were less than 10% higher for the water-dispersible C6-modified starch than for unmodified starch. Since the molecular weight calculated from Eqs. 2 and 3 depends on $\left(\frac{dn}{dc}\right)^2$, a small difference in $\left(\frac{dn}{dc}\right)$ can have a significant influence on the calculated molecular weight values. For example, a 10% error on $\left(\frac{dn}{dc}\right)$ introduces an error of over 20% on the molecular weight. For C3(0.05)-SNP-1 and C3(0.1)-SNP-1, similar minors difference in M_w were obtained

relatively to unmodified SNP-1 using the $\left(\frac{dn}{dc}\right)$ values calculated with Eq. 7. The measured D_h were likewise within 4 nm of unmodified SNP-1, indicating that the particles did not degrade nor cross-link in the reaction. SNP-2 had an M_w of 1.6×10^5 g/mol and a D_h of 14 nm. As expected, C6(0.05)-SNP-2 and C6(0.1)-SNP-2 had less than 15% difference in M_w compared to unmodified SNP-2, and D_h differences of less than 0.5 nm. C3(0.05)-SNP-2 and C3(0.1)-SNP-2 were synthesized from a different lot of SNP-2 than C6(0.05)-SNP-2 and C6(0.1)-SNP-2. Due to their different origin, the C3 particles had a M_w similar to unmodified SNP-2, but a noticeably different D_h . Warwel and coworkers²⁹ reported significant degradation in the synthesis of starch esters using octanoyl chloride and a catalytic amount of potassium methoxide. The M_w of their products was approximately 5 times lower than for octanoyl esters produced using an imidazolide intermediate and the same starch starting material. Winkler and coworkers³⁰ reported a significant increase in M_w after esterification with vinyl laurate in DMSO, using 3 mol% of Cs_2CO_3 with respect to the GPy units as catalyst. The M_w of their starch laurate with DS = 2.4, in a mobile phase of THF, increased more than 3-fold as compared to the starting material measured in DMSO. They cited an increase in sample recovery, from 72% for unmodified starch to 93% for the ester, to justify the large increase in M_w , but did not take into account the variation in $\left(\frac{dn}{dc}\right)$ of their products with the DS. The use of scanning electron microscopy (SEM) analysis has also been reported in the literature to monitor the integrity of starch after modification reactions.^{18,20,24} Unfortunately this approach only provides qualitative results, not comparable to the quantitative results obtained with GPC or dynamic light scattering

analysis. Panayiotou and coworkers¹⁸ utilized this method for gelatinized starch octanoate esters synthesized according to the procedure reported by Mullen and Pacsu.¹⁷ The only significant advantage of SEM is that it can be used to monitor granule integrity, for reactions done on whole starch granules. This method was favored by Hanna and coworkers as well as Foresti and coworkers.

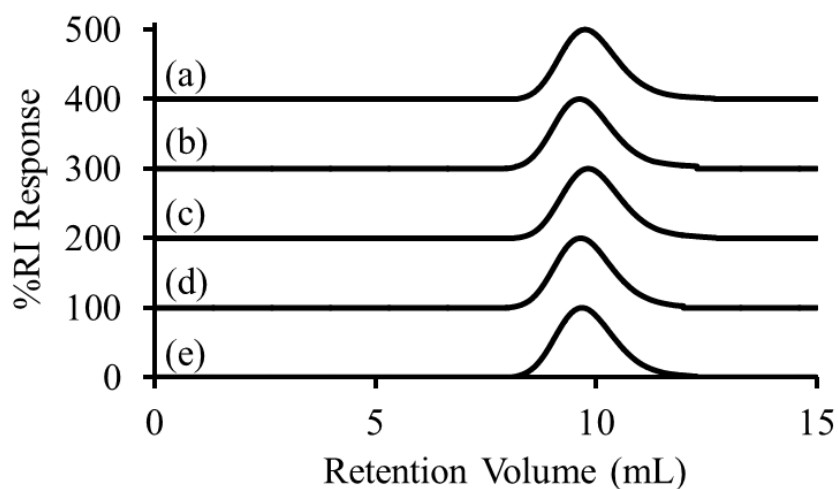


Figure 3.4. GPC baseline-subtracted RI elution curves of (a) SNP-1, (b) C6(0.05)-SNP-1, (c) C6(0.1)-SNP-1, (d) C3(0.05)-SNP-1, and (e) C3(0.1)-SNP-1. The position of each curve was adjusted on the vertical scale for clarity.

Table 3.1. Characteristics of SNPs and HMSNPs determined by GPC analysis.

Sample	dn/dc (mL/g)	M_w (g/mol)	D_h (nm)
SNP-1	0.066	5.4×10^6	54
C6(0.05)-SNP-1	0.063	5.9×10^6	58
C6(0.1)-SNP-1	0.061	4.8×10^6	50
C3(0.05)-SNP-1	0.064	6.1×10^6	58
C3(0.1)-SNP-1	0.063	5.6×10^6	56
SNP-2	0.066	1.6×10^5	14
C6(0.05)-SNP-2	0.063	1.4×10^5	14
C6(0.1)-SNP-2	0.061	1.4×10^5	14
C3(0.05)-SNP-2	0.064	1.2×10^5	10
C3(0.1)-SNP-2	0.063	1.5×10^5	8

3.5 Conclusions

Starch esters were successfully prepared by reacting SNPs with hexanoic and propionic acid anhydrides in the presence of pyridine and DMAP. The DS of the products, determined by ¹H NMR analysis, revealed that this solvent and catalyst system yielded a RE of 100% over the entire DS range tested. There was no difference in reactivity observed between hexanoic and propionic acid anhydrides nor between SNPs of different size under these conditions. The integrity of the products was maintained, as confirmed by GPC analysis, since there were no substantial changes in molecular weight nor hydrodynamic size. This indicates that the reaction conditions used did not degrade the starch backbone, and that the addition of hydrophobic microdomains did not influence the size of the HM-SNPs in DMSO.

While starch and the native SNPs are hydrophilic, the addition of C6 and C3 groups would be expected to induce amphiphilic behavior for the molecules. These hydrophobic microdomains within the SNPs have the potential to stabilize insoluble materials such as hydrophobic drugs in aqueous solutions. For this reason, the materials synthesized will be further characterized both in the solid state and in solution. The highly controlled synthesis of HM-SNPs would be useful to tune the hydrophobic character of the SNPs, which could serve as biodegradable drug delivery vehicles, beyond other potential applications as associative thickeners, colloidal stabilizers, compatibilizers, and food additives.

Chapter 4

Castor Oil–Isocyanate Prepolymers as Cross-linkers for Starch

4.1 Abstract

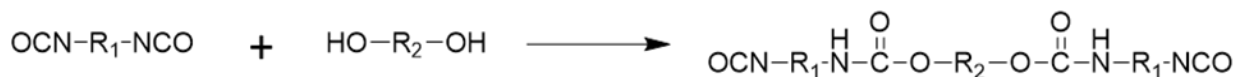
Petroleum-based products have been considered advantageous due to their widespread availability, low cost and tailorable properties, but depleting oil supplies have created a need for materials derived predominately from natural building blocks. One way to address this issue is to develop materials from renewable biopolymers that are readily available and cost-effective. In the current investigation, a method was developed to synthesize polyurethane prepolymers (PUPs) from castor (bean) oil in the absence of solvents. Ricinoleic acid, the most common fatty acid component in castor oil, contains one hydroxyl group, and the castor oil triglyceride contains 2-3 hydroxyls per molecule. Castor oil and toluene diisocyanate (TDI) were reacted at an OH:NCO ratio of 1:2.0, catalyzed by either dibutyltin dilaurate (DBTDL), bismuth 2-ethylhexanoate (K-KAT 348), or without catalyst. The PUPs were synthesized with complete hydroxyl group conversion, %NCO contents between 7.35 and 7.77, and less than 10 wt% unreacted diisocyanate, to be used without further purification since no by-products were formed. The PUPs were reacted with starch at various weight loadings in a batch melt mixer with water as plasticizer and without additional catalysts. In most cases a reaction efficiency (RE) greater than 90% was achieved. Gel permeation chromatography (GPC) analysis of the products showed that the molecular weight and diameter of the starch molecules decreased due

to shearing in the mixer. The materials synthesized have potential applications as associative thickeners and colloidal stabilizers for paints, paper coatings, and adhesives.

4.2 Introduction

Polyurethanes (PUs) are a class of polymeric materials with a wide range of applications including coatings, adhesives, sealants, binders and foams.^{1,2} The urethane functionality is obtained by the reaction of an alcohol and an isocyanate.³ The alcohols used to synthesize PUs are commonly referred to as polyols, as they contain at least two alcohol functional groups,⁴ and are reacted with diisocyanates such as 4,4-methylene diphenyl diisocyanate (MDI), toluene diisocyanate (TDI) or 1,6-hexamethylene diisocyanate (HMDI). Polyurethanes can include other functional groups such as ethers, esters, or aromatic components. The properties of the resulting PU materials not only depend on the monomers used, but also on the presence of cross-links. One drawback of PUs is that the diisocyanate monomers are volatile and toxic.⁵ To overcome this issue polyurethane prepolymers (PUPs), formed by step polymerization between a polyol and an excess of diisocyanate, can be used (Scheme 4.1).^{6,7} All the hydroxyl groups react and form urethane linkages, while a fraction of the isocyanate groups do not react such that the resulting product has at least two residual isocyanate groups available for subsequent reactions.⁷ PUPs are effectively polyisocyanates with a higher viscosity and molecular weight than the starting diisocyanate small molecules, while their isocyanate content by weight (%NCO) and vapor pressure are lower.⁵ Since the reaction between a hydroxyl and an isocyanate group does not produce small molecule by-products, the product does not need to be purified, albeit

unreacted diisocyanate may remain. If desired, unreacted diisocyanate may be removed in a thin film evaporator⁷ at high temperature and high vacuum, keeping in mind that isocyanates can form ureas, biuret or allophanates that alter the product properties under these conditions.⁵ It would thus be advantageous to minimize the amount of unreacted diisocyanate in PUPs.



Scheme 4.1. Reaction of a polyol with a diisocyanate to form a PUP.

One drawback of PUPs is the source of polyols and diisocyanates, as these are typically derived from petroleum products. Overdependence on petroleum-based products and depleting oil supplies have created a need for materials derived predominantly from naturally sourced building blocks.⁸ While petroleum-based products are generally considered advantageous due to their widespread availability, low cost and properties tailorable to a multitude of applications,⁹ most petrochemical products ultimately accumulate in landfills or in the environment, thus complicating waste disposal and leading to the contamination of different ecosystems. To address these issues, there is an impetus to use renewable biopolymers as readily available and cost-effective materials.¹⁰

One class of hydrophobic materials derived from agricultural products is vegetable oils.¹¹ These materials have been extracted from different sources for thousands of years, and have found many applications as both edible and industrial materials.¹² Vegetable oils are triglycerides

(Figure 4.1), containing a glyceryl moiety bound to three fatty acids via ester bonds.¹³ The composition of the fatty acids varies with the plant source. The fatty acids vary in length and may contain double bonds (e.g. linoleic acid), a hydroxyl functional group (e.g. ricinoleic acid), or a saturated carbon chain (e.g. stearic acid). The fatty acids in castor oil are composed of 87% ricinoleic acid tails, thus castor oil contains 2.7 hydroxyls per triglyceride on average. An in-depth analysis of castor oil revealed that 70% of triglycerides contain three hydroxyl groups, 30% contain 2 hydroxyl groups, and no triglycerides contain zero or one hydroxyl group.¹⁴ Given that the triglycerides in castor oil contain exclusively two or three hydroxyl groups, it would be well-suited as polyol in the synthesis of PUPs.

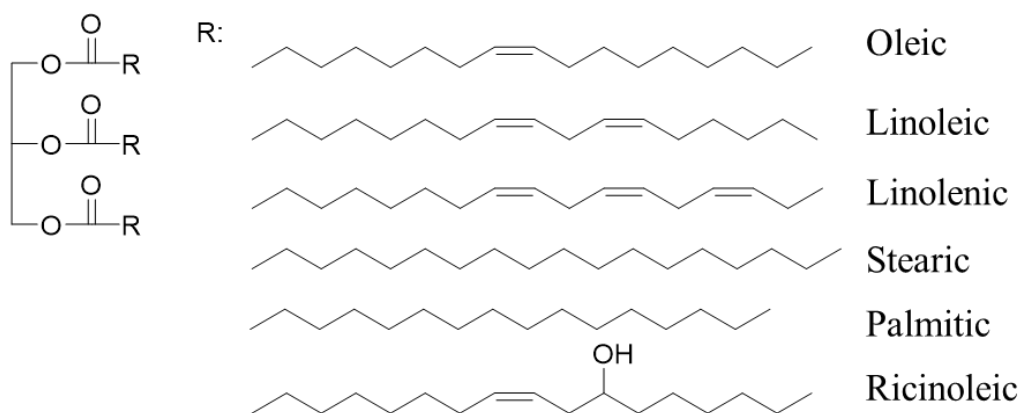


Figure 4.1. Structure of a triglyceride and common fatty acids.

Starch is a natural biopolymer that is renewable, readily available, biodegradable and cost-effective.¹⁵ These attributes make it an attractive feedstock for industrial applications.¹⁶ Common sources of starch include but are not limited to cereals like corn or wheat, tubers such

as potatoes, and roots (e.g. tapioca).¹⁵ Starch is composed of glucopyranose (GPy) units connected through α -1,4 linkages, with branching introduced through α -1,6 linkages.¹⁷ The use of native starch to replace petroleum products is not necessarily advantageous due to its water sensitivity and brittleness, even when plasticized.¹⁸ To overcome these issues, starch is commonly modified to tailor its properties.¹⁹ The hydrophobic modification of starch with either acetic anhydride or octenylsuccinic anhydride (OSA) is thus common.²⁰ The reaction between a hydroxyl group in starch and acetic anhydride yields an acetate ester, while acetic acid (or its salt) is formed as a by-product.²¹ The starch derivative therefore needs to be purified before it can be used. The reaction between starch and OSA introduces octenylsuccinate ester groups on the starch, with hydrophobicity of the product increasing directly with the degree of substitution.²⁰ The carboxylate groups that forms through esterification with OSA remains covalently bound to the starch, because of the cyclic structure of OSA. No small molecule by-products are formed, but a proton may be lost if the carboxylic acid is neutralized with a base. Another common modification of starch is cross-linking.²¹ Cross-linked starch typically has reduced swellability, solubility, and water-binding capacity.²² Starch is commonly cross-linked with dialdehydes including glyoxal and glutaraldehyde, polyfunctional epoxides such as epichlorohydrin, by phosphorylation with reagents such as sodium trimetaphosphate, or with diisocyanates.¹⁶ The reaction between starch and a diisocyanate is particularly interesting because it results in zero atoms loss (100% atom economy), since the reaction does not yield any

small molecule by-products, which also makes it industrially advantageous.²³ The economic viability of modified starches is indeed often compromised by requisite purification steps.¹⁶

The main objective of this study was to prepare cross-linked starches in an environmentally friendly fashion, while at the same time imparting hydrophobicity to the product. To achieve this, castor oil was used to synthesize a biobased PUP. The OH:NCO ratio was set to at most 1:2, to minimize the amount of unreacted diisocyanate in the PUP. The products were characterized by ¹H NMR spectroscopy, dibutylamine titration (to determine %NCO content) and gel permeation chromatography (GPC). The PUPs were subsequently reacted with starch in a melt mixer at different PUP weight loadings. The melt mixer was used to mimic reactive extrusion conditions on a smaller scale.²⁴ The materials synthesized have multiple potential applications including drug delivery carriers, associative thickeners, colloidal stabilizers, paper coatings, and adhesives.

4.3 Experimental Section

4.3.1 Materials

Waxy maize starch (waxy pearl 1108) was purchased from Cargill Inc. (Burlington, Canada). Dibutyltin dilaurate (DBTDL) was purchased from Air Products and Chemicals, Inc. (Allentown, USA). K-KAT 348 was purchased from King Industries, Inc. (Norwalk, USA). The remaining chemicals were purchased from Sigma Aldrich. All chemicals were used as received.

4.3.2 Synthesis of Castor Oil PUPs

Castor oil was dried by heating to 80 °C in a vacuum oven for 16 hours under reduced pressure and stored in a desiccator over Drierite until use. Technical grade toluene-2,4-diisocyanate (TDI) (25.30 g, 145.2 mmol) and dibutyltin dilaurate (DBTDL; 0.0800 g, 0.13 mmol) was charged into a 3-neck round bottom flask equipped with an overhead mechanical stirrer, a glass dropping funnel loaded with castor oil (50.13 g, 53.79 mmol), a nitrogen inlet, and a gas bubbler. The system was degassed with nitrogen, heated to 40 °C, and the castor oil was added to the TDI drop-wise over 1 hour. After the addition was completed, the reaction was continued for 2 hours with constant stirring at 40 °C. The clear viscous product was stored at -20 °C until further use. A small sample of the product was reacted with methanol in a glass vial, by mixing 200 mg of it with 1.5 mL of methanol and 1 mL of acetone. After 16 hours the excess methanol and the acetone were removed first with a stream of nitrogen, and then in a vacuum oven at 40 °C for 16 hours. The methanol-blocked PUP sample was characterized by ¹H NMR spectroscopy and gel permeation chromatography (GPC) analysis. The same procedure was repeated using bismuth carboxylate 2-ethylhexanoic (K-KAT 348; 0.0800 g, 0.13 mmol) and no catalyst in replacement of DBTDL.

4.3.3 Determination of %NCO in Castor Oil PUP

The %NCO content of the synthesized PUPs was determined by the procedure described in ASTM D2572-97. The PUP (0.95 g) was weighed into a dry Erlenmeyer flask and dissolved

in 25.00 mL of toluene. After complete dissolution, 25.00 mL of 0.1 M di-*n*-butylamine solution in toluene was added. After 15 minutes, 100 mL of 2-propanol and 5 drops of bromophenol blue indicator (0.1% aqueous solution) were added, and the solution was titrated with standardized 0.1 M HCl. The procedure was repeated without PUP to determine the “blank” value. The %NCO was calculated using Eq. 1, where B is the volume of HCl solution used for titration of the blank (mL), V is the volume of HCl for titration of the PUP (mL), N is the HCl concentration (mol/L), W is the mass of PUP (g), and 0.0420 represents the weight of 1 meq. of NCO groups.

$$\%NCO = \frac{[(B-V) \times N \times 0.0420]}{W} \times 100\% \quad (1)$$

4.3.4 Modification of Starch with Castor Oil PUP in a Melt Mixer

Uncooked waxy starch (22.0 g, 0.136 mol) and distilled water (4.4 mL, 0.244 mmol, 20 wt% wrt starch) were loaded into a melt mixer (Half size mixer, C. W. Brabender, 30 mL capacity) fitted to an ATR Plasti-Corder Torque Rheometer (C. W. Brabender) preheated to 90 °C by circulating oil. The chamber was fitted with a thermocouple at the bottom to measure the temperature over the duration of the whole reaction (at most 15 minutes at 60 rpm). After 4 minutes, DBTDL-catalyzed castor oil PUP (0.36 g, 0.26 mmol, 1.6 wt%) was added slowly over 3 minutes to the mixing chamber. If torque exceeded 25 Nm, the mixer was stopped. After the reaction, the product was removed from the mixing chamber and ground to a fine powder in a coffee grinder. A 5-g portion of the product was purified by Soxhlet extraction with acetone for 48 hours before the solid product was dried in a vacuum oven at 80 °C overnight. The crude and

purified products were analyzed by ^1H NMR spectroscopy (300 MHz, $\text{DMSO-}d_6$), and the purified product by GPC. The procedure was repeated at DBTDL-catalyzed castor oil PUP loadings of 3.3, 5.0, 6.7, and 9.0 wt%. The procedure was also repeated for K-KAT 348-catalyzed PUP and catalyst-free castor oil PUP.

4.3.5 ^1H NMR Analysis

^1H nuclear magnetic resonance spectroscopy (NMR) was performed on a Bruker 300 MHz spectrometer. The concentration of all the samples was 15–30 mg/mL in CDCl_3 for the PUP samples, and 10–20 mg/mL in $\text{DMSO-}d_6$ with 4 mg LiBr and 6 drops of trifluoroacetic acid (TFA) for the modified starch samples. The reported chemical shifts are relative to the solvent protons at 7.27 ppm for CDCl_3 and 2.50 ppm for $\text{DMSO-}d_6$.

4.3.6 Gel Permeation Chromatography (GPC) Analysis

Analytical GPC measurements for the PUP samples were performed on a Malvern GPCmax instrument with a TDA 305 triple detector array, a 2600 UV detector, and two 300 mm \times 8.0 mm I.D. PolyAnalytik SuperesTM single pore columns with polystyrene molar mass ranges of up to 70 kDa and 1.5 kDa in series. A flow rate of 1.0 mL/min was used with tetrahydrofuran (THF) as the mobile phase at 35°C. Samples were prepared at a concentration of 1 mg/mL in THF and filtered through a 0.2 μm polytetrafluoroethylene filter.

Analytical GPC measurements for the modified starch samples were performed on a Malvern GPCmax instrument using a TDA 305 triple detector array equipped with a differential

refractive index (RI) detector, a dual angle light scattering detector with measurement angles of 7° and 90°, as well as an online viscometer. Separation was completed using a 300 mm x 8.0 mm I.D. PolyAnalytik Superes™ column having a theoretical linear PS molar mass range of up to 200 MDa. A flow rate of 0.6 mL/min was used with 0.05 M LiBr in DMSO as the mobile phase at 50 °C. A pullulan standard with a peak molecular weight $M_p = 200,000$ Da and $D = 1.09$ (PolyAnalytik) was used to calibrate the instrument and obtain absolute molecular weight (MW) values. The $\left(\frac{dn}{dc}\right)$ and intrinsic viscosity $[\eta]$ values supplied for this standard in DMSO were 0.066 mL/g and 0.65 dL/g, respectively. The samples were prepared at a concentration of 2 mg/mL and filtered through 0.45 μm nylon filters.

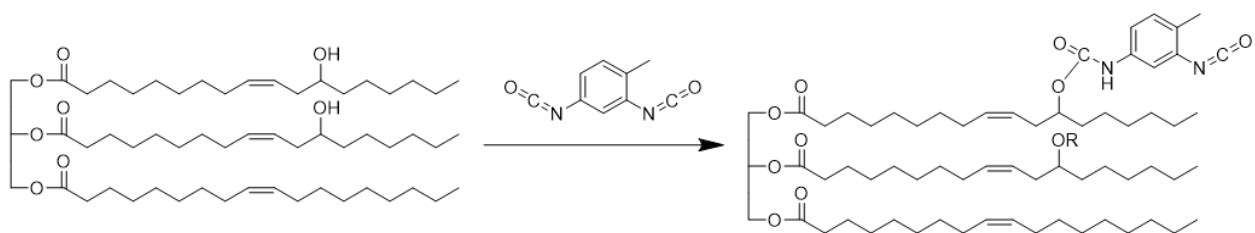
4.4 Results and Discussion

4.4.1 Synthesis of Castor Oil PUPs

Castor oil was selected as a polyol substrate for the PUP synthesis because of its high ricinoleic acid level,¹⁴ such that all the triglyceride molecules contain either 2 or 3 hydroxyl groups. The reaction between hydroxyl and isocyanate groups is commonly catalyzed by organometallic compounds such as DBTDL.²⁵ The catalytic cycle of DBTDL involves the formation of a complex with the hydroxyl group, forming a stannyl alkoxide, followed by coordination with the isocyanate group. The alkoxide attacks the isocyanate group, forming an N-stannylcarbamate intermediate, and the urethane linkage is released when another hydroxyl coordinates with the tin.²⁶ While tin compounds are effective catalysts, they are also toxic.²⁵

Catalysts such as bismuth carboxylates (K-KAT 348) are increasingly used to replace tin-based catalysts.² Castor oil was initially reacted with MDI and DBTDL as catalyst using the procedure described for TDI, but the reaction could no longer be stirred before all the castor oil was added. The product removed from the round bottom flask was likely cross-linked, as it was insoluble in common organic solvents. Since the isocyanate groups in MDI are on different aromatic rings, the two isocyanate groups react independently of each other. The diisocyanate was therefore replaced with TDI, for which the isocyanate group in the 4-position is known to be more reactive than the other group on the aromatic ring.⁵ The procedure (Scheme 4.2) was repeated with technical grade TDI, described as containing 80% 2,4-TDI and 20% 2,6-TDI, and a OH:NCO ratio of 1:2, using either DBTDL, K-KAT 348, or no catalyst. Castor oil was added to the TDI drop-wise over 1 h and allowed to react further for 2 h, to ensure complete conversion of the hydroxyl groups in castor oil. After the reaction, the clear liquid product was stored at -20 °C until further use without purification. A small aliquot of the product was reacted with methanol for structural characterization by ¹H NMR and GPC. Since the PUPs and methanol are not miscible, they were solubilized in acetone for the reaction.

The ¹H NMR spectrum obtained for methanol-blocked TDI (Figure 4.2(A)) contains methyl protons for the methanol-isocyanate adduct at 3.7 ppm, while the methoxy protons from unreacted methanol should appear at 3.5 ppm. The shift of the peak therefore confirms the presence of reactive isocyanate groups in the PUP.²⁷ The protons on the urethane linkages are at 8.8 and 9.6 ppm, while aromatic protons appear between 7.0 and 7.5 ppm and the methyl protons



Scheme 4.2. Reaction of castor oil with 2,4-TDI. The reaction can also happen at position 6 for 2,6-TDI present in the technical grade product (many isomers possible).

attached to the aromatic ring are at 2.1 ppm. The ^1H NMR spectrum obtained for castor oil (Figure 4.2(B)) is similar to previous reports,⁶ with the peak assignments shown in Figure 4.2(B). The ^1H NMR spectrum obtained for the methanol-blocked castor oil PUP synthesized with DBTDL (Figure 4.2(C)) contains peaks corresponding to methanol-blocked TDI and to castor oil, with three notable differences. First, the methine proton next to the urethane linkage shifted to 4.8 ppm following the reaction of the hydroxyl and isocyanate groups. This change in chemical shift is consistent with a previous report on the reaction of castor oil and isophorone diisocyanate (IPDI).⁶ Second, there is no peak remaining at 3.4 ppm, indicating that all the hydroxyl groups in castor oil reacted. Third, peaks corresponding to the protons on the urethane linkages appeared at 7.8 ppm. The ^1H NMR spectra obtained for the PUPs obtained with DBTDL, K-KAT 348, and without catalyst were identical.

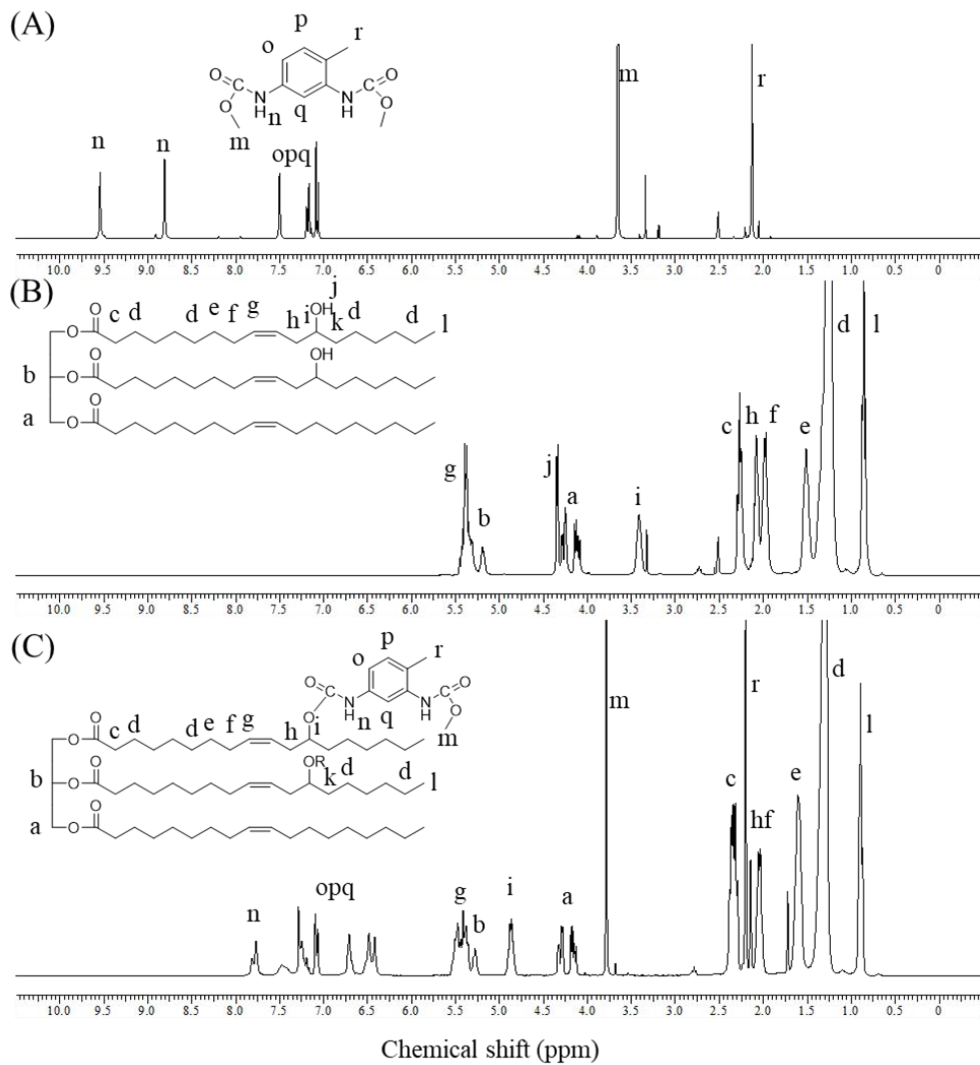


Figure 4.2. ^1H NMR spectra for (A) methanol-blocked 2,4-TDI, (B) castor oil and, and (C) the methanol-blocked castor oil PUP synthesized with DBTDL.

The %NCO content of the PUPs was determined by the ASTM D2572-97 method using dibutylamine.⁷ In this analysis technique, the isocyanate groups in the PUP are reacted with a

known amount of dibutylamine before titration of the remaining dibutylamine with standardized 0.5 M HCl. The %NCO content of the PUPs determined by that technique using Eq. (1) is provided in Table 4.1. For reactions between castor oil and TDI with a 1:2 ratio of OH:NCO, the theoretical %NCO would be 8.09% in the absence of oligomerization or unreacted TDI. Oligomer formation, resulting from the reaction of at least one TDI molecule with two different fatty acid hydroxyls, would result in a decreased %NCO content. Unreacted TDI in the product, on the other hand, would increase the %NCO content. The DBTDL-catalyzed product had the lowest %NCO content, followed by K-KAT 348 and the product obtained without catalyst. Decreasing the OH:NCO ratio below 1:2 led to mixing problems in the reaction, and hence that approach was not examined further. Because the castor oil PUP products were not purified, DBTDL and K-KAT 348 were also present at 0.1 wt% concentration in the corresponding PUPs, which were further reacted with starch in presence of the residual catalyst.

Table 4.1. Chemical characteristics of castor oil PUPs.

Catalyst Used	%NCO of PUP	Unreacted TDI monomer (wt%)
DBTDL	7.35	8.47
K-KAT 348	7.77	5.71
None	7.48	4.16

The GPC elution profiles obtained for the PUPs (Figure 4.3) reveal that a considerable amount of oligomerization occurred in the reactions. The DBTDL-catalyzed product visually

had the largest amount of oligomerization, followed by the K-KAT 348-catalyzed product and the PUP obtained without catalyst. As expected, all 3 PUPs had a decreased elution volume relatively to unreacted castor oil; the addition of TDI to the triglyceride increased the hydrodynamic volume of the product. Oleic acid (C₁₈ fatty acid) and methanol-blocked TDI were injected separately for comparison, to determine the origin of the low molecular weight peak eluted after the PUPs. Oleic acid had an elution volume different from any of the products present at a significant concentration in the PUPs. This shows that urethane formation did not lead to degradation of the triglycerides to fatty acids. The small peak eluting after the PUPs rather corresponds to methanol-blocked TDI. Since that peak was well-resolved from the other peaks, GPC analysis could be used to determine the concentration of unreacted TDI in the products. The response of the RI detector is directly related to the concentration of a component²⁸ according to Eq. (2),

$$S_{RI} = k_{RI} \times c \times \frac{dn}{dc} \quad (2)$$

where S_{RI} is the integrated RI signal intensity, k_{RI} is an instrument constant, c is the concentration (mg/mL), and $\left(\frac{dn}{dc}\right)$ is the refractive index of methanol-blocked TDI. To determine the $\left(\frac{dn}{dc}\right)$ value of methanol-blocked TDI, the chromatographic method of $\left(\frac{dn}{dc}\right)$ calculation was used.²⁸ To this end, the RI detector response was plotted against the methanol-blocked TDI concentration (Figure 4.4) and a straight line was fitted to the data points. The $\left(\frac{dn}{dc}\right)$ value determined by that method was 0.125 ± 0.005 mL/g. This value, specific to methanol-blocked TDI in THF at

35 °C, was used in combination with the area of the methanol-blocked TDI peak in the RI channel of the PUP injection to determine the concentration of unreacted TDI. The k_{RI} value was measured by injection of a polystyrene 3.5×10^4 g/mol narrow standard with a polydispersity (\mathcal{D}) of 1.1, a known $\left(\frac{dn}{dc}\right)$ value of 0.185 mol/g, at a concentration of 1.0 mg/mL, and an injection volume of 100 μ L. The measured $\left(\frac{dn}{dc}\right)$ values were 8.47, 5.71, and 4.16 wt% for the PUPs obtained with DBTDL, K-KAT 348 and without catalyst, respectively.

While this is not the first report on the synthesis of a castor oil-based PUP using TDI, the results reported herein show that using these specific conditions has significant advantages. Tran and Pham²⁷ indeed reported the reaction of castor oil with 2,6-TDI without solvent and found that the reaction required over 2 hours at 50 °C to reach a plateau in %NCO, however complete conversion of the hydroxyl groups was not achieved. While working at higher temperatures and with different diisocyanates, they reported the same viscosity/gelation issues which we encountered with MDI. Patel and coworkers²⁹ also investigated the reaction between castor oil and TDI, but using toluene as solvent and DBTDL as catalyst. They were mainly interested in the rate of the reaction, and unfortunately did not report the %NCO for any of their castor oil PUPs. Furthermore, neither investigation was concerned with the amount of unreacted TDI in the PUP products. Ferreira and coworkers synthesized a castor oil PUP from IPDI to prepare novel adhesives, likewise using an OH:NCO ratio of 1:2 and neither solvent nor catalyst. They characterized their PUP by FTIR, but they neither determined the %NCO nor quantified the unreacted IPDI in the product. Nayak and coworkers⁶ also achieved the synthesis of castor oil

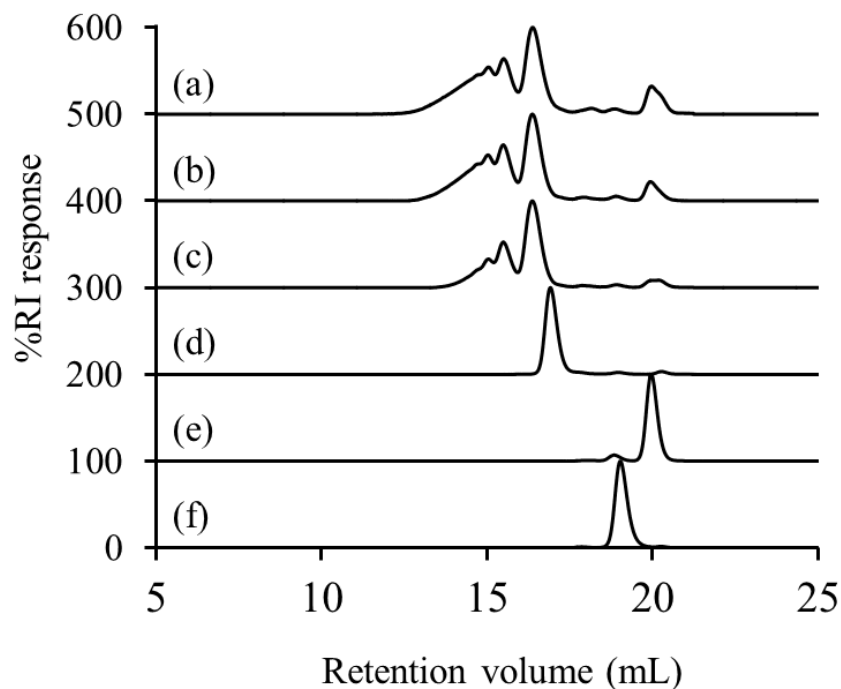


Figure 4.3. GPC elution curves from the RI detector for methanol-blocked castor oil PUP synthesized with (a) DBTDL, (b) K-KAT 348, and (c) without catalyst, as well as for (d) castor oil, (e) methanol-blocked TDI, and (f) oleic acid. The curves were normalized relatively to the maximum response and shifted vertically for clarity.

PUPs with IPDI without solvent at 75 °C with DBTDL, at an OH:NCO ratio as low as 1:0.5. Finally, Wu and coworkers³⁰ reported the synthesis of castor oil PUPs with MDI and no solvent nor added catalyst, and used their product to modify starch. Heating to 87 °C (significantly higher than the 40 °C used herein) was necessary for full conversion of the castor oil, as initial attempts at 60 °C were unsuccessful, and their product had a %NCO content of 7.0 %.

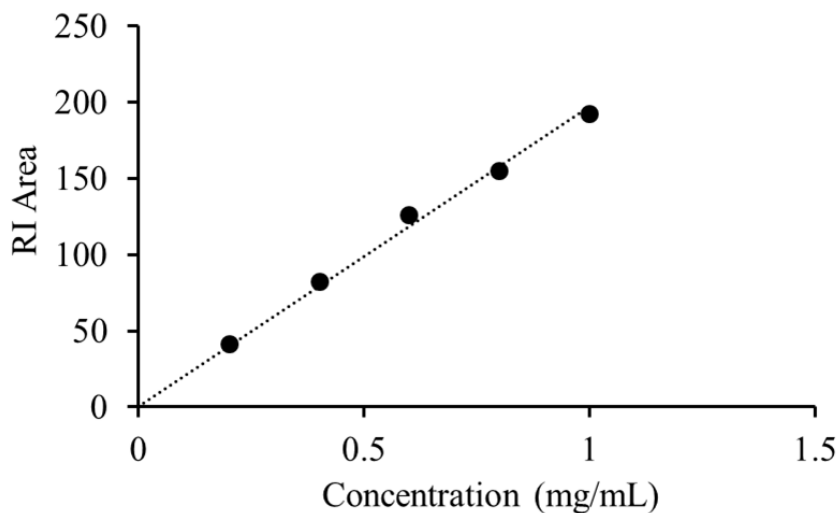


Figure 4.4. RI detector response calibration curve for methanol-blocked TDI.

In the current investigation, we report the synthesis of castor oil PUPs from TDI without solvents and catalysts, at an OH:NCO ratio of 1:2. In spite of the lower OH:NCO ratio, full conversion of the hydroxyl groups was achieved. This is an important detail since without full conversion, unreacted hydroxyls would continue to react in storage, resulting in lower %NCO contents for the PUPs and potentially leading to cross-linking. Furthermore, the reactions reported herein were completed at 40 °C to minimize the formation of ureas, biuret, or allophanates in the PUPs. GPC analysis of the products was carried out to ensure that there was no significant hydrolysis of the castor oil triglycerides, as well as to quantify the unreacted diisocyanate in the PUPs. All previous reports on castor oil PUP syntheses indeed neglected the

quantification of unreacted diisocyanate in the PUPs, even though this is the main underlying reason for using a low OH:NCO ratio.

4.4.2 Modification of Starch with Castor Oil PUPs

The chemical modification of starch is most commonly carried out in stirred reactors, but the direct reaction of starch granules under these conditions often yields products with an inhomogeneous composition. Another option is extrusion, whereby starch undergoes gelatinization after destruction of the granule structure. The process is irreversible and results in free chains of amylose and amylopectin producing a viscous solution.³¹ Reactive extrusion is clearly advantageous for starch modification due to the homogenous mixing achieved, as well as the ability to work at high starch concentrations and temperatures as compared with other techniques.³² On the down side, the amounts of reagents required for extrusion experiments can be very large, ranging from kilograms to the ton scale. For that reason, a smaller scale approach using a batch melt mixer operating on a 20-30 g scale to mimic extrusion conditions was preferred for the current investigation.

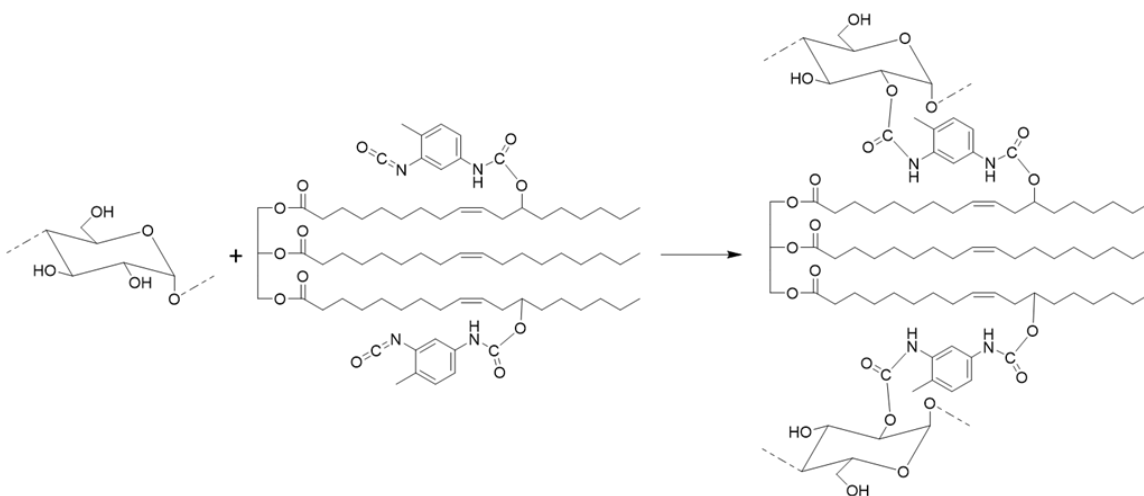
One significant advantage of using a PUP for starch modification is that the reaction of the hydroxyl groups of starch and isocyanates does not form any by-products. Water, present in starch and commonly added as a plasticizer for that material, can compete with starch for the reaction with the isocyanate groups. It is known that the reaction rate of water with isocyanate groups is comparable with primary alcohols, but more than three times that of secondary alcohols.³² Increasing the concentration of starch, and consequently decreasing the concentration

of water in the reaction, should therefore favor the reaction between starch and the PUP. Since the synthesized castor oil PUPs are polyfunctional, the reaction between starch and only one isocyanate per PUP molecule would be sufficient for the PUP to be covalently bonded to the starch and make it more hydrophobic. A lower reaction efficiency (RE) for the isocyanate groups can thus still lead to a high overall RE for the PUP with starch. Cross-linking of the starch, on the other hand, would require the reaction of at least two isocyanate groups per PUP molecule.

To mimic the reaction conditions encountered in a twin screw extruder on a smaller scale, a melt mixer was used²⁴ to first gelatinize the starch, and then for the reaction with the castor oil PUPs (Scheme 4.3) in a single process. The mixer was controlled by a torque rheometer, which enabled the continuous measurement of the torque throughout the reaction. Waxy maize starch (amylopectin content > 99%) and water as plasticizer (20 wt%) were added to the mixing chamber preheated to 90 °C, which resulted in a sharp increase in torque as the starch granules began to swell (Figure 4.5). In this high shear environment starch undergoes gelatinization quickly, which can be visualized as a drop in torque. After mixing the starch and water for 4 minutes, the castor oil PUP was slowly added (over 3 min) to the system. When the PUP was added too quickly, a sharp torque increase was observed and mixing could no longer be maintained. The torque increase was less pronounced and much more gradual with slow addition of the castor oil PUP. The addition of the castor oil PUP to the starch also resulted in a less than 5 °C temperature increase due to the higher torque and mechanical energy input (Figure 4.6) wrt the reaction without PUP, which can promote water losses from the system. For that

reason, the reaction was only allowed to proceed for up to 15 minutes from the moment when the starch was loaded, or else until the torque curve approached an infinite slope, which typically occurred between 25-30 Nm. A less pronounced increase in temperature accompanied the increase in torque. For all castor oil PUP reactions, the maximum torque was reached before the 15-minute set time limit. For increased weight loadings of castor oil PUP in the mixture, the upper torque limit was reached faster as expected. The increase in measured temperature was attributed to increased friction from the higher torque. The castor oil PUPs prepared with catalysts also reached the torque cut-off faster than the PUP without catalyst. As stated previously, the castor oil PUPs prepared with catalysts had more unreacted TDI and more oligomerization than the PUP without catalyst. Unreacted TDI may also act as a cross-linker for starch, but with a much lower molecular weight than the PUPs, thus increasing the molar equivalents of cross-linking molecules per gram of PUP. The effect of castor oil PUP oligomerization on cross-linking is unknown. After the reaction, the product was removed from the mixer, ground into a fine powder, and a portion was purified by Soxhlet extraction with acetone to remove any castor oil PUP not covalently bound to the starch.

The reaction of starch with the castor oil PUPs was confirmed by ^1H NMR analysis of the crude and purified products (Figure 4.7). Peaks corresponding to the GPy backbone protons on C2 and C4 overlap at 3.34 ppm, while the protons on C3, C5, and C6 overlap at 3.65 ppm. TFA was added to the NMR tube before analysis, to shift hydroxyl and any other labile protons



Scheme 4.3. Reaction of starch with castor oil PUP (many isomers possible). The reaction is drawn at the 2 position of the GPy units for simplicity, but reaction at the 2, 3 and 6 positions is possible.

present downfield. The signal for the proton on the anomeric (C1) carbon, appearing at 5.11 ppm, was used as reference when integrating peaks from the PUP components. Due to the low PUP loadings in the reactions, the only well-resolved peaks for the PUP component are upfield from the starch protons. The peak for the methyl protons of the fatty acid tails is visible at 0.82 ppm, the methylene protons not adjacent to functional groups appear at 1.23 ppm, and the peak from methylene protons beta to double bonds is at 1.49 ppm. The methyl peak at 0.82 ppm served to quantify the amount of PUP covalently bonded to the starch. The reaction efficiency (RE) was

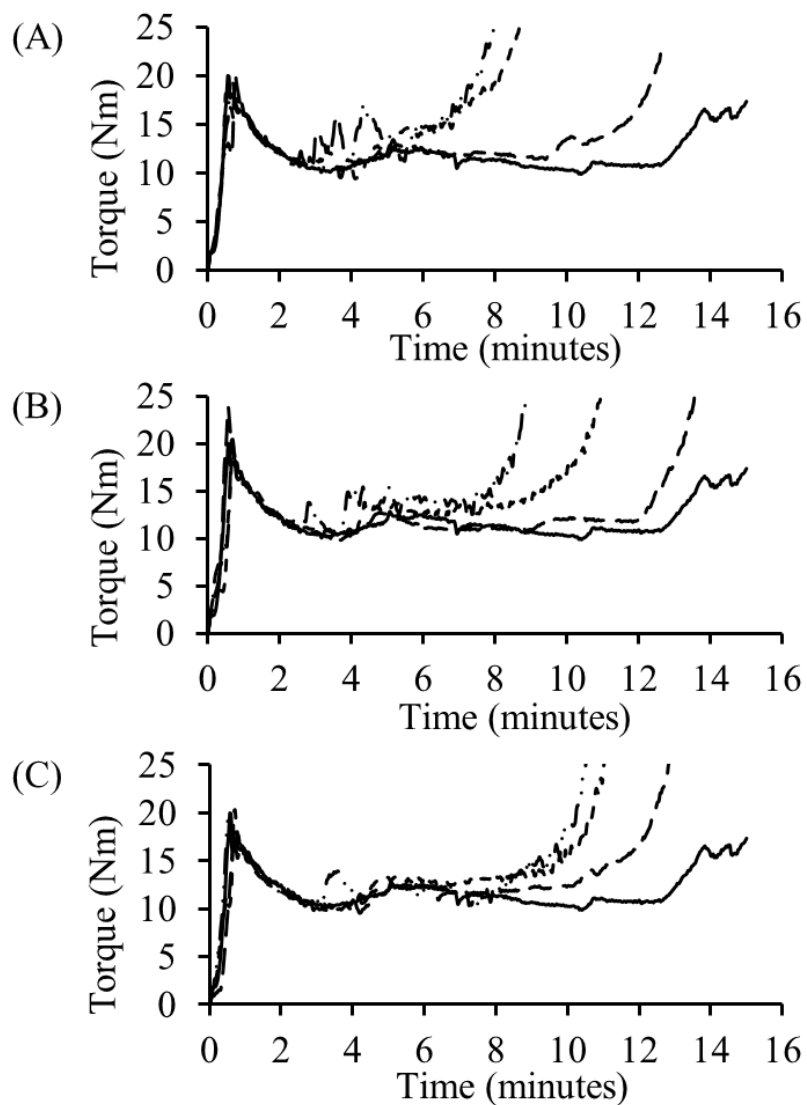


Figure 4.5. Typical torque curves for starch with water (—) and for starch reactions with (A) DBTDL-catalyzed PUP at weight loadings of 1.65 (— —), 4.84 (- - -) and 6.73 wt% (— . -); starch reactions with (B) K-KAT 348-catalyzed PUP at weight loadings of 1.62 (— —), 4.94 (- - -) and 6.86 wt% (— . -); starch reactions with (C) PUP without catalyst at weight loadings of 1.99 (— —), 5.05 (- - -) and 7.10 wt% (— . -).

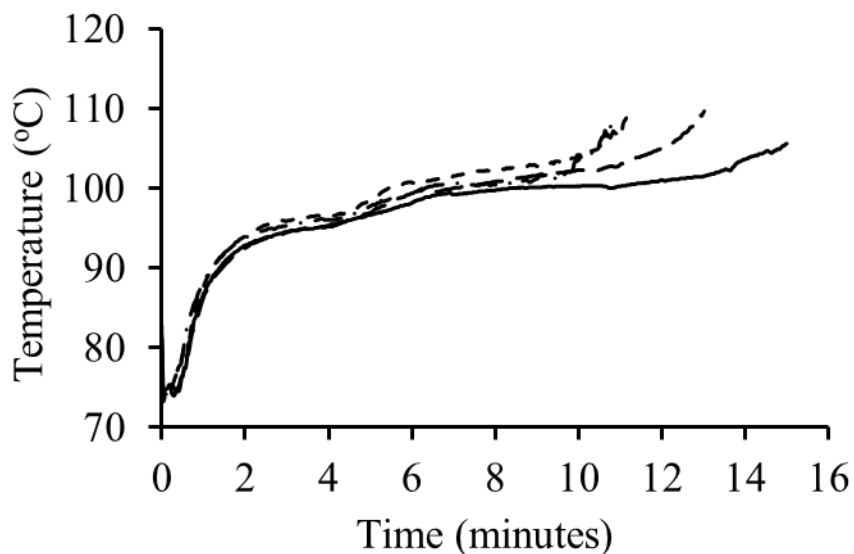


Figure 4.6. Typical temperature curves for starch with water (—) and for starch reactions with PUP without catalyst at weight loadings of 1.99 (— —), 5.05 (— — —) and 7.10 wt% (— . —).

determined by dividing the integral ratio for the methyl protons at 0.82 ppm and the peak at 5.1 ppm in the purified product, by the integral ratio for the same peaks in the crude product, and multiplying by 100%.

The RE was high (> 93%) for the reactions between starch and the DBTDL-catalyzed castor oil PUP at all weight loadings (Figure 4.8). Even the decreased reaction time, due to the fast torque increase, did not cause a noticeable decrease in RE, indicating that the reaction between the isocyanate groups and starch was fast. The reactions between starch and the K-KAT 348-catalyzed PUPs were also above 90% at all but the highest loading tested (9.0 wt%), where a RE of 80% was obtained. The reaction between starch and the PUP obtained without catalyst

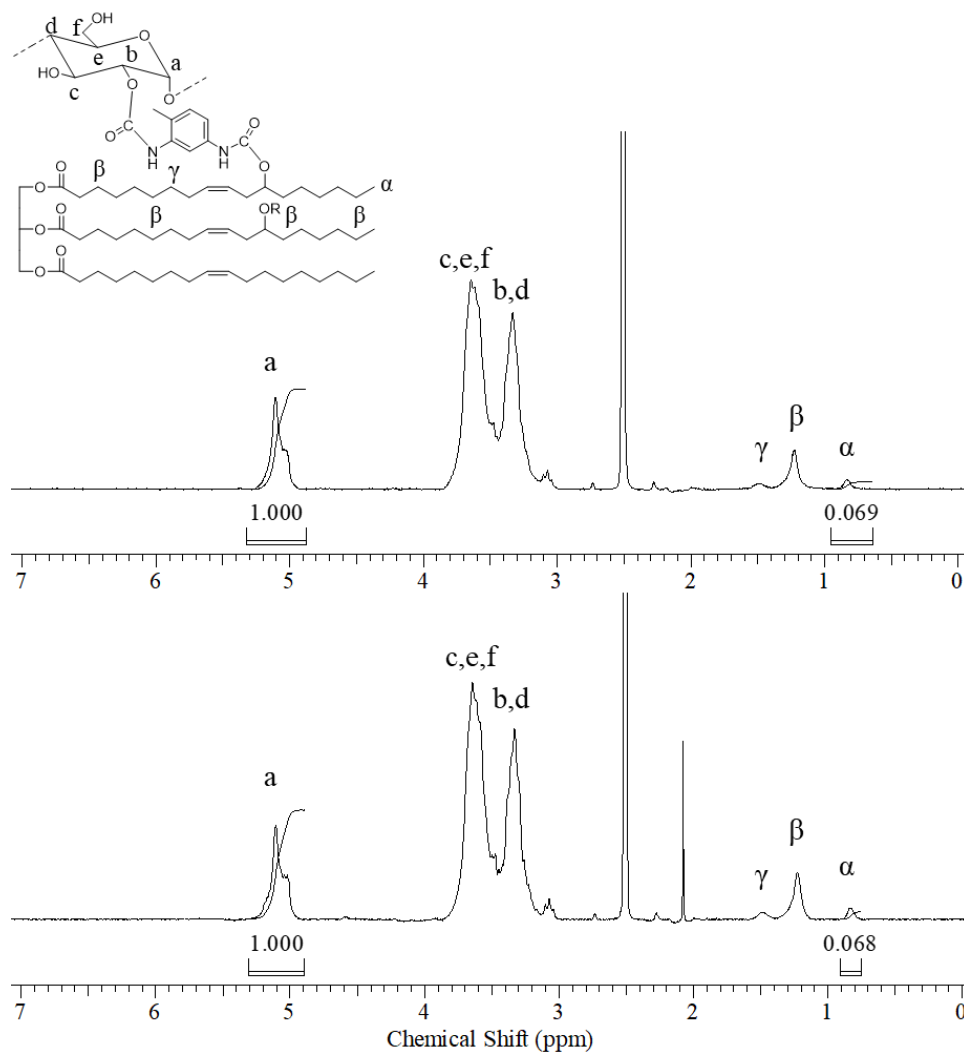


Figure 4.7. ¹H NMR spectra for the reaction between DBTDL-catalyzed PUP and starch at 4.84 wt% PUP loading, (top) before and (bottom) after purification.

followed the same trend as K-KAT 348, with the RE dropping to 82.4% at 9.4% loading. The small increase in temperature observed at higher loadings of PUPs did not result in an increase

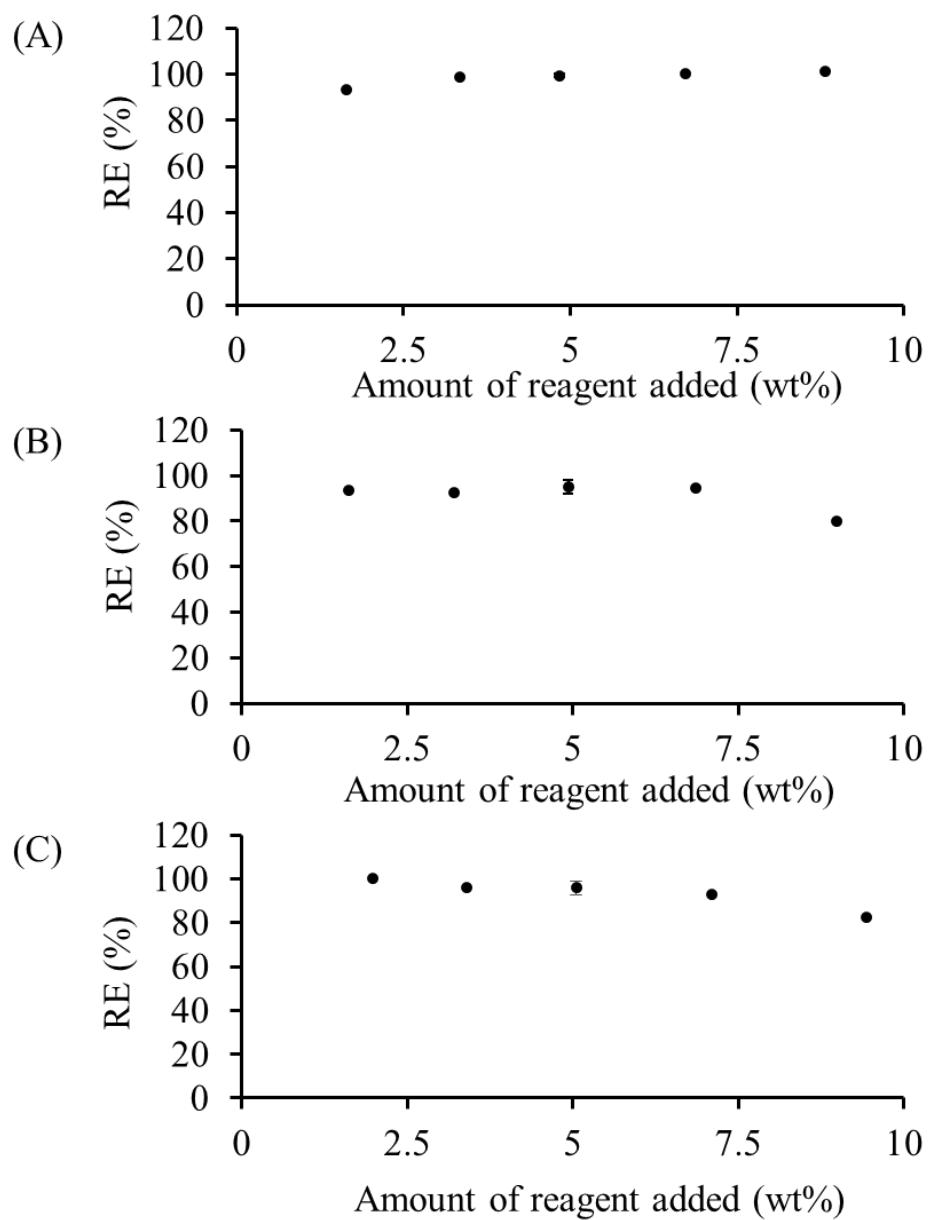


Figure 4.8. Reaction efficiency for starch and castor oil PUPs in a melt mixer catalyzed with (A) DBTDL, (B) K-KAT 348, and (C) without catalyst.

in RE. The high RE values achieved for the different PUPs in the melt mixer, in spite of the relatively short reaction times, indicate that the PUPs are tolerant to water and good candidates for extruder operations. Given the toxicity of TDI, it may be beneficial to purify the castor oil PUPs to remove monomeric TDI prior to these operations, however. Reactive extrusion would provide better mixing than the melt mixer used in the current investigation. Furthermore, higher temperatures and torques can be achieved in extrusion operations as compared with a melt mixer. Twin screw extruders have been shown to induce shear scission of the starch molecules in the melt phase, which could provide a further handle to control the molecular weight characteristics of the product.³³ Finally, the composition of the resulting vegetable oil-modified starch products should be more homogenous.¹⁶

4.4.3 Molecular Weight and Size of Castor Oil PUP-modified Starch

The solution properties of the different PUP-modified starch samples were examined by GPC analysis using 0.05 M LiBr in DMSO at 50 °C as mobile phase. The absolute molecular weight (MW) of each fraction (*i*) eluting from the column was calculated according to Eq. (3)

$$MW_i \cong \frac{LS_{Cal} \cdot RI_{Cal}}{n_o^3 \cdot v} \cdot \frac{LS_{i-\delta}}{RI_i} \quad (3)$$

where MW_i is the molecular weight corresponding to an elution volume V_i , LS_{Cal} and RI_{Cal} are the light scattering detector and differential refractive index detector response calibration factors, respectively, n_o is the refractive index of the mobile phase, v is the volume of the eluted fraction

(mL), RI_i is the RI detector signal, and $LS_{i-\delta}$ is the light scattering signal corrected for an offset δ with respect to the RI detector. Using an online viscometer, the specific viscosity of each slice of the eluent was also measured for the samples. Dividing the specific viscosity by the concentration (from the RI detector), the intrinsic viscosity $[\eta]$ was obtained and used to calculate the hydrodynamic radius (R_h) and diameter ($D_h = 2R_h$) of the starch molecules using Eqs. (3)-(7):

$$\eta = \eta_o (1 + 2.5\phi) \quad (4)$$

The Einstein equation (4) relates the viscosity of the sample solution η to the viscosity of the pure mobile phase (η_o) and the volume fraction ϕ of the molecules in solution. When transforming Eq. (4) to include the $[\eta]_i$, and expressing ϕ in terms of the volume of a sphere (Eq. (6)), Eq. (7) is obtained where N_A is Avogadro's number and n_i is the molar concentration.

$$V_h = \frac{4}{3} \pi R_h^3 \quad (5)$$

$$[\eta]_i MW_i = \frac{10\pi N_A}{3} \left(\frac{D_{hi}}{2}\right)^3 \quad (6)$$

$$D_h = \frac{\sum n_i D_{hi} [\eta]_i}{\sum n_i [\eta]_i} \quad (7)$$

The number-average molecular weight (M_n), weight-average molecular weight (M_w), \bar{D} , and D_h obtained for the starch samples are summarized in Table 4.2. To determine the MW of unmodified starch, waxy maize starch granules were subjected to the same procedure for the

PUP reactions with starch, except no PUP was added. The resulting starch product had $M_n = 1.9 \times 10^7$ g/mol, $M_w = 7.1 \times 10^7$ g/mol, $D = 3.7$, and $D_h = 150$ nm.

It was previously shown that the reaction of starch with a cross-linker under high shear can result in starch products with lower molecular weights and D_h as compared to starch processed under identical conditions without cross-linker.³⁴ The authors noted that it is not the addition of the cross-linker *per se* which leads to lower molecular weights. The addition of the cross-linker rather increases the torque and temperature, due to the formation of a cross-linked network, and it is the increased torque which is responsible for fragmentation of the starch, while the increased temperature also softens the starch and makes it more susceptible to shear-induced fragmentation. On that basis, decreases in molecular weight and D_h are expected following the addition of a castor oil PUP to starch in the melt mixer. This was not observed for the DBTDL-catalyzed castor oil PUP-modified starch. While the addition of DBTDL-catalyzed PUP to the starch indeed resulted in a torque increase, the reaction had to be stopped much before the 15 minute mark. The decreased reaction time presumably led to less fragmentation of the modified starch in comparison with the starch processed for 15 minutes without PUP. Using the K-KAT 348-catalyzed product to modify starch, a similar trend was observed with a similar small increase in MW and D_h . At higher loadings of K-KAT 348-catalyzed castor oil PUP (6.86 and

Table 4.2. Molecular weight and hydrodynamic diameter (D_h) of PUP-modified starch samples determined from GPC analysis.

PUP	PUP wt%	M_n (g/mol)	M_w (g/mol)	\bar{D}	D_h (nm)
N/A	0	1.9×10^7	7.1×10^7	3.7	150
DBTDL	1.65	4.5×10^7	1.1×10^8	2.4	180
	3.34	3.8×10^7	1.3×10^8	3.6	190
	4.84	4.1×10^7	1.3×10^8	3.1	190
	6.73	3.8×10^7	1.1×10^8	2.9	180
	8.82	2.6×10^7	7.7×10^7	2.9	160
K-KAT 348	1.62	6.9×10^7	1.4×10^8	2.0	200
	4.93	6.4×10^7	1.5×10^8	2.4	200
	6.86	1.1×10^7	3.2×10^7	3.0	110
	8.99	6.6×10^6	3.2×10^7	4.8	100
No catalyst	1.99	3.6×10^7	1.0×10^8	2.9	190
	5.05	1.5×10^7	5.7×10^7	3.9	140
	7.10	4.1×10^6	1.9×10^7	4.5	78
	9.43	3.2×10^6	1.7×10^7	5.2	84

8.99 wt%), a decrease in MW and D_h was nevertheless observed as compared to lower PUP loadings and unmodified starch. The MW of the higher loading K-KAT 348-catalyzed castor oil PUP-modified starch even decreased by more than a factor of 4 and the D_h decreased by 45% for the 6.86 wt%-modified starch product, and D_h decreased by 50% at 8.99 wt% PUP loading as compared to the 1.62 and 4.93 wt% loadings.

Interestingly, in the case of the castor oil PUP prepared without catalyst, the onset of fragmentation occurred at lower castor oil PUP weight loadings. Similarly to the other PUP systems, starch modified with 1.99 wt% PUP without catalyst had a small increase in MW and D_h as compared to the unreacted starch. At 5.05 wt% PUP loading without catalyst the MW and

D_h were similar to unmodified starch, while the MW of the products at 7.10 and 9.43 wt% loadings decreased more than 5-fold and the D_h decreased by more than 50% as compared to starch modified with 1.99 wt% PUP without catalyst.

While the MW and D_h decreased in many cases with the addition of PUP, the magnitude of the observed decreases varied for the different PUP systems. As expected, the decreases were more pronounced for longer mixing intervals under high torque. The duration of the reactions in the melt mixer followed the trend of DBTDL-catalyzed PUP < K-KAT 348-catalyzed PUP < PUP prepared without catalyst. The magnitude of the MW and D_h decreases was larger at higher PUP loadings, following the trend PUP prepared without catalyst > K-KAT 348-catalyzed PUP > DBTDL-catalyzed PUP. Interestingly, this is the same trend observed for the amount of unreacted TDI in the PUPs. The presence of catalyst and increased levels of monomeric TDI in the PUP led to decreased reaction time. A mechanistic study is required to determine the influence of each on the reaction duration and the decrease in MW and D_h of the products due to shear-induced fragmentation. It therefore appears that the trends observed are the result of the combined effects of the relative cross-linking reaction rate (and torque increase rate) and the total mixing time, determined by the upper torque limit set in the experiments.

Wu and coworkers^{30,36-40} reported a series of reactions for starch with different PUPs, including castor oil PUPs synthesized with MDI rather than TDI, in a melt mixer. In their case, the PUPs were mixed with the starch granules before gelatinization in a melt mixer. They also used water as plasticizer, but as much as 55 wt% with respect to the starch, much more than the

20 wt% content used herein. They also claimed to have a high RE, based on a gravimetric assay using a single extraction with butyl acetate. While they supplemented these results with FTIR analysis, no attempt was made to quantify the RE for each reaction formulation using (more reliable) spectroscopic analysis techniques. Dynamic light scattering analysis of a modified starch product obtained at 25 wt% PUP loading indicated an increase in average molecular size as compared with unmodified starch. In the current investigation, ^1H NMR analysis was used to quantify the amount of PUP covalently bonded to the starch, following exhaustive extraction on a Soxhlet apparatus to remove any free PUP from the samples. The RE was determined to remain relatively constant for PUP loadings of up to ca. 10 wt%. Through GPC measurements, the MW and D_h were shown to decrease at high PUP loadings under the conditions used, which is in contrast with the results of Wu and coworkers.

4.5 Conclusions

Starch was successfully cross-linked with castor oil PUPs in an environmentally friendly procedure using water as plasticizer. Castor oil was selected as a vegetable oil feedstock for the preparation of the PUPs, because its high ricinoleic acid content makes it attractive as a replacement material for petroleum-derived polyols. The hydroxyl groups in castor oil were fully reacted with TDI to form castor oil PUPs in the absence of solvents. Since no small molecule by-products were formed in the reaction, the products do not require further purification if properly handled (due to the presence of residual TDI). However if the PUPs are to be used on large scale (e.g. in extrusion operations), it may be advantageous to purify the products in a thin

film evaporator to remove unreacted TDI. Fortunately, this should be relatively easy to achieve since all the products obtained are liquid at room temperature and would flow easily in the evaporator, unlike PUPs synthesized with MDI.

While DBTDL is typically added to catalyze the reaction of alcohols with isocyanates, it was found that the uncatalyzed reaction yielded a PUP with a %NCO content similar to the DBTDL-catalyzed product, and the uncatalyzed PUP product contained about 50% less unreacted TDI in comparison to the DBTDL-catalyzed product. The PUPs obtained with the DBTDL and K-KAT 348 catalysts also contained more oligomerized triglycerides than the uncatalyzed PUP product, as determined by GPC analysis.

The reactions between starch and the castor oil PUPs were shown to proceed with a high overall RE, such that further purification of the product should not be necessary. The hydrophilic-hydrophobic balance of the modified starch could be predictably tuned for specific applications by that approach. Finally, the size of the resulting starch molecules can be controlled through the amount of castor oil PUP added, when the reaction is carried out under high shear.

Chapter 5

Maleation of Linseed and Soybean Oils

5.1 Abstract

Petroleum-based products have traditionally dominated the marketplace because of their low cost, but due to depleting petroleum supplies there is increasing need to develop new materials from sustainable feedstocks. Vegetable oils are a renewable resource that is cost-effective and hydrophobic. In the current investigation, linseed oil and soybean oil were reacted with maleic anhydride (MA) in an ene reaction. Reactions were completed in benchtop sealed high pressure and open glass reactors, and in a pilot plant open glass reactor. In contrast to soybean oil, the reaction between linseed oil and MA led to cross-linking of the product under most reaction conditions investigated. The reaction between soybean oil and MA was optimized in terms of temperature and time. The products were characterized by ^1H NMR, soap numbers and gel permeation chromatography (GPC) analysis. At low MA loading the benchtop sealed reactor was more efficient in terms of MA conversion, while at higher loadings the open reactor was more efficient. Following the benchtop reactions, the procedure was completed on a pilot plant scale in a glass reactor. These reactions were more efficient at lower loadings, but slightly less efficient than in the benchtop open reactor at the highest loading. Analysis by GPC revealed significant oligomerization and triglyceride degradation in the sealed reactor products. In comparison, the products synthesized in both open glass reactors had significantly less

oligomerization and no significant triglyceride degradation. A new procedure developed to quantify unreacted triglycerides in the maleated oils revealed that some of the products obtained contained less than 1 wt% unreacted triglyceride.

5.2 Introduction

Alkenyl succinic anhydrides (ASAs) are commonly used to modify starch, to make it more hydrophobic, for applications including FDA-approved food additives, binders in papermaking, and adhesives. Alkenyl succinic anhydrides are currently synthesized from petroleum-based alpha-olefins and maleic anhydride (MA).¹ This class of petroleum products have traditionally dominated the marketplace because they have a relatively low cost, are readily available and display desirable hydrophobicity characteristics. However due to depleting petroleum supplies, there is increasing need to develop materials from renewable feedstocks.²

One class of hydrophobic materials derived from agriculture are vegetable oils. They have been extracted from different sources for thousands of years, and have found many applications as edible and industrial materials. Vegetable oils are triglycerides (Figure 5.1), containing a glyceryl moiety bound to three fatty acids via ester bonds.³ The composition of the fatty acids varies with the plant source. The fatty acids vary in length and may contain a single double bond (e.g. oleic acid), two double bonds (e.g. linoleic acid), three double bonds (e.g. linolenic acid), or a saturated carbon chain (e.g. stearic acid). Vegetable oils are commonly classified into 3 different groups. Drying oils, such as linseed oil and tung oil, have a high degree of unsaturation and form hard cross-linked networks when exposed long enough to oxygen; they

have an iodine value (mass of iodine consumed per 100 grams of material) greater than 140.⁴ Non-drying oils, such as olive oil and peanut oil, have a low degree of unsaturation, do not harden when exposed to oxygen, and have iodine values of less than 125. Finally, semi-drying oils, such as soybean oil and corn oil, have a moderate unsaturation level, partially harden when exposed to oxygen long enough, and have iodine values between 125 and 140.⁵

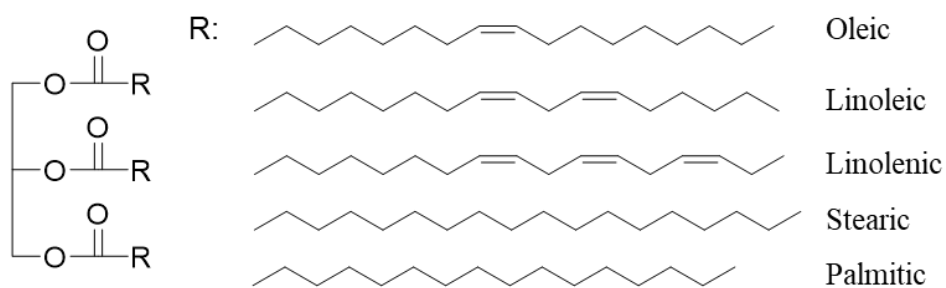


Figure 5.1. Structure of triglyceride and common fatty acids.

It has long been recognized that unsaturated fatty acids react with MA at high temperatures. Polyunsaturated fatty acids, such as linolenic and linoleic acid, are more reactive than mono-unsaturated fatty acids.⁶ Wool and coworkers⁵ suggested that the reaction proceeds through an ene (also referred to as Alder-ene) mechanism, in which the unsaturated fatty acid chains containing allylic hydrogen(s) act as the “ene”, and MA acts as the enophile (Figure 5.2). In the concerted reaction, a new carbon-carbon bond is formed between the fatty acid and the anhydride ring, while an allylic hydrogen shifts from the fatty acid to the anhydride ring, and there is migration of the double bond on the fatty acid tail by one carbon atom. The net result is

the loss of the double bond on maleic anhydride, and the formation of a new carbon-carbon single bond. Depending on the fatty acid involved, conjugated double bonds may be formed that could subsequently undergo Diels-Alder addition with another MA molecule. In their investigation, Wool and coworkers⁵ synthesized maleated soybean oil in a sealed reactor to prepare condensation polymers, by subsequent reaction with various polyols. They screened different catalysts for the reaction and reported that when a Lewis acid catalyst was used, the integrity of the anhydride ring may be lost. When a peroxide was used, there was an increase in viscosity of the product which they attributed to the copolymerization of maleic anhydride and the soybean oil. The resulting maleated soybean oil-based condensation polymers formed upon reaction with various polyols were not rigid solids, but rather soft and flexible as expected. Narayan and coworkers² reported using peroxides, 2,5-bis(*tert*-butylperoxy)-2,5-dimethylhexane (Luperox 101) and di-*tert*-butyl peroxide, as catalysts for the reaction between soybean oil and maleic anhydride. The authors hypothesized that the peroxide would catalyze the isomerization of the double bonds in linoleic acid, to form conjugated double bonds, followed by a Diels-Alder reaction between MA and the linoleic acid residues. The theoretical maximum incorporation by this approach would be one mole of maleic anhydride per mole of linoleic acid residues, corresponding to around 1.5-1.7 on average per triglyceride for soybean oil.⁴ In practice, the incorporation of maleic anhydride plateaued around one anhydride unit per triglyceride. Excess MA did not result in higher substitution and needed to be removed from the product, which was time-consuming and undesirable for large-scale production. Rosenau and

coworkers⁷⁻¹⁰ reported a series of thorough investigations on the synthesis, characterization, and applications of maleated vegetable oils. They first screened different oils, namely canola (rapeseed), high oleic sunflower, soybean, and linseed oils, as ene sources. They desired a low viscosity maleated product, to serve as bio-based paper sizing agent. It was found that canola and high oleic sunflower oil had the best properties for this application. In their procedure, excess MA had to be distilled off after the reaction, similarly to Narayan and coworkers. The chemical structure of high oleic sunflower oil and the maleated product was investigated, as well as the stability of the anhydride ring in the maleated products and the parent ASAs in aqueous environments comparable to those encountered in papermaking.

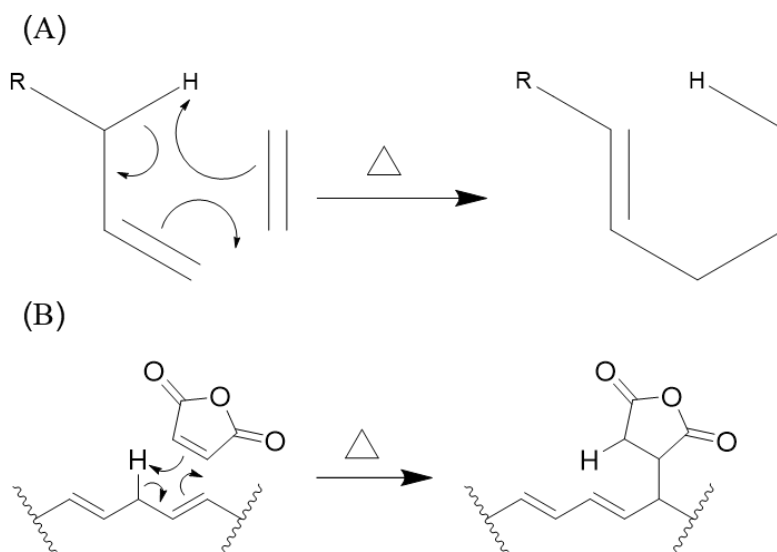


Figure 5.2. (A) Ene reaction mechanism between an ene and an enophile. (B) Ene reaction between a non-conjugated double bond (ene) with an allylic hydrogen and maleic anhydride (enophile).

The goal of the current investigation was to synthesize maleated vegetable oil, initially on a bench scale for proof of concept, followed by synthesis on a pilot plant scale, and characterization of the products. To be useful in subsequent reactions, such as the modification of starch, the product should contain minimal levels of free maleic anhydride, catalyst, solvent, and unreacted triglyceride. Linseed oil was initially selected as substrate because of its high linolenic acid and decreased low saturated fatty acid contents, but was replaced with soybean oil on the basis of the initial results obtained. The variables investigated included the reaction temperature and time, and the use of different solvents and reaction vessels. The maleated products were analyzed in terms of ^1H NMR spectroscopy, soap numbers, gel permeation chromatography (GPC), and the unreacted triglycerides content was determined by a novel procedure described herein.

5.3 Experimental Section

5.3.1 Materials

Organic solvents including toluene (ACS reagent, $\geq 99.0\%$), ethanol (reagent, $\geq 99.0\%$), hexanes (reagent, $\geq 99.0\%$), tetrahydrofuran (reagent, $\geq 99.0\%$), and deuterated chloroform (99.8% atom), and the reagents maleic anhydride (MA; reagent, 99%), potassium hydroxide (reagent, 99 %), monobasic potassium phthalate (ACS reagent), phenolphthalein (ACS reagent), pentaerythritol tetrakis(3-(3,5-di-*tert*-butyl-4-hydroxyphenyl)propionate) (Irganox 1010, 98%) were all purchased from Sigma Aldrich. Raw linseed oil and soybean oil, with assumed

molecular weights of 871 and 872 g/mol, and were purchased from Canadian Tire (Toronto, ON, Canada) and G&C Foods (Syracuse, NY, USA), respectively.⁴ All the chemicals were used as received from the suppliers.

5.3.2 Maleation of Linseed Oil in a Sealed High Pressure Reactor

Raw linseed oil (50 g, 57.3 mmol) and MA (25.3 g, 258 mmol, 4.5 eq) were charged into a 600 mL Parr 4563 reactor equipped with a stir-shaft, a pressure gauge, a sampling tube, a thermocouple thermometer, addition ports and a 4842 digital temperature controller. The reaction mixture was degassed by bubbling nitrogen through the sampling tube before heating to 200-230 °C for up to 4 hours. The heater was then turned off and the reactor was allowed to cool to 90 °C, the pressure was released and the reactor was emptied.

5.3.3 Maleation of Soybean Oil in a Sealed High Pressure Reactor

Similarly to linseed oil, soybean oil (50 g, 57.3 mmol) and MA (25.3 g, 258 mmol, 4.5 eq) were charged into the Parr reactor described above. After degassing with nitrogen, the reactor was heated to 200-230 °C for up to 4 h. The reactor was emptied after cooling to 90 °C and releasing the pressure. The same procedure was repeated using 1.7 and 3 equivalents of MA.

5.3.4 Maleation of Soybean Oil in an Open Glass Benchtop Reactor

Soybean oil (50 g, 57.3 mmol) was charged into a three-neck glass round-bottomed flask fitted with a nitrogen line, a thermocouple thermometer, a condenser, and a bubbler. MA (25.3

g, 258 mmol, 4.5 eq) was added when the soybean oil reached 200 °C. After 4 h, heating was stopped and the reaction mixture was removed after cooling. The procedure was repeated using 1.7 and 3 equivalents of MA.

5.3.5 Maleation of Soybean Oil on a Pilot Plant Scale

Soybean oil (15.3 kg, 17.5 mol) was charged into a 30 L glass reactor equipped with an impeller mechanical stirrer, a nitrogen line, a thermocouple thermometer, a condenser, an addition port, a bubbler, and a heating mantle. When the soybean oil reached 200 °C, the melted MA (7.7 kg, 78.5 mol, 4.5 eq) was added in 3 aliquots under positive nitrogen pressure at 30 minute intervals, for a total reaction scale of 23 kg. Four hours after completing the MA addition the heat was removed, the reaction mixture was allowed to cool to 90 °C, and drained from the reactor. The procedure was repeated using 1.7 and 3 equivalents of MA, while maintaining a reaction scale of 23 kg.

5.3.6 Soap Number Determination (ASTM D94-07)

Soap numbers for the oil samples were determined following ASTM D94 – 07.¹¹ The oil (0.6883 g) was weighed into an Erlenmeyer flask and 20.00 mL of 0.5 M KOH in ethanol were added. The mixture was refluxed for 1 h, several drops of phenolphthalein (1% solution in methanol) were added and the mixture was titrated against standardized HCl until no purple color persisted. The soap number, expressed in milligrams of KOH per gram of oil sample, was calculated using Equation 1, where B is the volume of acid required for titration of 20.00 mL of

0.5 M KOH without oil (mL), A is the volume of acid required for titration of the sample (mL), N is the concentration of standardized HCl (mol/L), M_{KOH} is the molar mass of KOH (56.1 g/mol), and C is the sample weight (g).

$$SN = \frac{(B-A) \times N \times M_{\text{KOH}}}{C} \quad (1)$$

5.3.7 ^1H NMR Analysis

^1H nuclear magnetic resonance (NMR) spectroscopy was performed on a Bruker 300 MHz spectrometer. The concentration of all the samples was 15–30 mg/mL in CDCl_3 and 32 scans were averaged. The chemical shifts were determined using the residual solvent proton signal at 7.27 ppm as reference.

5.3.8 Gel Permeation Chromatography (GPC) Analysis

Analytical GPC measurements for the oil samples were performed on a Malvern GPCmax instrument with a TDA 305 triple detector array, a 2600 UV detector, and two 300 mm \times 8.0 mm I.D. PolyAnalytik SuperesTM single pore columns having linear polystyrene molar mass ranges of up to 70 kDa and 1.5 kDa in series. A flow rate of 1.0 mL/min was used with tetrahydrofuran (THF) as the mobile phase at 35°C. Samples were prepared at a concentration of 1 mg/mL in THF and filtered through a 0.2 μm polytetrafluoroethylene filter.

5.3.9 Quantification of Unreacted Triglycerides

Maleated soybean oil (5.31 g) was loaded onto a silica gel column (25 mm diameter × 350 mm length; bed volume 60 mL) in hexanes. The column was first eluted with hexanes (500 mL), followed by THF (300 mL), and the two fractions were collected. The solvents were removed with an air stream under mild heating. The residual products were redissolved and transferred into tared glass vials, dried for 16 hours at 80 °C under reduced pressure and weighed. The products were characterized by ¹H NMR and GPC analysis.

5.4 Results and Discussion

5.4.1 Maleation of Linseed Oil

Linseed oil was initially selected as a maleation substrate because of its high unsaturation level, with 57.8% of linolenic acid and 15.7% linoleic acid tails. As stated above, these two fatty acids have a higher reactivity towards MA as compared to oleic acid. Linseed oil also has a lower amount of saturated fatty acids, 3.2% of which are stearic acid and 5.6% palmitic acid, both being unable to react with MA in an ene reaction. The remaining 17.7% fatty acid is the monounsaturated oleic acid. Among all the vegetable oils produced on a large scale, linseed oil appeared to have the most promising combination of polyunsaturated fatty acids (73.5% content overall) and minimal saturated fatty acids (8.8%). One of the goals was to minimize the amount of unreacted triglycerides in the product. The rationale for this was that unreacted triglycerides would be unable to participate in subsequent reactions in replacement for ASAs. A high

unsaturation level should also favor a high reaction efficiency (RE) for MA. Consequently, linseed oil was first reacted with MA in a sealed high pressure reactor as a proof of concept. The reaction products were characterized by ^1H NMR and soap numbers analysis. The influence of an antioxidant (Irganox 1010) and a solvent (toluene) on the maleation reaction was also investigated for linseed oil. The reaction temperature and time were then optimized.

The reaction between linseed oil and MA, when carried out at 230 °C for 4 h (following the procedure of Wool and coworkers⁵), yielded a dark solid product that was difficult to remove from the reactor. The procedure was repeated after adding 5 wt% toluene to the reaction, but the product was still incompletely soluble in chloroform and other common organic solvents. The ^1H NMR spectrum obtained for linseed oil (Figure 5.3(A)) is similar to that reported for high oleic sunflower oil,⁸ with distinct integration ratios due to the different fatty acid distribution. The peaks at δ 5.3 and 4.25 ppm correspond to the glyceryl backbone protons. The methyl protons from the fatty acid tails are at 0.8 ppm, except for linolenic acid residues that have a resonance at 1.0 ppm. The methylene protons not adjacent to functional groups appear at 1.3 ppm, while those beta to carbon-carbon double bonds are at 1.6 ppm, and methylene protons alpha to double bonds are at 2.1 ppm. Methylene protons alpha to carbonyl groups are at 2.3 ppm, and methine protons are at 2.8 ppm. Finally, the signals from alkene protons of unsaturated fatty acid tails overlap with a glyceryl proton at 5.3 ppm. There was no significant peak downfield from chloroform, indicating that there were no free carboxylic (fatty) acids in the material. Analysis of the soluble fraction of the reaction product (Figure 5.3(B)) revealed no

detectable amount of unreacted maleic anhydride, as evidenced by the absence of peaks for MA at 7.04 ppm, and for maleic acid around 6.5 ppm. The resonance signals in the product are broader than in the linseed oil substrate, which suggests the formation of oligomeric species. New broad peaks in the product appeared between 2.5 and 3.5 ppm, corresponding to protons in succinic anhydride rings bound to the fatty acid tails, and to the proton on the tertiary carbon covalently bound to the anhydride ring, respectively. In addition to reduced mobility of the oligomers, the broad peaks are likely due to the fact that linseed oil is a statistical mixture of triglycerides with different fatty acids tails, which can yield a large number of regioisomers in the product. These broad peaks overlap with the methine proton signals, making quantification of the maleation level solely by ^1H NMR analysis inaccurate. Finally, the alkene protons no longer appear as a singlet but rather as broad multiple peaks, due to the migration of double bonds during the reaction.

To determine the average number of anhydride units incorporated per triglyceride, soap numbers were determined according to Eq. 2, by refluxing the product with a known amount of excess base (KOH) in ethanol, to ensure that all the hydrolysable groups reacted. The sample was then back-titrated with a standardized hydrochloric acid solution, to determine how much base was consumed in the first step. This quantity is reported in mg of KOH consumed per g

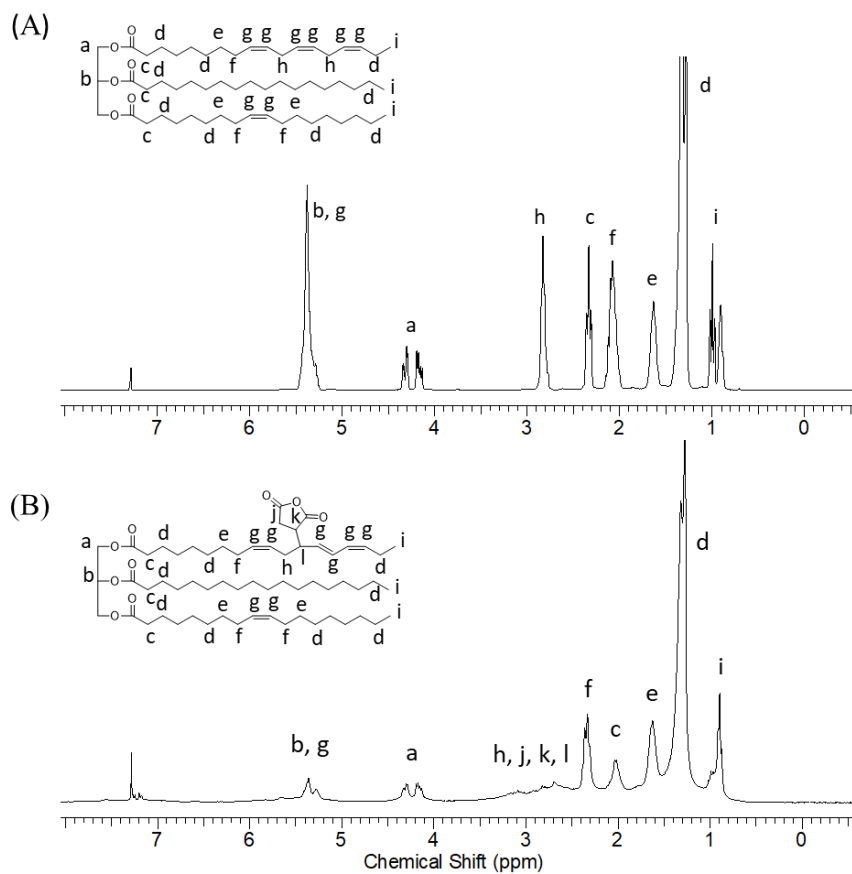


Figure 5.3. ^1H NMR spectra for (A) raw linseed oil and (B) maleated linseed oil synthesized with 4.5 eq. of MA in a sealed reactor with 5 wt% toluene added.

of sample. A triglyceride contains 3 ester bonds, each consuming 1 equivalent of base during saponification, producing one molecule of glycerol and 3 potassium fatty carboxylate salts. Each anhydride ring introduced in the triglyceride will consume 2 equivalents of base (one to open the anhydride ring, and one to neutralize the additional carboxylic acid group produced). The

average molar mass of the maleated oil will also increase by the mass of the MA units added. From the soap numbers obtained for the maleated products, the average number n of maleic anhydride units incorporated per triglyceride (MA/TG) was calculated by rearranging Eq. 2 (for the soap number) into Eq. 3, where M_{KOH} is the molar mass of potassium hydroxide (56.1 g/mol), M_{Oil} is the average molar mass of the oil before modification (assumed to be 871 g/mol for linseed oil), and M_{MA} is the molar mass of MA (98.1 g/mol). Eqs. 2 and 3 are valid as long as no residual MA is present in the sample.

$$SN = \frac{(3+2n) \times M_{KOH} \times 1000 \frac{g}{mg}}{M_{Oil} + M_{MA} \times n} \quad (2)$$

$$n = \frac{3 * M_{KOH} \times 1000 \frac{g}{mg} - SN \times M_{Oil}}{SN \times M_{MA} - 2 \times 1000 \frac{g}{mg} \times M_{KOH}} \quad (3)$$

During saponification all the insoluble (cross-linked) maleated linseed oil component became completely soluble, in contrast to the samples prepared for NMR analysis, indicating that the polyfunctional fatty acid tails play a role in the cross-linking reaction. In an attempt to decrease cross-linking of the triglycerides, an antioxidant, Irganox 1010, was added to the reaction along with toluene. The addition of small amounts of Irganox 1010 (up to 1 mol% with respect to the oil) did not suffice to prevent cross-linking, the resulting product being incompletely soluble in chloroform, but dissolving as the ester bonds were hydrolysed in the soap number determinations. The products obtained with the addition of 50 wt% toluene had a low viscosity when removed from the reactor, but were very viscous after removal of the toluene

under reduced pressure. Toluene was nevertheless most effective at preventing extensive cross-linking, the maleated products being completely soluble in organic solvents irrespective of whether Irganox was added. The RE, expressed as the fraction of MA added becoming incorporated in the maleated product, reached 33-38% in all cases (Table 5.1) regardless of whether Irganox 1010 was present, indicating that the antioxidant did not inhibit the ene reaction. Finally, there was no significant change in RE upon dilution with toluene, with less than 2% difference as the toluene content was increased from 5 to 50 wt% (Table 5.1). On the basis of these results, 50% toluene was added to the maleation procedure with linseed oil to obtain a very viscous, albeit soluble liquid product.

Table 5.1. Soap numbers and MA incorporation in Alder-Ene reaction with linseed oil, using 4.5 MA/TG at 230 °C for 4 h.

Toluene (wt%)	Irganox 1010 (mol %)	SN (mg KOH/ g oil)	<i>n</i> (MA/TG)	RE (%)	Solubility in CDCl₃
5	0	346	1.7	37.8	-
5	0.2	330	1.5	33.3	-
5	1	343	1.7	36.9	-
50	0	330	1.5	33.3	+
50	0.2	336	1.6	35.1	+

The maleation of linseed oil was optimized using 4.5 molar equivalents of MA/TG and toluene (50 wt%) at 230 °C in a sealed high-pressure reactor, by removing samples at time $t = 0$, 0.25, 0.5, 0.75, 1, 1.5, 2, 3, and 4 h, to monitor the consumption of MA over time by ¹H NMR

analysis. The reaction was considered complete when there was less than 0.15 molar equivalent (1.7 wt%) of unreacted MA/TG in the product (Table 5.2). The procedure was repeated at 200 °C for linseed oil with toluene (50 wt%). When the reaction was carried out at 200 °C instead of 230 °C, there was a significant increase in MA incorporation level. The reaction time had to be increased to 1.5 hour to maintain a residual MA content below 2 wt%. This indicates that the addition of MA to the double bonds in the fatty acid tails competes with the degradation of MA. Given that toluene was necessary to produce a non-cross-linked product from linseed oil, soybean oil was selected for the subsequent work.

Table 5.2. Soap numbers and MA incorporation in ene reaction with linseed oil, using 4.5 eq. MA and 50 wt% toluene in a sealed reactor.

Temperature (°C)	Time (h)	<i>n</i> MA/TG	RE (%)	Unreacted MA (wt%)
230	0.5	2.1	47.8	< 0.1
200	1.5	2.5	55.1	< 0.1

5.4.2 Maleation of Soybean oil

While linseed oil was initially selected as substrate due its high unsaturation level, the complications encountered with cross-linking led to considering a different oil feedstock for maleation. Similarly to linseed oil, soybean oil contains a large fraction of polyunsaturated fatty acids. The main difference is that soybean oil contains only 8.1% of linolenic acid and 53.7% of

linoleic acid fatty acid tails, as compared with 57.8% and 15.7% in linseed oil, respectively. As stated above, these two fatty acids are expected to have a higher reactivity towards MA and represent 61.8% of the fatty acids in soybean oil. Similarly to linseed oil, soybean oil has a low amount of saturated fatty acids (4.3% stearic acid and 10.1% palmitic acid). While this is higher than in linseed oil (8.8% in all), it should be low enough to minimize the amount of unreacted triglycerides in the final product. Soybean oil was therefore reacted with MA under the same conditions used for linseed oil, except that no toluene addition was necessary. In this case, the reaction mixture included only soybean oil and MA. Reactions were first completed in a sealed reactor. The reaction temperature and duration were optimized using 4.5 eq. of MA. After determining the optimal temperature, a range of maleated soybean oil products were synthesized using 1.7, 3, and 4.5 eq. of MA. The procedure was then adapted to a small scale benchtop open reactor before moving to a pilot plant scale open glass reactor. All the reaction products were characterized by ^1H NMR and soap numbers. Unlike linseed oil, the soybean oil products were completely soluble, which allowed their analysis by GPC.

Reaction of soybean oil with MA in a sealed reactor. The reactions of soybean oil with MA, without catalyst or solvent, yielded a dark viscous liquid product that was completely soluble in organic solvents, even without toluene addition. The ^1H NMR spectrum for soybean oil (Figure 5.4(A)) is similar to linseed oil, but since it contains less than one percent linolenic acid, the methyl proton signal is predominantly at δ 0.8 ppm. The peak at 5.3 ppm is also less intense than for linseed oil, because soybean oil contains fewer double bonds per triglyceride.

The ^1H NMR spectrum for the product (Figure 5.4(B)) reveals a trace amount of MA at δ 7.04 ppm, but no detectable maleic acid around 6.5 ppm. Similarly to maleated linseed oil, the proton peaks in the soybean oil product are broader than in the starting material, which is indicative of the formation of oligomers. Since soybean oil is also a statistical mixture of triglycerides with different fatty acids tails yielding multiple isomers, the protons characteristic for the added MA units appear between 2.5 and 3.5 ppm. As with linseed oil, the alkene protons no longer form a singlet due to the changes in alkene populations.

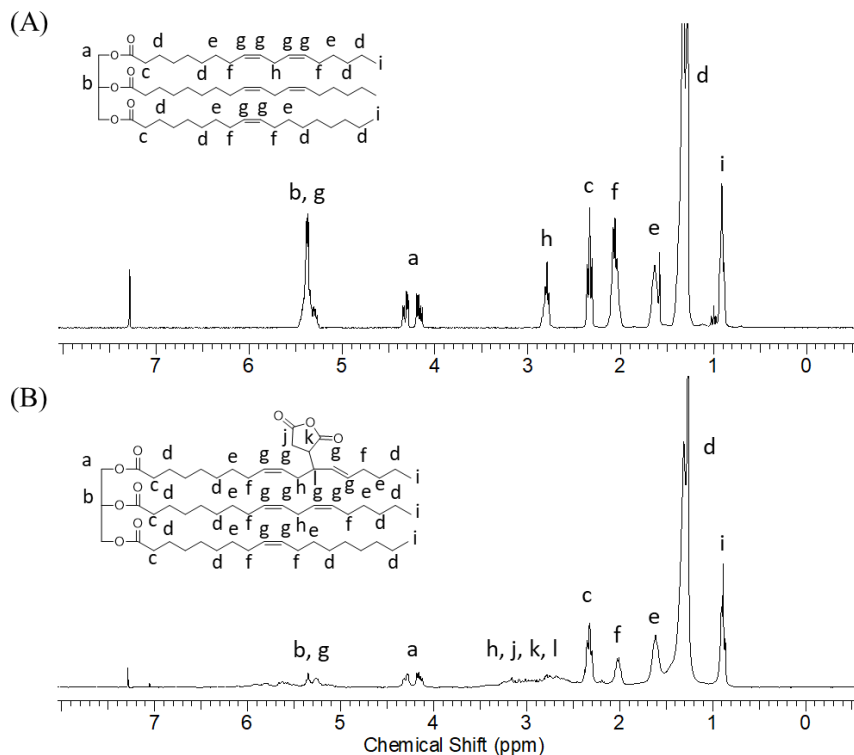


Figure 5.4. ^1H NMR for (A) raw soybean oil and (B) maleated soybean oil synthesized with 4.5 eq. of MA in a sealed reactor.

Going forward, only soybean oil was used in the maleation reaction because it did not require solvent, which is more cost-effective, since toluene adds to the cost and must be removed after the reaction. Since the maleated linseed oil products were very viscous, it would also have been necessary to use vacuum for extended time periods to remove all the toluene. Furthermore, maleated linseed oil had a strong pungent odor while maleated soybean oil did not, and linseed oil was best stored under nitrogen to avoid auto-oxidation making it a potential fire hazard.

Using the same procedure described for linseed oil, the maleation of soybean oil was first optimized using 4.5 molar equivalents of MA/TG at 230 °C in a sealed reactor, removing samples at time $t = 0, 0.25, 0.5, 0.75, 1, 1.5, 2, 3,$ and 4 h. The reaction was considered complete when there was less than 0.15 molar equivalent (1.7 wt%) of unreacted MA/TG by ^1H NMR analysis of the product. The procedure was repeated at 200 °C. As expected, the reaction required more time to go to completion (Table 5.3) as compared to linseed oil, because soybean oil contains fewer double bonds on average. As with linseed oil, when the reaction was carried out at 200 instead of 230 °C, there was a considerable difference in the incorporation level of MA, indicating again that the degradation of MA is competing with the ene reaction.

The MA content was varied in the sealed reactor from 1.7 to 4.5 eq. per triglyceride (Table 5.4). It was found that while the reaction with 1.7 eq. required 1.5 h for completion at 200 °C, the reaction with 3 eq. was done after 2 h. The ^1H NMR spectrum obtained for the products with the lower maleation level resembled that for the 4.5 eq. product, with two key

Table 5.3. Soap numbers and MA incorporation in ene reaction with soybean oil, using 4.5 eq. MA in a sealed reactor.

Temperature (°C)	Time (h)	<i>n</i> MA/TG	RE (%)	Unreacted MA (wt%)
230	0.8	1.9	42.0	< 0.1
200	2.0	2.1	47.6	0.2

differences: The peaks corresponding to the anhydride ring and the proton on the tertiary carbon between δ 2.5 and 3.5 ppm were less intense, and the peak corresponding to unreacted alkene protons was more intense. For the 1.7 eq. product the RE for MA incorporation was 63.5%, but decreased to 57.7% for 3 eq. MA, and again to 47.6% for 4.5 eq. MA. It is not surprising that the RE was higher at a lower loading of MA, as the excess of polyunsaturated linolenic and linoleic acids is larger under these conditions. As stated earlier, soybean oil contains 61.8% of polyunsaturated fatty acids. At the beginning of the reaction the concentration of polyunsaturated fatty acids is high, but it decreases as the reaction proceeds. At higher MA loadings it is expected that all the polyunsaturated fatty acids should react, and the only way in which the reaction can proceed further is through the oleic acid residues, which are less reactive. Consequently, the competing thermal decomposition reaction of MA becomes more significant, and the RE decreases when a larger amount of MA is used in the reaction.

Table 5.4. Soap numbers and MA incorporation in ene reaction with soybean oil in sealed and open glass reactors at 200 °C.

Reactor Type	Mol Eq. MA	Time (h)	<i>n</i> MA/TG	RE (%)	Unreacted MA (wt%)
Sealed	1.7	1.5	1.1	63.5	< 0.1
Sealed	3	2	1.7	57.7	0.9
Sealed	4.5	2	2.1	47.6	0.2
Open	1.7	4	1.0	58.8	1.8
Open	3	4	1.8	59.3	2.6
Open	4.5	4	2.6	57.8	0.8

Reaction of soybean oil with MA in an open reactor. In the “open” glass reactor, 4 hours were required at 200 °C for full consumption of the MA, as it condensed on the cooler glass surface in the headspace of the reactor. It should be noted that the products obtained in the open reactor were less viscous and lighter in color than those from the sealed reactor. While the RE varied in both the open and sealed reactors, the trends were opposed: The open reactor was slightly (4.7%) less efficient than the sealed reactor at the lowest loading (1.7 eq. MA), but the difference decreased to less than 2% at 3 eq. MA, and it was larger by over 10% at 4.5 eq. MA. A possible explanation for these differences is that, in contrast to the sealed reactor, the glass reactor had a condenser allowing the condensation (recycling) of MA back into the reaction rather than staying in the headspace of the reactor. At lower MA loadings, the sealed reactor also required a shorter reaction time however, which led to less anhydride degradation.

Narayan and coworkers² reported reaction conditions using a peroxide catalyst that were near 100% efficient for MA/TG ratios up to 1. They were unable to exceed that value however,

even when increasing the amounts of MA or catalyst used. Their reaction required polyunsaturated fatty acids but did not reach the theoretical maximum values of 1.5-1.7 MA/TG for different triglycerides, and reactions were not possible with oleic acid. Their products also needed to be purified by removing unreacted MA and were contaminated with peroxide. The procedure reported herein did not use a catalyst, and no purification of the product was needed. The liquid product drained from the reactor was free of by-products because the degradation products of MA, namely CO₂, CO, and ethyne,¹² are all gaseous. Rosenau and coworkers⁷ reported a RE of 50% for reactions between MA and soybean oil using either 1 or 2 eq. of MA per triglyceride in a sealed reactor. The reaction conditions used herein yielded higher RE values, with 63.5% in a sealed reactor and 58.8% in a glass reactor, when using a loading of 1.7 eq. MA, similar to Rosenau and coworkers. The procedure of Rosenau and coworkers also involved a reaction time of 6-8 hours, followed by the distillation of excess MA under reduced pressure. In the current procedure, a reaction time of up to 1.5 hours was required in the sealed reactor, and 4 hours in the open reactor when using 1.7 eq. MA. Most importantly, the current approach does not require purification after the reaction, which would make that procedure less problematic for large scale production. Finally, the highest MA/TG ratio reported by both Narayan and Rosenau for soybean oil was 1.0 (up to 2.0 for linseed oil), while an MA/TG ratio of 2.6 was achieved in an open reactor for soybean oil in the current investigation. Consequently, the previous limit of an MA/TG ratio of 1.0 for soybean oil has been largely surpassed with the new procedure developed.

GPC analysis of maleated soybean oil. The GPC elution profiles obtained for maleated soybean oil prepared in a sealed reactor (Figure 5.5) reveal that significant oligomerization occurred in the reaction. The product with the highest MA/TG ratio contained the largest amount of oligomers. A control reaction under the same conditions, without MA, produced negligible oligomerization of the oil. This indicates that either MA or some of the MA degradation products play a role in the oligomerization of the product. All the maleated products from the sealed reactor also contain material with a hydrodynamic volume population smaller (with a higher elution volume) than the triglyceride. Oleic acid, when injected in the GPC, was found to have an elution volume matching this smaller hydrodynamic volume population. This suggests that the rightmost peak in the chromatograms corresponds to single fatty acids, and that the intermediate peak eluted after the triglyceride is for diglycerides, slightly larger in size than free fatty acids. The GPC elution profiles for maleated soybean oil prepared in an open reactor (Figure 5.6) reveal that significantly less oligomerization occurred as compared to a sealed reactor. Given that the reaction temperature in the different reactors was identical, the main difference is that the gaseous by-products of MA decomposition, namely carbon monoxide, carbon dioxide, and ethyne,¹² would escape from the open reactor but remain trapped in the sealed reactor. It is therefore suggested that the degradation products, particularly ethyne (acetylene), may be predominantly responsible for the formation of oligomers in the product. Similarly to the sealed reactor, the products from the open reactor with the highest MA/TG ratios contain the largest amounts of oligomers. Furthermore, the open reactor products contained

minimal amounts of material with a hydrodynamic radius smaller than a triglyceride. This indicates that the reactions in the open reactor led to negligible decomposition of the triglycerides into free fatty acids and diglycerides.

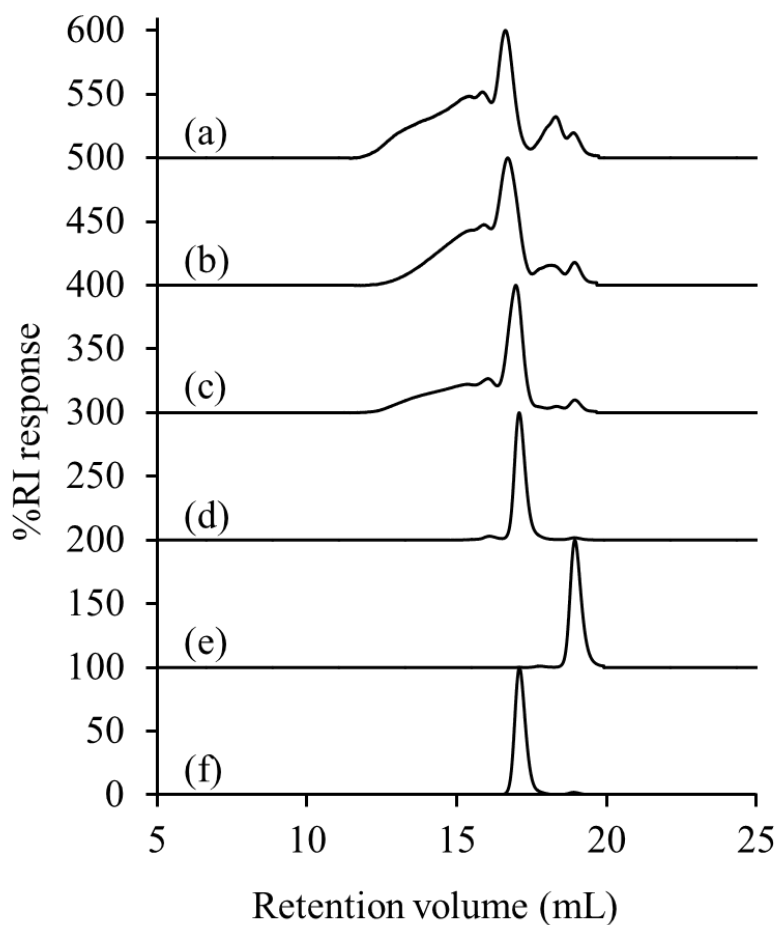


Figure 5.5. GPC elution curves for maleated soybean oil from a sealed reactor with an average of (a) 2.1, (b) 1.7, (c) 1.1 MA/TG, (d) soybean oil heated at 200 °C for 2 h in a sealed reactor without MA, (e) oleic acid, and (f) soybean oil substrate.

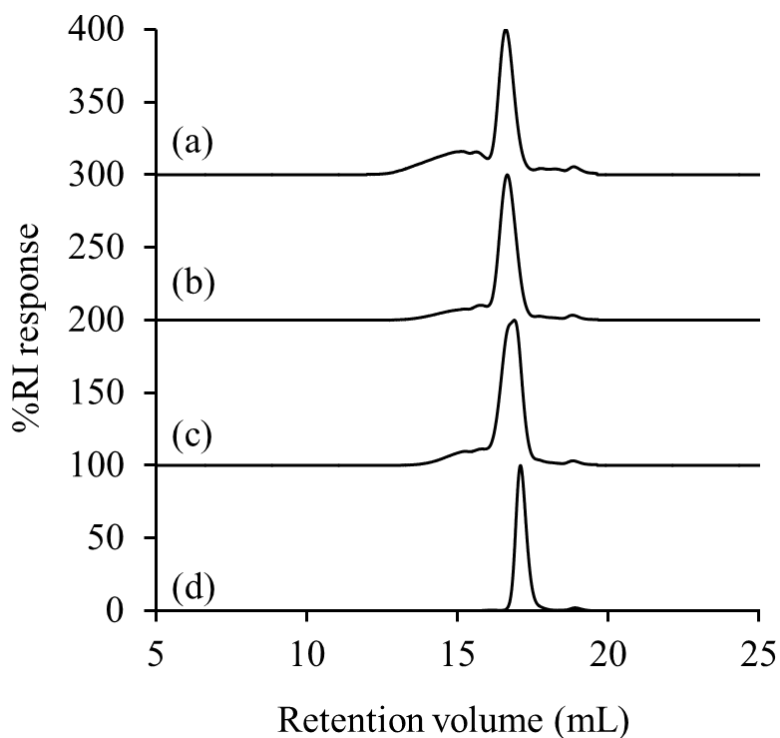


Figure 5.6. GPC elution curves for maleated soybean oil from an open glass reactor with an average of (a) 2.6, (b) 1.8, (c) 1.0 MA/ TG and (d) soybean oil substrate.

5.4.3 Quantification of Unreacted Triglycerides

The maleated soybean oil product from a sealed reactor (Figure 5.7(A)) was dissolved in a minimal amount of THF and loaded onto a silica column prepared in hexanes. The column was then flushed with hexanes to elute all the hydrophobic species (not containing anhydride groups) from the mixture. The dark color of the maleated product allowed its visual monitoring, and it was clear that it remained in the top 20% of the column. A very faint yellow band, similar to the raw oil, eluted from the column. A large volume of hexane, 6 times the silica gel bed volume,

was used to ensure that all the hexane-soluble material was eluted from the column. The column was then flushed with THF to elute the remaining material, as confirmed visually by the dark-colored band traveling down the column. The THF-soluble product precipitated upon mixing with the hexane which previously eluted from the column. After drying, the products collected in the hexane and THF fractions were weighed to determine the amount of unreacted triglyceride in the product, determined as the mass of the hexane-soluble product divided by the sum of the hexane- and THF-soluble products, multiplied by 100%. By collecting both fractions it was possible to determine the total product recovery in the procedure, to ensure that all the material had eluted from the column. The small excess recovery is attributed to trace amounts of solvent in the samples. The ^1H NMR spectrum for the hexane-soluble product (Figure 5.7(B)) was quite similar to soybean oil, with peaks corresponding to most of the triglyceride protons. However the absence of peaks between δ 5.5 and 6 ppm, as well as the sharp peak at 5.3 ppm suggest that there was no significant amount of conjugated di-unsaturated (linoleic) fatty acids in the hexane-soluble product. The ^1H NMR spectrum for the THF-soluble product (Figure 5.7(C)) is essentially identical with that for the sealed reactor product. GPC traces for the whole maleated soybean oil, the hexane- and THF-soluble products, and soybean oil in THF are compared in Figure 5.7(D). As mentioned previously, soybean oil contains a single population while the maleated soybean oil from the sealed reactor has a significant amount of oligomers. The THF-soluble product is almost identical with the sealed reactor product, as for NMR analysis. There appears to be a small increase in oligomer population for the THF-soluble fraction, which could

be due to residual double bonds in the maleated triglyceride reacting further with oxygen while the THF was being removed. Interestingly, the hexane-soluble fraction has an elution profile similar to raw soybean oil. The retention volume at the peak maximum is identical for both samples, which indicates that the small change in retention volume observed for the maleated product is due to the presence of the anhydride rings on the fatty acid tails. The procedure was repeated except that a small amount, 2 wt%, of unmodified soybean oil was added to the product before loading onto the column (Table 5.6) to confirm the effectiveness of the procedure. The product was eluted from the column first with hexane, followed by THF. The fractions were dried, weighed, and analyzed by ^1H NMR. The ^1H NMR spectra for the hexane- and THF-soluble fractions were identical with Figures 5.7(B) and 5.7(C), respectively. The gravimetric method developed in this work can therefore reliably quantify minor changes in unreacted triglycerides in the maleated products.

Table 5.5. Gravimetric study of unreacted triglycerides in maleated soybean oil prepared in a sealed reactor, with an average $n = 2.1$ MA/TG, after column chromatography on silica gel.

Sample	Mass (g)	Percent
Starting material	5.31	100
Hexanes fraction	0.024	0.4
THF fraction	5.38	101.2
Total recovery	5.40	101.7

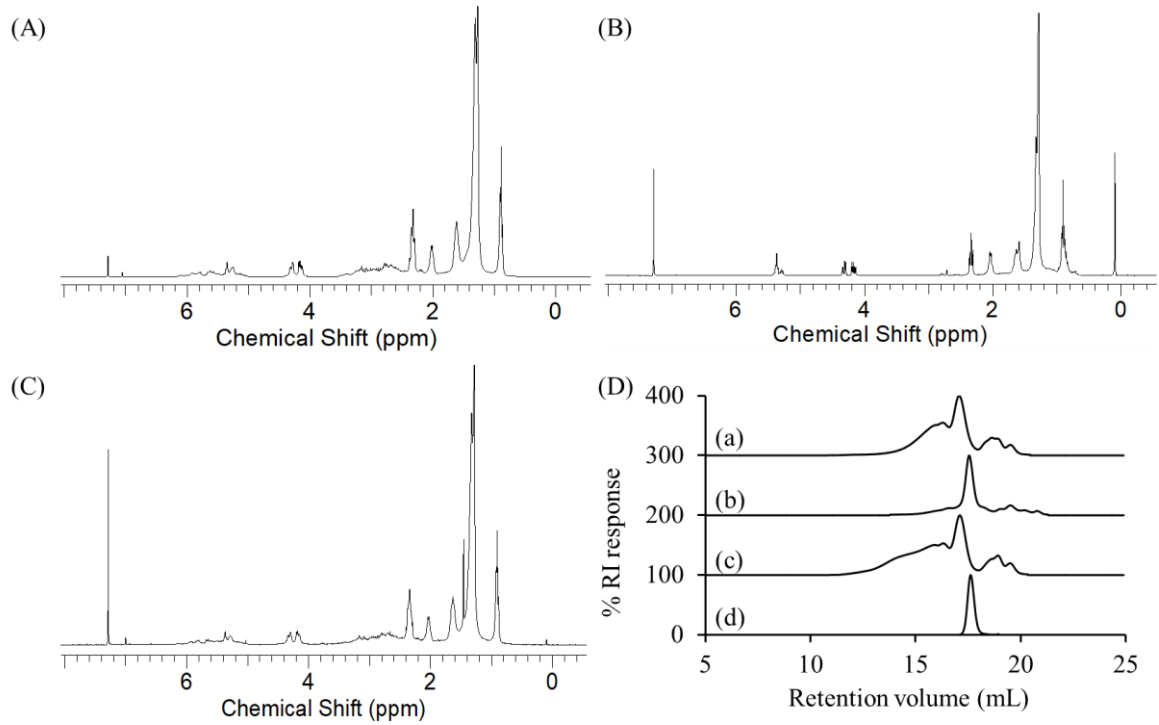


Figure 5.7. ^1H NMR spectra for (A) maleated soybean oil from a sealed reactor with an average of 2.1 MA/TG, (B) hexanes-soluble fraction, (C) THF-soluble fraction, and (D) GPC traces for (a) maleated soybean oil from a sealed reactor with an average of 2.14 MA/TG, (b) hexanes-soluble fraction, (c) THF-soluble fraction, and (d) soybean oil.

Table 5.6. Gravimetric study of unreacted triglycerides in maleated soybean oil prepared in a sealed reactor, with an average $n = 1.1$ MA/TG, after column chromatography on silica gel.

Sample	Mass (g)	Percent
Starting material	4.85	98.0
Soybean Oil	0.10	2.0
Total mass	4.95	100
Hexanes fraction	0.21	4.2
THF fraction	4.50	90.9
Total recovery	4.71	95.1

5.4.4 Scaled-up Maleation Reaction

The maleation reaction was conducted in an open reactor on a pilot plant scale, to determine whether the process was scalable, at the same MA loadings previously used. A large glass reactor was used, with a bubbler to prevent oxygen from entering the reaction and allow gaseous products to escape. The products obtained in the scaled-up procedure were visually light orange in color, similarly to the reactions done in the open reactor on a benchtop scale. The scaled-up reaction was more efficient (Table 5.7) than both the sealed and open reactor processes at loadings of 1.7 and 3 eq. MA. The scaled-up reaction was less efficient than in the benchtop open reactor, but more efficient than in the sealed reactor at 4.5 eq. MA loading. The unreacted MA content in the scaled-up products was comparable to the open reactor (Table 5.4) at 1.7 and 3 eq. MA loadings, but higher at 4.5 eq. MA, and higher than for all the sealed reactor products. Unreacted triglycerides were quantified by the same procedure described above. The product

containing the lowest amount of MA (1.1 MA/TG) contained 0.89 wt% unreacted triglycerides. For increasing MA loadings, the amount of unreacted triglyceride decreased to 0.31 wt% (2.0 MA/TG) and 0.13 wt% (2.3 MA/TG).

Table 5.7. MA incorporation, unreacted MA and unreacted triglycerides in the ene reaction with soybean oil in a pilot plant scale open glass reactor.

Sample	MA/TG	RE (%)	Unreacted MA (wt%)	Unreacted TG (wt%)
1.7	1.1	67	1.4	0.89
3	2.0	65	1.9	0.31
4.5	2.3	51	4.6	0.13

The GPC elution profiles for the scaled-up maleated soybean oils (Figure 5.8) were similar to those obtained for the benchtop open reactor products. The pressure in the large glass reactor was minimal, as in the open benchtop reactor, which allowed the gaseous by-products of MA decomposition (carbon monoxide, carbon dioxide, and ethyne) to escape during the reaction. It is therefore not surprising that, similarly to the other methods, the maleated products with the highest MA/TG ratios contained the largest amounts of oligomers. As for the small-scale open reactor products, the scaled-up products contained minimal amounts of materials with a hydrodynamic volume smaller than a triglyceride, indicating marginal decomposition of the triglycerides. The products only contained amounts of free fatty acids similar to the starting oil, and no diglycerides.

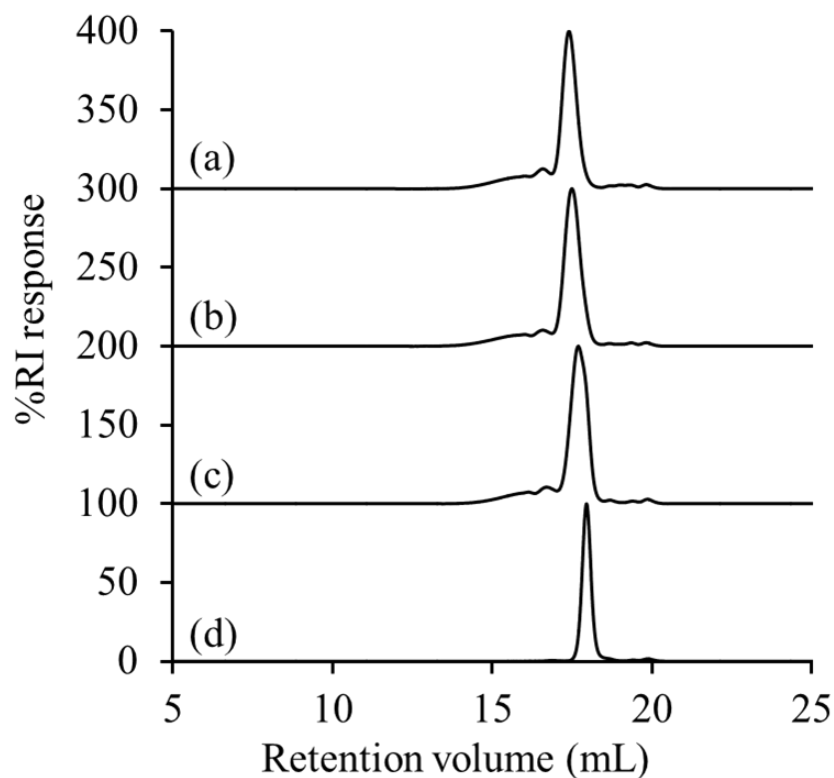


Figure 5.8. GPC elution curves for maleated soybean oil synthesized in a pilot scale glass reactor with an average of (a) 2.3, (b) 2.0, (c) 1.1 MA/TG, and (d) soybean oil.

5.5 Conclusions

A range of maleated vegetable oils, containing more than one anhydride group per triglyceride on average, were successfully synthesized from raw linseed oil. The success of the reaction was confirmed by changes in the ^1H NMR spectra, and anhydride incorporation was quantified with soap numbers. When using raw linseed oil, extensive cross-linking became a serious issue; anti-oxidants were ineffective at preventing cross-linking, and toluene was only

effective at high concentrations. Consequently, soybean oil was preferred as a vegetable oil substrate, because it had a lower unsaturation level than linseed oil and a low saturated fatty acid content. This made the use of solvents or catalysts in the reaction unnecessary. The maleation of soybean oil required longer reaction times to consume all the MA in a sealed reactor and was less efficient, but the resulting products were completely soluble in organic solvents. Maleated soybean oil products were synthesized containing up to 2.6 anhydride units on average per triglyceride, which greatly exceeds the maximum value of 1.0 anhydride units on average per triglyceride reported in the literature.^{2,7}

The maleation level of soybean oil was controlled by varying the amount of MA in the reaction, using either a benchtop sealed high pressure reactor, a benchtop open glass reactor, or a large pilot scale open glass reactor. Interestingly, the large scale reaction was most efficient at loadings of 1.7 and 3 eq. MA/TG, while the benchtop open reactor was most efficient at 4.5 eq. MA/TG. The type of reactor used had a pivotal influence on the physical properties of the products, as GPC analysis indicated that the sealed reactor approach led to significant oligomerization of the maleated triglycerides. This is the first report demonstrating that a significant portion of triglycerides in sealed maleation reactions of soybean oil undergoes oligomerization. The products from both open reactor methods were predominantly isolated triglycerides, suggesting that the oligomerization reaction could be related to the buildup of ethyne in the sealed reactor in relation to MA degradation. The sealed reactor approach also led to a small amount of degradation of the triglycerides to diglycerides and fatty acids.

For the first time, a procedure was developed to determine the weight fraction of unreacted triglycerides remaining in the maleated oil. By monitoring and minimizing the amount of unreacted triglyceride, the synthesis of new biobased materials can be optimized by avoiding costly purification processes, thereby decreasing overall production costs. For the scaled-up reactions, less than 1 wt% of the product did not contain any anhydride groups.

The new biobased materials reported herein should be useful as “green” replacements for ASA, as hydrophobic modifiers for starch or other polysaccharides. At higher MA loadings, the triglycerides contained more than two anhydride groups on average. These highly functionalized maleated oils could be useful as cross-linkers or monomers to synthesize new polyesters, food additives, binders in paper making, and adhesives, among others.

Chapter 6

Production of Cyclic Anhydride-Modified Starches

6.1 Abstract

Modified starches offer a biodegradable, readily available, and cost-effective alternative to petroleum-based products. The reaction of alkenyl succinic anhydrides (ASAs), in particular, is an efficient method to produce amphiphilic starches with numerous applications in different areas. While ASAs are typically derived from petroleum sources, maleated soybean oil can also be used in an effort to produce materials from renewable sources. The reaction of gelatinized waxy maize starch with octenylsuccinic anhydride (OSA), dodecenylsuccinic anhydride (DDSA), a maleated fatty acid (TENAX 2010), phthalic anhydride (PA), 1,2,4-benzenetricarboxylic acid anhydride (trimellitic anhydride, TMA), and three maleated soybean oil samples was investigated under different conditions. To minimize the reaction time and the amount of water required, the outcome of the esterification reaction was compared for starch dispersions in benchtop dispersed reactions, for starch melts in a heated torque rheometer, and for reactive extrusion with a pilot plant scale twin screw extruder. The extent of reaction was quantified by ^1H NMR analysis, and changes in molecular weight and diameter were monitored by gel permeation chromatography (GPC) analysis. The outcome of the reactions varied markedly in terms of reaction efficiency, molecular weight distributions and average

hydrodynamic diameter, for the products derived from the different maleated reagents used, as well as for the different reaction protocols.

6.2 Introduction

Starch is a natural biopolymer that is renewable, readily available, biodegradable and cost-effective.¹ These attributes make it attractive not only for food, but also as a feedstock for industrial applications.² Common sources of starch include but are not limited to corn, wheat and potatoes.³ In most plants starch is synthesized as two different macromolecules, namely amylose and amylopectin.⁴ Amylose (Figure 6.1(A)) is an essentially linear molecule composed of glucopyranose (GPy) units connected by α -1,4 glycosidic linkages.^{5,6} Similarly to amylose, amylopectin (Figure 6.1(B)) incorporates GPy units connected by α -1,4 glycosidic linkages,⁷ but also branching introduced through α -1,6 linkages.⁸ Amylose is composed of approximately 200-1200 GPy units, whereas amylopectin can have more than 100,000 GPy units per molecule.³ The proportions of amylose and amylopectin vary with the plant species; as an example, regular corn (maize) starch typically contains 28% amylose, whereas tapioca (cassava root) has 17% amylose.⁹ Some mutant plant strains are enriched in amylose, such as amylomaize containing > 50% amylose, or enriched in amylopectin, such as waxy maize starch containing > 99% amylopectin.¹⁰

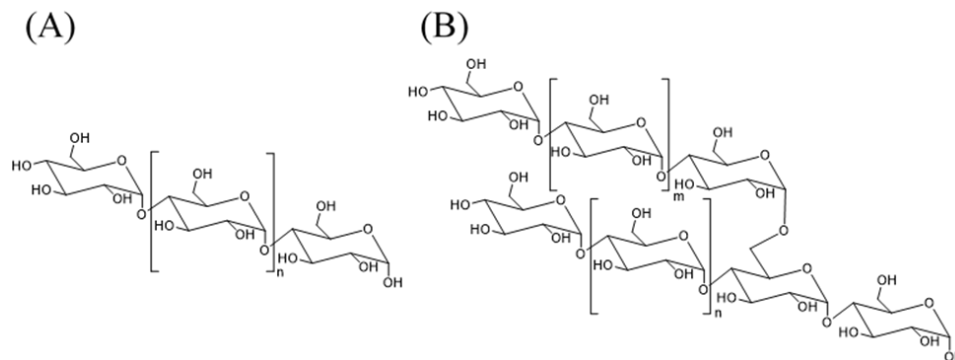


Figure 6.1. Chemical structure of (A) amylose and (B) amylopectin.

Amylose and amylopectin chains in starch granules are deposited as alternating semi-crystalline and amorphous layers.^{11,12} The semi-crystalline layers contain the linear amylose segments, while the amorphous layers are composed of branched amylopectin segments.¹⁰ The location of the amylose is not as defined as for amylopectin: In wheat starches, it is concentrated in the amorphous layers, while in maize starch it is more evenly distributed across the amorphous and semi-crystalline layers, and in potato starches it is crystallized with linear amylopectin segments.¹³ Native starch has several drawbacks for industrial applications; for example, it is brittle unless it is suitably plasticized,¹⁴ but can become soft and weak while plasticized.¹⁵ Finally, the mechanical properties of starch can deteriorate upon exposure to water, either in liquid or vapor forms.¹⁶ One solution to address these issues is to hydrophobically modify starch.² Octenyl succinic anhydride (OSA), an alkenyl succinic anhydride (ASA) with an 8-carbon chain bound to a succinic anhydride moiety, has long been studied as a starch modifier.¹⁷ OSA-modified starch is currently FDA-approved for use in food products at up to 3 wt% OSA

contents with respect to starch; at least 2.7 wt% OSA must be bound to the starch, and up to 0.3 wt% can be free in solution, which represents a 90% reaction efficiency (RE).¹⁸ It can be difficult to achieve a RE of 90%, because the granular structure of starch physically inhibits the diffusion of the anhydride inside the granules. Gelatinization is the process of disrupting hydrogen bonds within the granule structure, which results in the release of individual amylose chains and amylopectin side chains.¹⁹ The process is irreversible and requires a plasticizer, such as water or glycerol, and heat.²⁰ The amounts of heat and plasticizer required for full gelatinization varies with the starch composition, amylose being more crystalline and requiring more energy to disrupt the ordered structure in the granules.²¹ The mechanical treatment of starch is not required but it accelerates the process. After cooling, the gelatinized (cooked) starch thickens but does not display the same properties as native starch granules.²⁰ Starch is commonly gelatinized on a large scale in batch processes using blenders and melt mixers, as well as continuous techniques such as single or twin screw extruders.²¹ Gelatinized starch simply refers to the absence of granular structure, which could be lost in more than one way, while thermoplastic starch (TPS) is plasticized starch gelatinized through thermomechanical treatment. Thermomechanical treatment results in mechanical work on the starch, which ultimately results in a decrease in molecular weight of the starch chains.²² Gelatinized starch and TPS are hydrophilic, but their hydrophilic character and other physical properties can be tuned with hydrophobic reagents such as OSA, since hydrophobicity of the products increases directly with their level of substitution.⁶

OSA and other ASAs are produced by the reaction of maleic anhydride (MA) and unsaturated hydrocarbons, typically containing a terminal alkene.²³ They are produced by an ene reaction (also referred to as Alder-ene reaction) between an electron-poor double bond (MA) and a compound with an allylic hydrogen (an alkene).²⁴ Terminal alkenes, like 1-octene for OSA, are almost exclusively derived from petrochemicals.²⁵ With depleting oil supplies and increasing prices, it would be advantageous to shift to naturally sourced materials that are still cost-effective.²⁶ Vegetable oils and their derivatives are renewable, cost-effective, and biodegradable.²⁴ Depending on their source, vegetable oil triglycerides (TGs) may contain multiple double bonds and allylic hydrogens per molecule. Soybean oil, one of the most readily available vegetable oils, contains on average over 4 double bonds per TG.²⁷

This study concerns the reaction of starch with different cyclic anhydrides, namely two commercially available ASAs (OSA and dodecanyl succinic anhydride, DDSA), TENAX 2010 (a commercially available maleated fatty acid), phthalic anhydride (PA), 1,2,4-benzenetricarboxylic acid anhydride (trimellitic anhydride, TMA) and three maleated soybean oil products developed in our laboratory containing 1.1, 2.0, and 2.3 anhydride rings per TG. These reactions are generally completed on granular starch in batch stirred reactions for extended times. With granular starch the reaction is heterogeneous, requires a lot of water with respect to the starch, and a base. In the current study, the reactivity was investigated using gelatinized waxy maize starch in “classical” benchtop batch reactions, following methodologies previously reported for the modification with ASAs. To implement the reactions on an industrial scale, the

reactions were then transferred to a melt mixer, also referred to as a heated torque rheometer or internal roller mixer, to modify the TPS at high solids (80 wt% starch), with and without NaOH. Finally, starch was modified by a continuous pilot plant scale twin screw extrusion process using DDSA, TENAX and maleated soybean oil containing on average 1.1 anhydride rings per TG. While the removal of solvents and contaminants such as catalysts in starch modification often impairs the economic viability of processes,²¹ the procedures reported herein use only water as solvent and NaOH, so as to minimize the need for purification. The products obtained were characterized by ¹H NMR spectroscopy and gel permeation chromatography (GPC). The hydrophobically modified starch products synthesized have numerous potential uses as food thickeners, binders in paper making, or as adhesives.⁶

6.3 Experimental Section

6.3.1 Materials

Waxy maize starch (waxy pearl 1108) was purchased from Cargill Inc. (Burlington, Canada). OSA and DDSA were purchased from Dixie chemicals, and TENAX 2010 was acquired from MeadWestvaco Corporation. The remaining chemicals were purchased from Sigma Aldrich. All chemicals were used as received. Native waxy maize starch was gelatinized by extrusion through a pilot plant scale twin screw extruder.

6.3.2 Modification of Dispersed Starch with Cyclic Anhydrides (Benchtop Procedure)

Gelatinized waxy maize starch (60.0 g, 0.370 mol) was dispersed in 120 mL of distilled water (33 wt%) in a glass beaker and the pH was adjusted to 10 using 20 w/v NaOH. The mixture was stirred with an overhead mechanical stirrer until the starch solution was homogenous. OSA (1.50 g, 7.13 mmol, 2.5 wt% wrt starch) was dissolved in acetone (approximately 50 wt%) before slow addition (over 10 minutes) to the stirred reaction. The pH was monitored with a pH meter (Thermofisher Scientific) and maintained between 9 and 10 over 60 minutes by addition of 20 wt% NaOH solution. The reaction was stopped by addition of HCl (1.5 M) to adjust the pH to 6.5-7.0. The crude product was dried by heating under an airstream, while a portion was also purified by precipitation in acetone followed by Soxhlet extraction with acetone for 48 hours. The solid products were dried in an oven at 80 °C at reduced pressure overnight. The crude and purified products were analyzed by ¹H NMR spectroscopy, and the purified product by GPC. The procedure was repeated for anhydride loadings of 5, 7.5, and 10 wt%. The procedure was also repeated with the other cyclic anhydrides (DDSA, PA, TMA, TENAX 2010 and three maleated soybean oils).

6.3.3 Modification of Starch in a Melt Mixer

Uncooked waxy starch (22.0 g, 0.136 mol) and distilled water (4.4 mL, 0.244 mmol, 20 wt% wrt starch) were loaded into a melt mixer (Half size mixer, C. W. Brabender, 30 mL

capacity) fitted to an ATR Plasti-Corder Torque Rheometer (C. W. Brabender) preheated to 90 °C by circulating oil. The chamber was fitted with a thermocouple at the bottom, to measure the internal temperature over the duration of the whole reaction (up to 15 minutes at 40 rpm). After 4 minutes, OSA (0.55 g, 2.62 mmol) was added slowly to the mixing chamber. After the reaction, the product was removed from the mixing chamber and ground to a fine powder in a coffee grinder. A portion of the crude product was purified by Soxhlet extraction with acetone for 48 hours. The solid products were dried in an oven at 80°C at reduced pressure overnight. The crude and purified products were analyzed by ¹H NMR spectroscopy (300 MHz, DMSO-*d*₆) and by GPC for the purified product. The procedure was repeated for anhydride loadings of 5, 7.5, and 10 wt%. The procedure was also repeated with the other cyclic anhydrides (DDSA, PA, TMA, TENAX 2010, and three maleated soybean oils). All the reactions were completed either without added base or with 1.1 eq. of NaOH with respect to the anhydride. When NaOH solution was added, the amount of distilled water used in the procedure was decreased so as to maintain the overall water concentration constant.

6.3.4 Modification of Starch with Cyclic Anhydrides in a Pilot Plant Scale Twin Screw Extruder

The modification of waxy maize starch with DDSA, TENAX 2010 or maleated soybean oil containing on average 1.1 MA units per TG (1.1 MA/TG) was accomplished by reactive extrusion similarly to a reported procedure.^{28,29} Reactive extrusion was also accomplished while adding 20 wt% NaOH w/w (1.1 eq. wrt anhydride) to the starch melt during extrusion. The

overall amount of water added was adjusted to remain at a consistent level for all the products. Extrusion-modified starch samples were ground into a fine powder with a coffee grinder, purified by Soxhlet extraction with acetone for 48 hours, and dried at reduced pressure in an 80 °C oven overnight. The crude and purified products were analyzed by ^1H NMR spectroscopy (300 MHz, DMSO), and the purified product by GPC.

6.3.5 ^1H NMR Analysis

^1H nuclear magnetic resonance (NMR) spectroscopy was performed on a Bruker 300 MHz instrument. The concentration of all the samples was 15–30 mg/mL in dimethyl sulfoxide- d_6 with 7 drops of trifluoroacetic acid (TFA), or deuterium oxide for PA- and TMA-modified samples, and 64 scans were averaged. The reported chemical shifts are relative to the residual solvent protons at 2.50 ppm for dimethyl sulfoxide- d_6 and 4.79 for deuterium oxide.

6.3.6 Gel Permeation Chromatography (GPC) Analysis

Analytical gel permeation chromatography (GPC) measurements for modified starch samples were performed on a Malvern GPCmax instrument with a TDA 305 triple detector array and one 300 mm x 8.0 mm I.D. PolyAnalytik SuperesTM column having a theoretical linear PS molar mass range of up to 200 MDa. A flow rate of 0.6 mL/min was used with 0.05 M LiBr in DMSO as the mobile phase at 50 °C. Samples were prepared at a concentration of 2 mg/mL in 0.05 M LiBr in DMSO and filtered through a 0.2 μm nylon filter. A pullulan standard with a peak molecular weight $M_p = 334,000$ Da and $M_w/M_n = 1.10$ (PolyAnalytik) was used to calibrate

the instrument to obtain absolute molecular weight (MW) values. The $\left(\frac{dn}{dc}\right)$ and intrinsic viscosity $[\eta]$ values supplied for this standard in DMSO were 0.066 mL/g and 0.65 dL/g, respectively. The absolute MW of each fraction (i) eluted from the column was calculated according to Eq. (1)

$$MW_i \cong \frac{LS_{Cal} \cdot RI_{Cal}}{n_o^3 \cdot v} \cdot \frac{LS_{i-\delta}}{RI_i} \quad (1)$$

where MW_i is the molecular weight of a sample fraction corresponding to an elution volume V_i , LS_{Cal} and RI_{Cal} are the light scattering detector and differential refractive index detector response calibration factors, respectively, n_o is the refractive index of the mobile phase, v is the volume of the eluted fraction (mL), RI_i is the RI detector signal, and $LS_{i-\delta}$ is the light scattering signal corrected for an offset δ with respect to the RI detector. Using the online viscometer, the specific viscosity of each slice of the eluent was measured for the samples. Dividing the specific viscosity by the concentration (from the RI detector), $[\eta]$ was obtained and used to calculate the hydrodynamic radius (R_h) and diameter ($D_h = 2R_h$) of the starch samples using the Einstein equation, Eq. (2)

$$\eta = \eta_o (1 + 2.5\phi) \quad (2)$$

relating the viscosity of the sample solution η , the viscosity of the pure mobile phase η_o , and the volume fraction ϕ of the molecules in solution. When transforming Eq. (2) to include $[\eta]_i$, Avogadro's number (N_A), molar concentration (n_i), and expressing ϕ in terms of the volume of a sphere (Eq. (3)), Eq. (4) is obtained

$$V_h = \frac{4}{3} \cdot \pi R_h^3 \quad (3)$$

$$[\eta]_i MW_i = \frac{10\pi N_A}{3} \cdot \left(\frac{D_{hi}}{2}\right)^3 \quad (4)$$

$$D_h = \frac{\sum n_i D_{hi} [\eta]_i}{\sum n_i [\eta]_i} \quad (5)$$

6.4 Results and Discussion

The reaction of starch with cyclic anhydrides in the presence of water has been widely investigated, starting with Caldwell and Wurzburg³⁰ in 1953 who used different alkenyl succinic anhydrides and sodium carbonate as base. The reaction mixture was a “slurry”, in that granular starch was simply suspended in water.³¹ After 14 hours the reaction was neutralized with hydrochloric acid (HCl) to reach a final pH of 7.0, the solid product was collected by gravity filtration and washed with either water or ethanol. While changes were made to this method, it is still widely used to produce hydrophobic starch nowadays. One drawback of that procedure is that since granular starch is used, the GPy units on the surface are free to react while GPy units inside the granules are inaccessible. The hydrophobic anhydride must diffuse through the hydrophilic starch granule to react.³² The longer the chain length, the more hydrophobic the anhydride, which makes this process more difficult. One solution to this problem is to use gelatinized starch, so that the amylose chains and amylopectin molecules are free in solution and able to react with the anhydride.³³ In the current study, gelatinized waxy maize starch was

modified with different cyclic anhydrides. The esterifying agents used were OSA, DDSA, TENAX 2010, PA, TMA and three maleated soybean oil products developed previously in our laboratory (Figure 6.2). The reaction time for the starch modification reaction was set to one hour for reactions in the dispersed state. To further optimize esterification, the state of the system was changed from a dispersed phase to a melt phase. Industrial starch esterification is typically achieved in a continuous twin screw extruder,²¹ as this method does not require that the starch be dispersed in a solvent but simply plasticized.³⁴ Correspondingly, some reactions were first carried out in a melt mixer as batch reactions in the melt phase under shear, to mimic TPS preparation conditions achieved in a twin screw extruder, and over less than 15 minutes rather than hours. The native waxy maize starch granules were gelatinized *in situ* under high shear before addition of the anhydride,³⁵ and the reactions were completed with and without base. The starch was also modified in a pilot plant scale continuous twin screw extrusion process using DDSA, TENAX and maleated soybean oil with 1.1 MA/TG. The extent of reaction was determined by ¹H NMR analysis, while GPC measurements were used to determine whether the starch products suffered chain scission during the modification procedure.

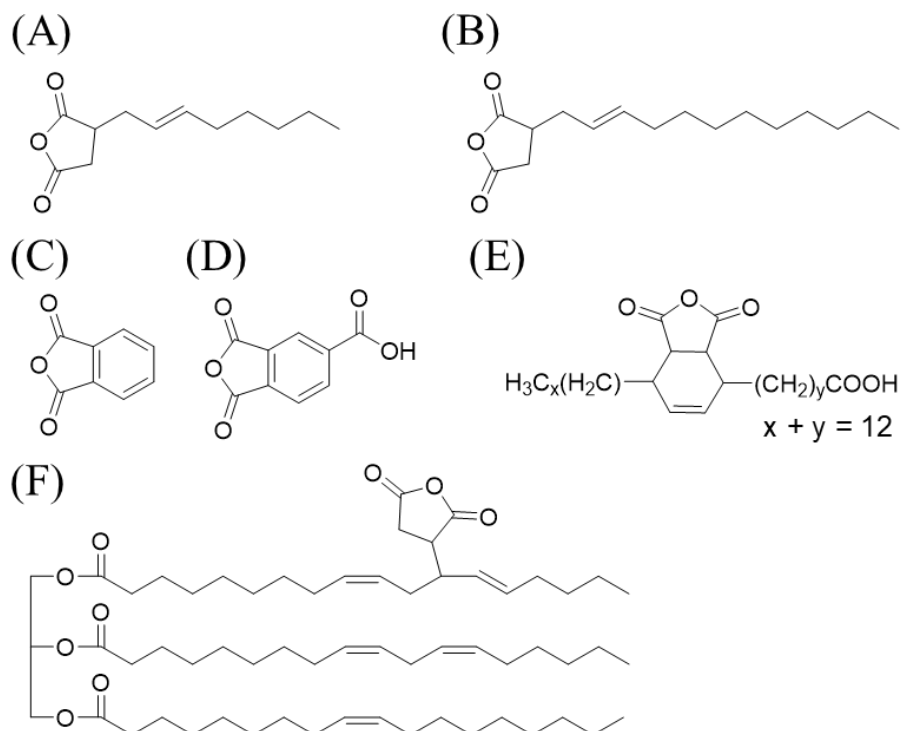


Figure 6.2. Chemical structure of (A) OSA, (B) DDSA, (C) phthalic anhydride, (D) 1,2,4-benzenetricarboxylic acid anhydride, (E) TENAX 2010, and (F) maleated soybean oil with one equivalent of maleic anhydride (many isomers possible).

6.4.1 Reaction of Starch with OSA and DDSA in Dispersions and in the Melt

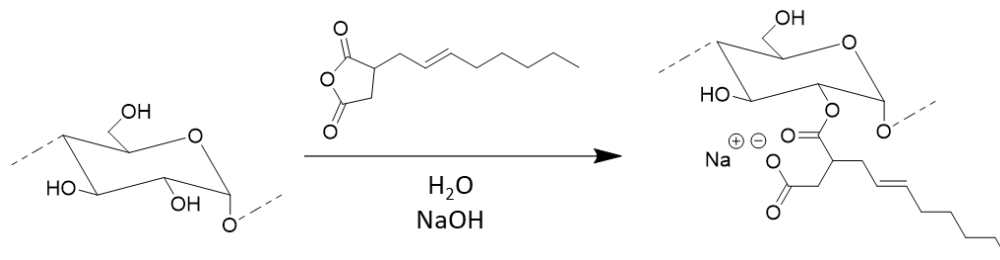
Mixer

To study the reaction of OSA with starch (Scheme 6.1), gelatinized waxy maize starch was first dispersed in water at 33 wt% solids content at room temperature and the pH was

adjusted to 10.0 through drop-wise addition of 20 wt% NaOH. When a homogenous dispersion was obtained, OSA diluted with acetone (to lower the viscosity and facilitate its controlled addition, and avoid a high local concentration of anhydride) was added drop-wise to the reaction mixture. The pH of the reaction was maintained between 9 and 10 through the addition of 20 wt% NaOH during this process. The reaction was stopped after 1 hour by adjusting the pH to 6.5-7.0 with 1.5 M HCl. After neutralization, a small amount of sample was removed and dried without purification. The purification of another portion of the crude product was achieved by precipitation in acetone, followed by Soxhlet extraction with acetone for two days with occasional stirring to break up clumps, and then drying in a vacuum oven for 16 hours at 80 °C. To determine the RE, ¹H NMR analysis was completed on the unpurified and purified products for each reaction. The spectra obtained for OSA-modified starch (Figure 6.3) were consistent with those found in previous reports.³⁶ The peaks between 3 and 4 ppm correspond to protons on the starch backbone, while the peak at 5.1 ppm, for the anomeric proton of starch, can serve as reference to compare with the integrated signals for the hydrophobic side chains. The methyl signal at 0.8 ppm can serve to quantify the hydrophobic alkyl chains in the mixtures. The peak at 1.3 ppm is for methylene protons in the alkyl group, while the resonance at 1.9 ppm is for aliphatic methylene protons α to carbon-carbon double bonds. Finally, the signals at 5.35 and 5.5 ppm are for the alkene protons. These peaks can potentially interfere with the starch anomeric proton signal (5.1 ppm), although at low anhydride loadings this should not be an issue. The RE was determined by dividing the integral ratio for the peaks at 0.8 ppm and 5.1 ppm for the

purified product through the same integral ratio for the unpurified product, multiplied by 100%.

The procedure was completed for 2.5, 5, 7.5, and 10 wt% OSA loadings with respect to starch.



Scheme 6.1. Reaction of starch with OSA. The ester is drawn in the C2 position, but esterification is possible at C2, C3 or C6.

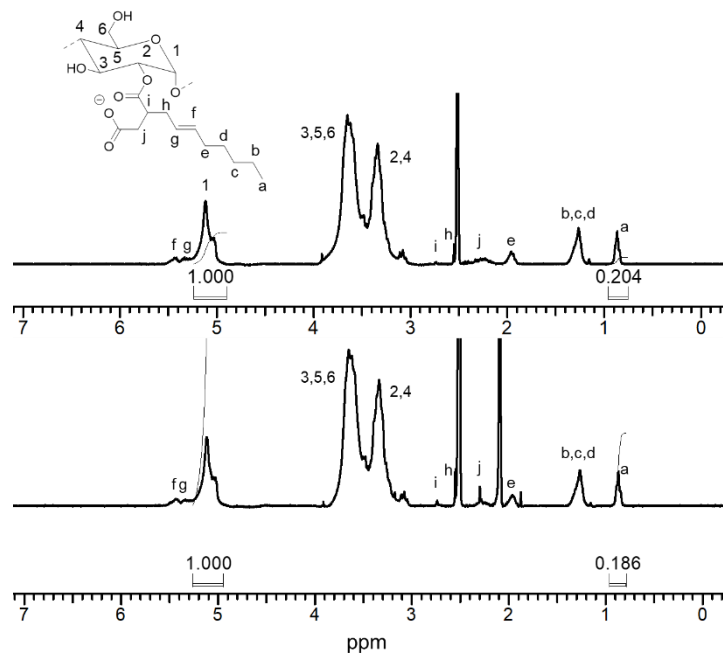


Figure 6.3. ¹H NMR spectra for OSA-modified starch in DMSO-*d*₆ (top) prior to purification and (bottom) after purification with acetone.

The RE for OSA-modified starch (Figure 6.4(A)) prepared in the dispersed phase was 99.1% at 2.5 wt% loading. Increasing the amount of OSA used did not change the RE significantly, as the RE values were between 95.6 and 100%. The high RE achieved with OSA in solution under the conditions described herein are consistent with some previous reports, and higher than for others. For example, Miao and coworkers⁵ achieved a RE > 95% for gelatinized maize starch, and above 80% for waxy maize starch granules in 30 wt% dispersions. Bai and Shi³⁷ quoted values of RE > 99% for water-soluble starch samples, and above 80% for waxy maize starch granules in 40 wt% dispersions. Qi-he and coworkers³⁸ reported RE values of up to 83% for potato starch granules in 35 wt% dispersions, but decreasing to 33% at 10 wt% OSA loading. He and coworkers¹⁴ achieved REs of up to 78% using rice starch granules in 30 wt% dispersions, while Zhu and coworkers³⁹ reported 68.5% RE for gelatinized waxy maize starch vs. 74.6% for waxy maize starch granules, albeit the starch concentrations used were unspecified.

To complete reactions in the melt phase under homogenous conditions, a melt mixer was used initially. Granular starch was loaded into the melt mixer along with water as plasticizer (20% wt% to starch) at 40 rpm. The time and torque recording started as soon as a torque of 1.0 Nm was obtained (Figure 6.5). Upon loading the starch in the melt mixer there was a sharp rise in torque, followed by a less intense broad peak resulting from water diffusing into the starch granules.³⁵ The diffusion of water into the granules increases the internal pressure and viscosity within the mixing chamber.⁷ After gelatinization, the torque plateaued to a lower value.⁴⁰ It is possible for the plasticizer, in this case water, to evaporate at high temperatures, which would

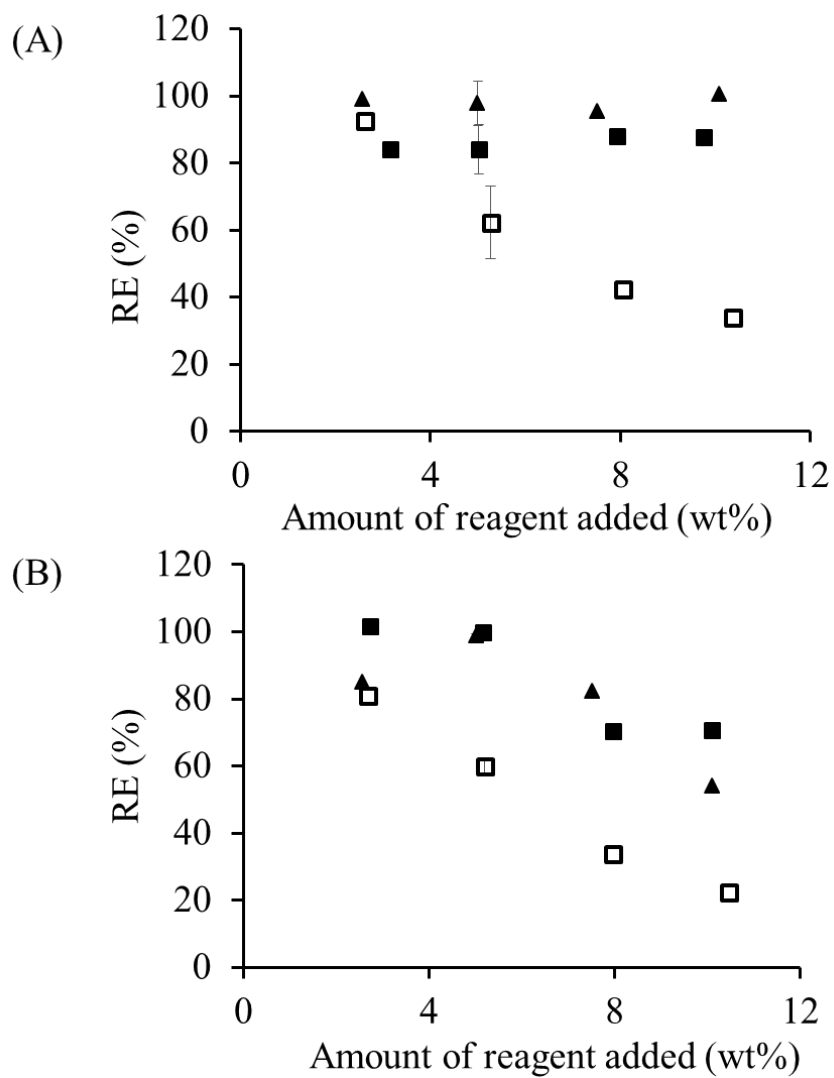


Figure 6.4. Modification of starch with (A) OSA and (B) DDSA. Conversion at different weight loadings for (▲) gelatinized starch dispersions, (□) melt mixer reactions without base, and (■) melt mixer reactions with base.

result in a slow torque increase.⁷ For that reason, a maximum temperature of 90 °C was selected for the reaction with 15 minutes of mixing to avoid significant water losses. The anhydride was added slowly to prevent pooling of the anhydride in the starch melt, and led to expected small decreases in torque and temperature.⁷ As the reaction progressed, the starch melt became more viscous again, which also led to an increase in temperature due to the higher torque. Water condensate was also visible on the mouth of the mixer above the reaction, confirming water losses from the reaction mixture. After the reaction the modified starch product was removed from the melt mixer, ground into a fine powder, and part of the material was purified by Soxhlet extraction with acetone for two days to remove all unreacted anhydride. Preliminary experiments revealed that dialysis in acetone with three solvent changes was insufficient to achieve similar results. Soxhlet extraction solved this issue by providing continuous solvent exchange. Products were prepared with loadings of 2.5, 5, 7.5, and 10 wt% OSA, similarly to the dispersed phase reactions. The procedure was also repeated using 1.1 eq. of NaOH with respect to OSA in the reaction. The volume of water added initially was reduced by the volume of 20 wt% NaOH solution in that case, so as to maintain 20 wt% water in the reaction.

Increasing the OSA loading led to decreased RE within the 2.5-10 wt% range tested. While the RE at 2.5 wt% OSA loading was 92.6%, close to the 95% RE for the dispersed phase reactions, it did not plateau at higher loadings as seen in other studies³¹ but rather dropped to 33.8% at 10% loading. Besides hydrolysis of the anhydride, possible explanations for a drop in RE include the limitations of using a melt mixer to mimic reactive extrusion conditions. It is also

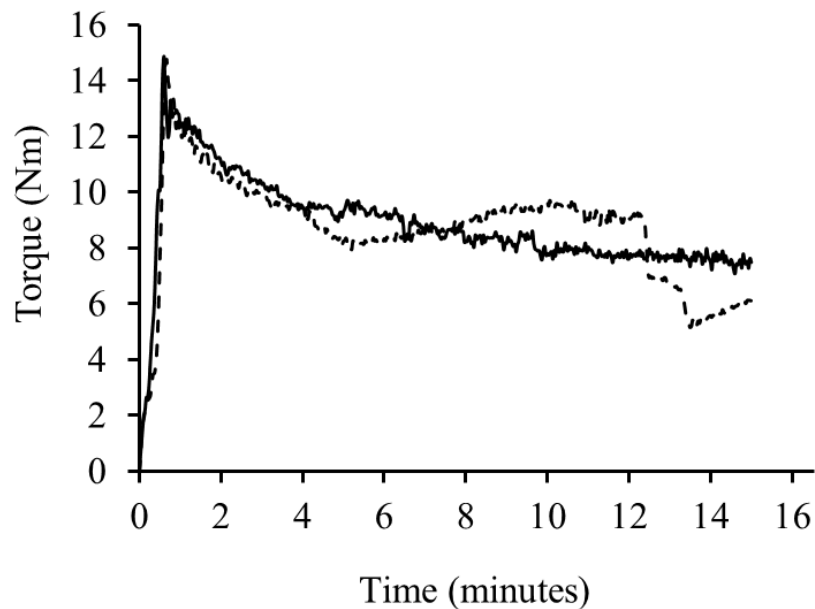


Figure 6.5. Typical torque variation at 90 °C and 40 rpm for starch with water (—) and starch with water and OSA (- - -).

possible that the starch was not fully gelatinized, limiting the number of hydroxyls available to react. The reaction time was significantly lowered to 11 minutes as compared to 1 hour for dispersion modification. Longer reaction times may result in higher REs, however long reaction times cannot be attained with a single pass through an extruder, and thus these conditions were not pursued. Furthermore, the reaction between the starch hydroxyls and the anhydride depend on the reactivity of the hydroxyl groups. The addition of a base increases the rate of reaction, and literature reports mostly concern reactions completed with a base.²¹ The RE with added base

was indeed significantly increased, ranging between 80% and 90%, but still lower than for dispersed phase reactions (RE > 95% in all cases).

When the procedures described above were repeated with DDSA, different trends were observed (Figure 6.4(B)): For the dispersed phase reactions, a RE of 85.1% was achieved at 2.5 wt% loading, even increasing to 99.0% at 5 wt%. Unfortunately the reaction mixture began foaming at higher loadings, which suggests DDSA hydrolysis leading to the formation of surface-active sodium dodecyl succinate. Accordingly, the RE decreased to 82.3% at 7.5 wt% loading, and finally to 54.0% at 10 wt% DDSA. These results are consistent with previous reports on DDSA, such as Gross and coworkers³¹ who achieved REs of 80 and 63% at 5 and 10 wt% loadings, respectively, when using waxy maize starch granules for a 6 h reaction time and a starch concentration of 31 wt%. They also found that increasing the DDSA loading beyond 10 wt% did not yield increased substitution levels. Wang and coworkers¹⁶ reported lower RE values of 71.1% and 42.7% at 3 and 10 wt% loadings, respectively, for maize starch granules at 30 wt% concentration.

The RE for DDSA-modified starch in the melt phase without base followed the same decreasing trend as the melt reactions with OSA without base as a function of anhydride loading, except for 5 wt% loading which was highest. When NaOH was used 100% RE was achieved for both 2.5 and 5 wt%, but the efficiency dropped to 70% at the higher loadings (Figure 6.4(B)).

The molecular weight distribution of the modified starch products was determined by GPC analysis using a mobile phase of 0.05 M LiBr in DMSO. The dispersed phase products of

OSA and DDSA (Figure 6) displayed no significant differences in their elution profile with respect to unmodified gelatinized waxy maize starch. Unmodified starch had an absolute number-average molecular weight $M_n = 2.2 \times 10^6$ g/mol and an absolute weight-average molecular weight $M_w = 4.5 \times 10^6$ g/mol, corresponding to a polydispersity index $\mathfrak{D} \equiv M_w/M_n = 2.0$. The weight-average D_h of the molecules determined using Eq. (5) was 50 nm. The fact that the elution curves (Figure 6.6) and the molecular weight averages (Table 6.1) for the unmodified and modified starches only displayed minor variations strongly suggests that no significant degradation or chain scission occurred during the dispersed phase reactions. This is consistent with the report of Miao and coworkers,⁵ for which a reaction with 3 wt% OSA under similar conditions resulted in no decrease in molecular weight when using gelatinized maize starch, however there was significant (57%) decrease in molecular weight when the reaction was completed on waxy maize starch granules.

To generate reference samples for reactions completed in the melt mixer, granular waxy maize starch employed in the melt mixer experiments were processed with water for 15 minutes in the melt mixer under the same conditions as the anhydride reactions. The processed starch prepared at 40 rpm had an absolute $M_n = 5.6 \times 10^6$ g/mol, an absolute $M_w = 1.9 \times 10^7$ g/mol ($\mathfrak{D} = 3.4$) and $D_h = 80$ nm, all higher than the materials used in the dispersed phase reactions. The same starch grade was used for the dispersed phase reactions and the melt mixer reactions, however the starch originated from different lots. The observed differences in absolute molecular weight among the lots are attributed to a combination of variance in year-to-year growth

conditions, which have previously been shown to result in more than one order of magnitude difference in M_w for maize starch, and the fact that the gelatinized starch was prepared in a twin screw extruder, under higher shear conditions than in the melt mixer.^{8,11}

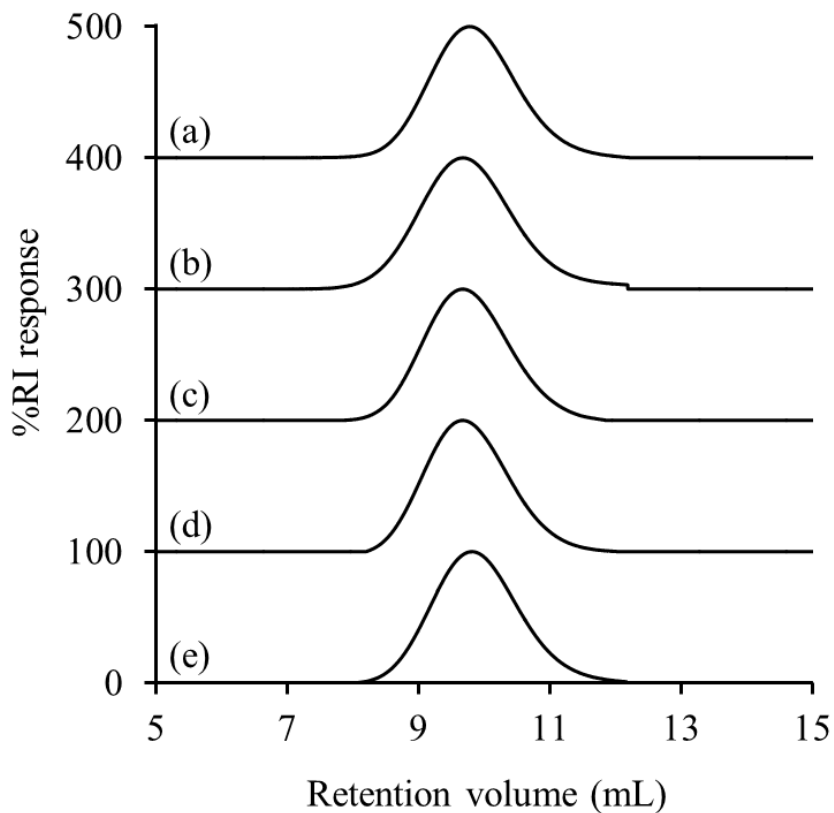


Figure 6.6. GPC elution curves for the baseline-subtracted normalized RI detector response for (a) unmodified gelatinized starch, gelatinized starch modified with (b) 5 wt% OSA, (c) 10 wt% OSA, (d) 5 wt% DDSA, and (e) 10 wt% DDSA in dispersed phase reactions. The position of each curve was shifted on the vertical axis for clarity.

Table 6.1. Absolute molecular weight averages determined by GPC analysis of starch modified in the dispersed phase with OSA and DDSA.

Reagent	Weight loading (wt%)	M_n (g/mol)	M_w (g/mol)	Đ	D_h (nm)
N/A	0	2.2 × 10 ⁶	4.5 × 10 ⁶	2.0	50
OSA	5	2.2 × 10 ⁶	5.7 × 10 ⁶	2.7	56
OSA	10	2.5 × 10 ⁶	5.0 × 10 ⁶	2.0	54
DDSA	5	2.7 × 10 ⁶	5.2 × 10 ⁶	1.9	54
DDSA	10	1.9 × 10 ⁶	4.0 × 10 ⁶	2.1	48

Absolute molecular weight analysis was attempted using the light scattering detector on the GPC system for the starch modified on the melt mixer. Unfortunately, the low-angle light scattering (LALS) detector signal was saturated for samples with a large high-molecular weight shoulder (Figure 6.7) preventing reliable molecular weight measurements. A high molecular weight shoulder was visible in the RI signal for the products independently of the anhydride used, or whether a base was used (Figure 6.8). While this appears somewhat unlikely under the conditions used, the free carboxylate groups formed in the esterification with the anhydrides could participate in Fischer (also referred to as Fischer-Speier) esterification.⁴¹ The mechanism of this acid-catalyzed reaction involves protonation of the carboxylic acid, followed by intermolecular nucleophilic attack of a starch hydroxyl on the protonated acid, to produce an ester linkage and a water molecule. The acid catalyst is produced by the reaction of starch with the anhydride, at least in the case of reactions not involving a base. In addition to Fischer esterification, there is a potential for dehydration of carboxylic acid groups leading to the intermolecular formation of

anhydride linkages. Starch has indeed been modified with carboxylic acids such as citric acid to cross-link starch via anhydride linkages.⁴² These reactions are likewise acid-catalyzed and favored at high temperatures.⁴³ Considering the very high molecular weight of starch (well over 10^6 g/mol), the intermolecular formation of ester or anhydride bonds could very well explain the appearance of the shoulders in the GPC traces of Figure 6.8.

6.4.2 Reaction of Starch with Phthalic Anhydride (PA) and 1,2,4-Benzenetri-carboxylic Acid Anhydride (TMA) in Dispersions and in the Melt Mixer

While the reaction of starch with OSA or DDSA introduces a hydrophobic alkyl tail, PA and TMA introduce an aromatic ring onto starch. Dispersed phase reactions with PA and TMA were completed similarly to OSA and DDSA, except that PA was not completely soluble in acetone at 50 wt%. For that reason, PA was dissolved in THF (50 wt%) rather than acetone. ^1H NMR analysis was completed in D_2O for both PA- and TMA-modified products, because the peak from TFA in $\text{DMSO-}d_6$ overlapped with the aromatic signal used for quantification at 7.37 and 7.43 ppm. The RE for the PA derivatives (Figure 6.9(A)) followed a trend similar to OSA, with high RE values for the dispersed phase reactions and the base-catalyzed melt phase reactions: A RE of 86.1% was achieved in the dispersed phase at 2.6 wt% loading, increasing to 98.6% at 10 wt% loading. The RE likewise decreased for increasing loadings in the melt phase reactions without base, from an apparent RE > 100% (attributed to integration errors in the ^1H

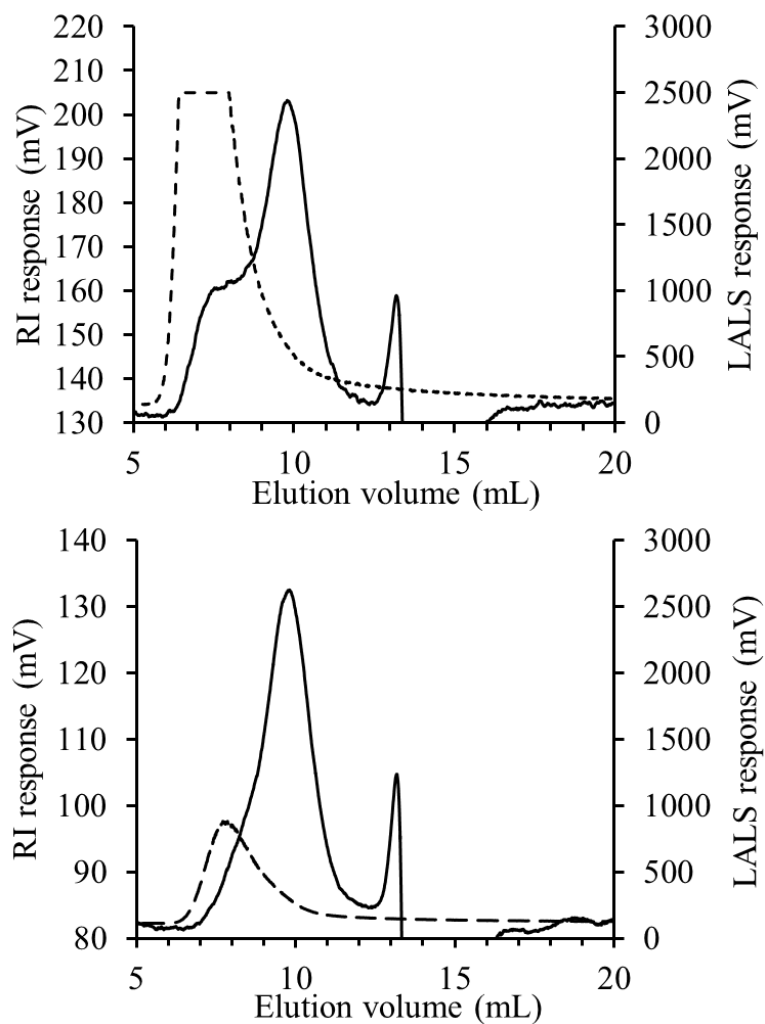


Figure 6.7. GPC elution curves with RI (—) and LALS (- - -) detector responses for starch modified in a melt mixer under identical conditions, leading to LALS detector saturation (top; 5 wt% DDSA without base) and no saturation (bottom; 10 wt% OSA with base).

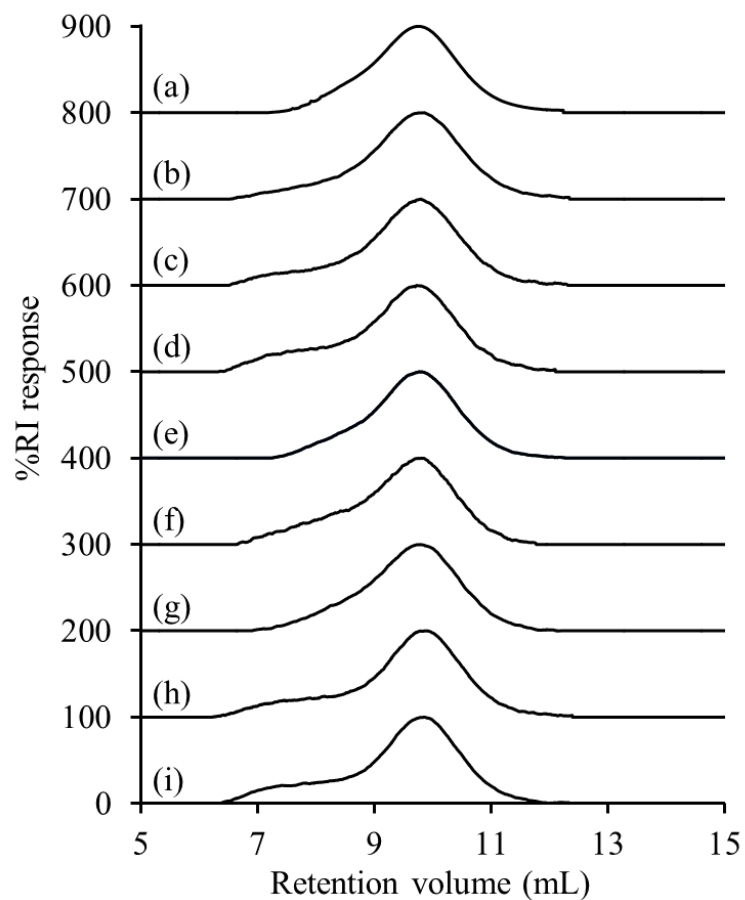


Figure 6.8. GPC elution curves with baseline-subtracted normalized RI detector response for starch modified in the melt mixer: (a) unmodified starch, and starch modified with (b) 5 wt% OSA, (c) 10 wt% OSA, (d) 5 wt% DDSA, and (e) 10 wt% DDSA without base; starch modified with (f) 5 wt% OSA, (g) 10 wt% OSA, (h) 5 wt% DDSA, and (i) 10 wt% DDSA with base. The position of each curve was shifted on the vertical axis for clarity.

NMR spectrum) at 2.6 wt% loading, decreasing to 39.9% at 10.1 wt% loading. The corresponding PA reactions in the melt mixer with base also had a RE > 100% for 2.5 wt%, remaining above 85% at the higher loadings. Only one report has been published on the reaction of PA with starch in the presence of water⁴⁴ and concerned reactions done in a twin screw extruder rather than a batch mixer. Interestingly, it was determined that at PA loadings above 2.5 wt%, using either 20 or 30 wt% aqueous sodium carbonate as buffer and 30 rpm at 110 °C led to hydrolysis of the anhydride. Reactions completed with 0.5 and 1.0 wt% PA under the same conditions were reported as “near quantitative” by the authors.

The RE for TMA in the dispersed phase (Figure 6.9(B)) was above 95% at all loadings tested (2.5-10 wt%), similarly to OSA and PA. For reactions in the melt phase without base, RE values of 92.6, 94.5, 98.4, and 85.3% were achieved at loadings of 2.5, 5.1, 7.5, and 10 wt%, respectively. There was therefore no substantial decrease in RE of the type observed for OSA, DDSA, and PA without base. For the base-promoted reactions, due to the presence of a carboxylic acid group in TMA, the procedure was attempted using both 1.1 and 2.2 eq. of base per anhydride. The first equivalent of base is expected to neutralize the free carboxylic acid, while the second equivalent would neutralize the acid formed during esterification of the starch. With 2.2 eq. NaOH, RE > 90% were achieved, while the RE with 1.1 eq. of base was likewise high, within 5% of the reactions without base. Additional base therefore did not lead to much improvement in RE for TMA. To the best of our knowledge, this is the first report on the reaction of TMA with starch under aqueous conditions.

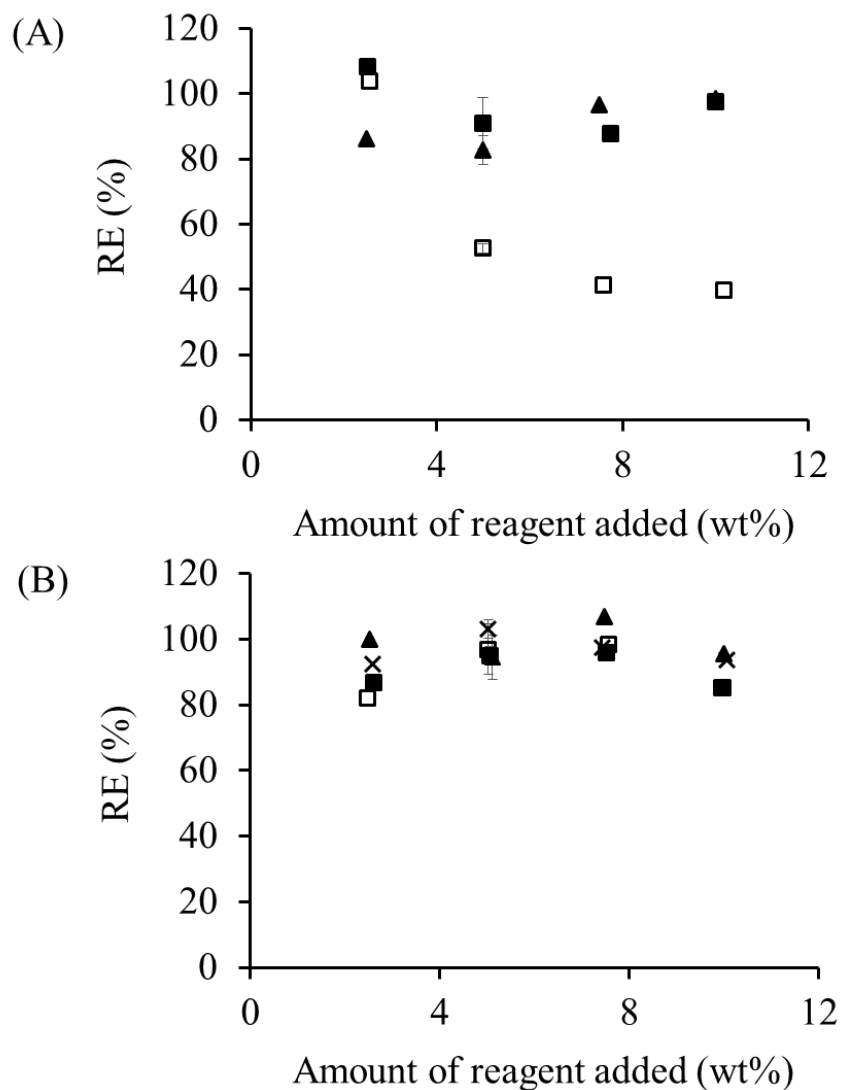


Figure 6.9. Modification of starch with (A) PA and (B) TMA. Reaction efficiency at different weight loadings for (▲) dispersed starch, (□) melt mixer reactions without base, (■) melt mixer reactions with 1.1 eq. of NaOH, and (x) melt mixer reactions with 2.2 eq. NaOH.

The absolute molecular weight averages (Table 6.2) and D_h for the PA- and TMA-modified products prepared in the dispersed phase, as with OSA and DDSA, were similar to the unmodified starch. The corresponding RI elution profiles were likewise identical to unmodified starch, indicating that no degradation or cross-linking occurred during the reaction.

Table 6.2. Absolute molecular weight averages determined by GPC analysis of starch modified with PA and TMA in the dispersed phase.

Reagent	Loading (wt%)	M_n (g/mol)	M_w (g/mol)	\bar{D}	D_h (nm)
N/A	0	2.2×10^6	4.5×10^6	2.0	50
PA	5	1.9×10^6	3.9×10^6	2.1	48
PA	10	1.9×10^6	4.0×10^6	2.2	48
TMA	5	2.2×10^6	4.3×10^6	2.0	48
TMA	10	2.1×10^6	4.2×10^6	2.0	50

The molecular weight and D_h of PA-modified starch prepared in the melt mixer without base decreased considerably with respect to unmodified starch (Table 6.3): The M_n and M_w of starch modified with 5 wt% PA decreased by more than one order of magnitude, while the D_h decreased by almost a factor of 4. The effect was even more pronounced at 10 wt% PA loading, in particular for M_w , weighted more heavily towards the longer chain components of the molecular weight distribution. Interestingly, the variations in molecular weight averages and D_h for the PA derivatives obtained in the melt mixer with a base did not display the same trends.

The 5 wt% PA derivative had a large high molecular weight shoulder in the RI elution curve, resulting in larger molecular weight and D_h values. The 10 wt% PA-modified starch, in contrast, displayed a small decrease in molecular weight and D_h , albeit not comparable with the reaction products obtained without base. A possible explanation for this result is a combination of cross-linking (through intermolecular ester or anhydride bond formation) and chain cleavage occurring during the reaction.

Table 6.3. Absolute molecular weight averages determined by GPC for starch modified with PA and TMA in a melt mixer.

Reagent	Loading (wt%)	Base (eq)	M_n (g/mol)	M_w (g/mol)	\bar{D}	D_h (nm)
---	0	0	5.6×10^6	1.9×10^7	3.4	80
PA	5	0	2.6×10^5	1.5×10^6	5.6	28
PA	10	0	2.3×10^5	9.6×10^5	4.2	24
TMA	5	0	4.7×10^5	1.8×10^6	3.8	31
TMA	10	0	4.4×10^5	1.8×10^6	4.1	31
PA	5	1.1	2.7×10^6	5.8×10^7	21.6	103
PA	10	1.1	2.6×10^6	8.7×10^6	3.4	55
TMA	5	1.1	1.7×10^6	7.1×10^6	4.3	52
TMA	10	1.1	1.7×10^6	1.1×10^7	6.3	57
TMA	5	2.2	4.1×10^6	1.2×10^7	3.0	68
TMA	10	2.2	3.2×10^6	1.4×10^7	4.4	65

The reactions with TMA followed the same trends observed for PA, with the M_n and M_w of the products without base decreasing by more than one order of magnitude and the D_h decreasing more than 2-fold. The M_n , M_w , and D_h of the TMA-modified products prepared without base were nevertheless larger than the corresponding PA derivatives. As for the PA reactions, the decrease in molecular weight and D_h of the products was minimized with base addition, the reactions with 2.2 eq. of base having M_n , M_w , and D_h values most comparable to the starch substrate.

Previous reports on starch modification with a base showed signs of degradation,¹⁴ but this was not observed in the current investigation. If acid-catalyzed hydrolysis were the only cause for the decrease in molecular weight and D_h , the TMA derivatives prepared without base should have a lower molecular weight since unreacted TMA contains a free carboxylic acid group. As that was not the case, hydrolysis cannot be the only factor coming into play. Similarly, the decrease in molecular weight and size did not scale linearly with the TMA loading, as the 5 and 10 wt% TMA products had nearly identical characteristics. This suggests that acid-catalyzed chain cleavage and cross-linking both played a role in the trends observed.

6.4.3 Reaction of Starch with Maleated Vegetable Oil in Dispersions and in the Melt Mixer

All the starch derivatives reported so far were synthesized using anhydrides derived from petroleum products.²⁵ TENAX 2010 is a commercially available maleated fatty acid derived from tall oil.⁴⁵ Beyond TENAX 2010, reactions were also completed using three different

maleated soybean oil products (Table 6.4) previously synthesized in our lab. While TENAX is produced from C₁₈ fatty acids, maleated soybean oil is an entire TG containing over 50 carbons. The hydrophobic domains introduced in starch by reaction with one mole of maleated soybean oil would therefore be much larger than for one mole of the ASAs reported above. While the reaction with starch involves anhydride rings, subsequent reactions of the modified starch could focus on the carbon-carbon double bonds, for example by cross-linking with atmospheric oxygen for coatings applications.⁴⁶

Reactions between starch and TENAX in the dispersed phase were completed in the same manner described above, except that the starch was dispersed at 25 wt% instead of 33 wt%. This is because, for reactions with 5 wt% TENAX loadings and above, the viscosity of the reaction increased to the extent that the reaction formed a solid mass around the impeller of the mechanical stirrer. This impeded mixing and pH control in the reactions, but did not result in a drop in RE, which remained above 90% at all weight loadings (Figure 6.10(A)). Foaming of the type observed with hydrophobic DDSA (containing a C₁₂ alkyl tail) was not observed for reactions with TENAX. Foaming was likely suppressed due to the higher RE for the TENAX reactions, leading to a lower succinate salt concentration in solution acting as surfactant, in addition to the increase in viscosity. The increased viscosity also suggests that reactions with TENAX may be more suitable for melt mixer or extruder operations, designed for these conditions. To the authors' best knowledge, this is the first report on reactions between TENAX 2010 and starch.

Table 6.4. Maleated soybean oil products synthesized in Chapter 5, used for the modification of starch.

Sample	MA/TG	Unreacted MA (wt%)	Unreacted TG (wt%)
MSO-1.1	1.1	1.4	0.89
MSO-2.0	2.0	1.9	0.31
MSO-2.3	2.3	4.6	0.13

Modifications to the reaction conditions were also required for the vegetable oil-based anhydrides in the melt mixer, since at 40 rpm the torque immediately dropped to zero upon addition of the oil, indicating that homogeneous mixing was not achieved. This problem was avoided when the reactions with vegetable oil-based anhydrides were completed at 60 rpm. The reactions in the melt phase, with or without base, followed trends similar to DDSA since increasing the loading of anhydride resulted in a decrease in RE. The highest RE achieved for reactions without base varied from 72.9 to 22.3%, and from 98.6 to 43.0% with base. In contrast to reactions completed in the dispersed phase with gelatinized starch, reactions in the melt mixer had uniform mixing throughout the whole procedure. Similarly to the OSA, DDSA and PA reactions, a base led to higher RE values.

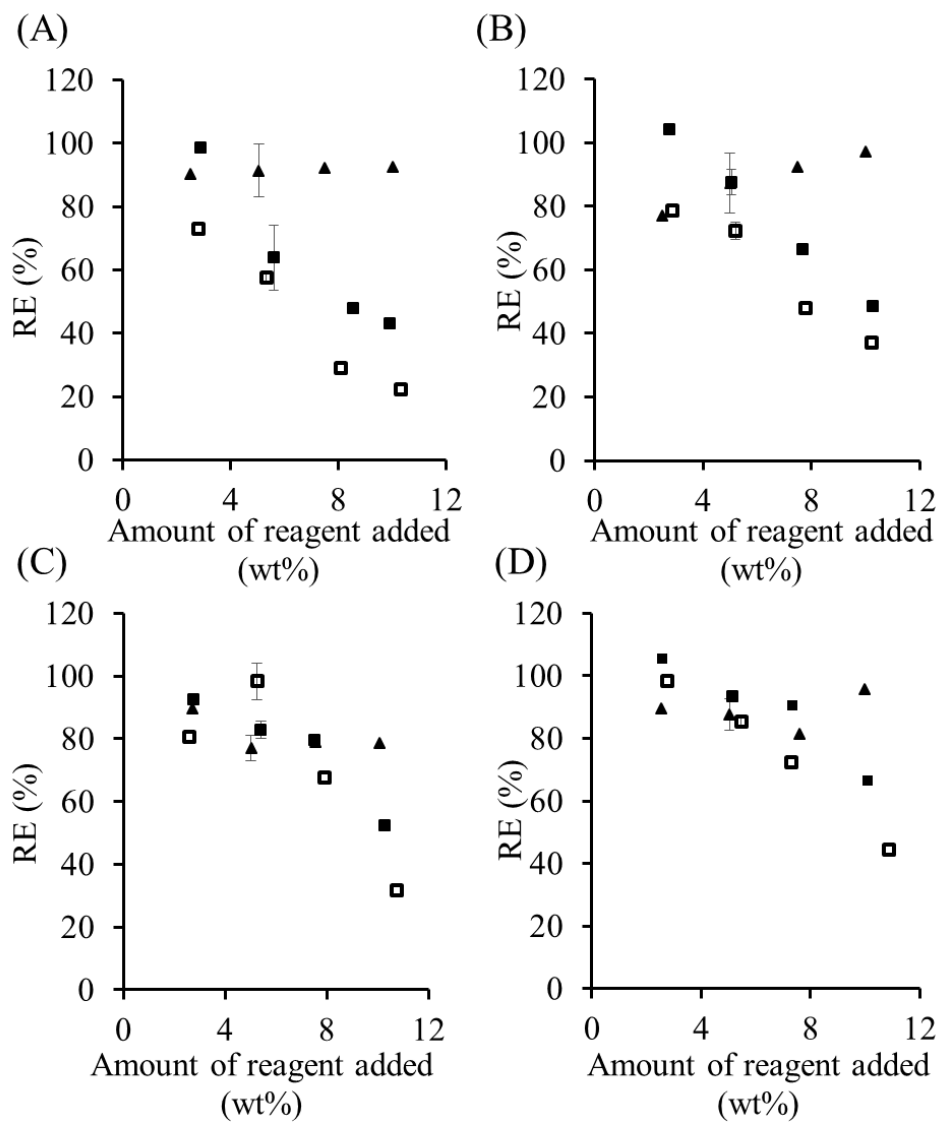


Figure 6.10. Modification of starch with (A) TENAX 2010, (B) MSO-1.1, (C) MSO-2.2, and (D) MSO-2.3. Conversion at different weight loadings for (▲) dispersed starch and melt mixer reactions (□) without and (■) with base.

Dispersed phase reactions between starch and the maleated soybean oils were completed as described for TENAX, since at weight loadings of 5 wt% and above, the reaction mixture likewise formed a solid mass around the impeller of the stirrer. For dispersed phase reactions with MSO-1.1, a RE of 77.2% was achieved at 2.8 wt%, increasing to 97.3% at the highest loading of 10.0%. The two remaining maleated oils did not show the same RE dependence on oil loading, as for MSO-2.0 a RE of 89.7% was achieved at 2.7 wt%, decreasing to 78.0% at higher loadings, while for MSO-2.3 the lowest RE of 81.4% was obtained at 7.6 wt% loading and the highest RE was 95.9% 10.0 wt% loading.

The melt phase reactions with maleated soybean oil also proceed differently. While a small decrease in torque was observed upon addition of the other reagents to the melt mixer, maleated soybean oil yielded an increase in torque (Figure 6.11). Such an increase in torque is characteristic for starch cross-linking.⁴⁷ In the absence of base the torque increased gradually throughout the reaction, reflecting increased shear forces on the starch derivative. With added base, the torque increased more rapidly. Within 2 minutes from the sharp torque increase, the plasticized starch returned to a powder form and the torque dropped to near zero since melt mixing was no longer achieved. Due to the loss of melt integrity when a base was added, the maleated oil samples had less time to react in a homogenous phase, in contrast to the other anhydrides which had approximately 11 minutes to react in the melt phase. The torque increase prior to melt breakdown was proportional to the maleation level of the soybean oil, which is further evidence for cross-linking. In spite of the melt breakdown issue, the RE remained higher

in the presence of a base: While for MSO-1.1 the RE decreased from 78.7% at 2.9 wt% to 37.1% at 10.2 wt% loading without base, the RE increased “above 100%” at 2.8 wt% and decreased to 48.7% at 10.3 wt% loading when base was used. Similarly for MSO-2.0 without base, the RE was highest (95.4%) at 5.3 wt% loading, decreasing to 31.6% at a 10.8 wt% loading. When base was used, the RE varied from 92.5% at 2.8 wt% loading to 52.5% at 10.3 wt% loading. Thus, despite the significantly reduced time spent in the melt phase, a higher RE was achieved in the presence of a base at all but the 5.3 wt% loading level. Finally, for MSO-2.3 without base, a RE of 98.3% was achieved at 2.8 wt% loading, decreasing to 44.5% at 10.9 wt% loading, while with base the RE varied from 100%, within error limits, to 66.4% over a similar composition range. Even though increasing the MA content in the maleated soybean oil product resulted in a higher RE over a shorter time period, reactive extrusion requires the starch derivative to remain as a melt throughout the procedure. If this cannot be achieved, the reaction of starch with high MA/TG oils in a twin screw extruder may be troublesome.

The molecular weight averages (Table 6.5) of the TENAX- and maleated soybean oil-modified starch products in the dispersed phase had more variance than the products previously synthesized in the dispersed phase. The TENAX-modified starch had M_n , M_w and D_h values comparable with unmodified starch, and the elution profiles were essentially identical, without high molecular weight shoulder or large D_h increase that would be expected in the presence of cross-linking.

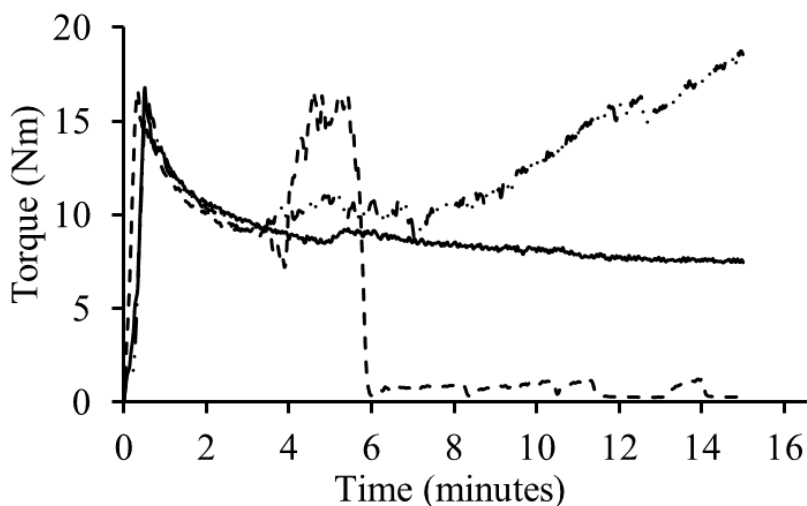


Figure 6.11. Typical torque curves at 90 °C and 60 rpm for starch with water (—), and for starch, water and MSO-2.0 without base (— . . .) and with base (- - -).

The starch processed with water in the melt mixer at 60 rpm had decreased molecular weights and D_h values (Table 6.5) as compared to starch processed at 40 rpm (Table 6.3), with $M_n = 3.8 \times 10^6$ g/mol, $M_w = 1.3 \times 10^7$ g/mol, and $D_h = 62$ nm. The decrease in molecular weight was expected, as it has been shown that increasing the specific mechanical energy exerted on starch results in starch molecules of decreased size.^{48,49} Consequently, the molecular weight of TENAX-modified starch produced in the melt phase without base are about double that of unmodified starch, with only a minor increase in D_h (Table 6.6). A possible explanation for this increase is that the torque dropped significantly upon addition of TENAX to the starch, which

Table 6.5. Absolute molecular weight averages of starch modified with TENAX and maleated soybean oil in the dispersed phase.

Reagent	Loading (wt%)	M_n (g/mol)	M_w (g/mol)	Đ	D_h (nm)
N/A	0	2.2×10^6	4.5×10^6	2.0	50
Tenax	5	2.5×10^6	7.0×10^6	2.8	64
Tenax	10	3.2×10^6	7.8×10^6	2.4	60
MSO-1.1	5	2.0×10^6	4.3×10^6	2.2	48
MSO-1.1	10	2.0×10^6	2.5×10^6	2.2	50
MSO-2.0	5	2.2×10^6	6.9×10^6	3.1	48
MSO-2.0	10	1.9×10^6	7.6×10^6	4.1	56
MSO-2.3	5	1.3×10^6	2.7×10^6	2.0	42
MSO-2.3	10	1.2×10^6	2.3×10^6	2.0	40

may have resulted in reduced chain scission. The peak elution volume and shape of unmodified starch and the TENAX-modified starch products was essentially identical in terms of RI response, indicating that there was no change in molecular weight distribution. While the TENAX-modified starch prepared with added base had a slightly higher molecular weight than unmodified starch, there was likewise no significant change in the RI peak elution volume, again indicating that the addition of base did not cause much change in molecular weight or D_h .

As stated previously, the TG molecules of maleated soybean oil contained more than one anhydride ring and could therefore act as cross-linkers. Increasing the MA/TG ratio (oil maleation level) should increase the likelihood of cross-linking. For the lowest MA/TG ratio (MSO-1.1), the starch modified in the melt phase only displayed a slight increase in molecular weight and D_h as compared to unmodified starch (Table 6.5). There was no change in the RI

Table 6.6. Absolute molecular weight averages and hydrodynamic diameter of starch modified with TENAX and maleated soybean oil in the melt mixer.

Reagent	Loading (wt%)	Base (eq)	M_n (g/mol)	M_w (g/mol)	Đ	D_h (nm)
N/A	0	0	3.8×10^6	1.3×10^7	3.3	62
Tenax	5	0	7.9×10^6	2.3×10^7	3.0	90
Tenax	10	0	7.7×10^6	2.0×10^7	2.6	81
Tenax	5	1.1	8.4×10^6	1.9×10^7	2.2	82
Tenax	10	1.1	7.3×10^6	1.5×10^7	2.0	75
MSO-1.1	5	0	6.5×10^6	1.6×10^7	2.5	76
MSO-1.1	10	0	5.6×10^6	1.3×10^7	2.3	70
MSO-1.1	5	1.1	4.9×10^6	2.0×10^7	4.1	81
MSO-1.1	10	1.1	9.0×10^6	2.8×10^7	3.1	99
MSO-2.0	5	0	3.6×10^6	8.8×10^6	2.4	59
MSO-2.0	10	0	8.6×10^5	2.2×10^6	2.6	31
MSO-2.0	5	1.1	3.0×10^6	1.6×10^7	5.5	77
MSO-2.0	10	1.1	4.2×10^6	3.1×10^7	7.3	96
MSO-2.3	5	0	1.4×10^5	4.5×10^5	3.2	17
MSO-2.3	10	0	1.1×10^5	3.7×10^5	3.4	15
MSO-2.3	5	1.1	5.2×10^6	1.5×10^7	2.8	63
MSO-2.3	10	1.1	7.8×10^6	2.2×10^7	2.8	73

peak elution volume, indicating a relatively unchanged molecular weight distribution. As in the previous cases, the addition of base resulted in higher molecular weight and D_h averages. For reactions completed without base there was no change in the RI peak elution volume.

The molecular weight and D_h for MSO-2.0-modified starch at 5 wt% loading prepared without base in the melt phase were slightly lower than for unmodified starch, but these values were much lower at 10 wt% loading without base, with M_n decreasing 4-fold, M_w decreasing 6-fold, and D_h decreasing 2-fold. The corresponding RI peak was shifted to noticeably higher elution volumes, consistently with the observed decrease in D_h . It should also be noted that the

decreases observed were apparently mainly due to degradation of the longer chain components, as there was a major loss in the high molecular weight portion of the distribution. When base was added to the reaction for MSO-2.0-modified starch at 5 wt% loading prepared with base, there was no significant change in either molecular weight or D_h , and the corresponding RI peak elution volume was similar to unmodified starch. The RI elution curve for the MSO-2.0-modified starch at 10 wt% loading prepared with base had a noticeable high molecular weight shoulder, which is likely responsible for the increased M_w value.

The MSO-2.3-modified products without base in the melt phase suffered substantial reductions in molecular weight, with M_n and M_w both decreasing by over one order of magnitude and D_h decreasing 4-fold. The RI peak elution volume increase was consistent with the D_h reduction also observed. As with the MSO-2.0 starch product at 10 wt% loading, the high molecular weight population was strongly affected. Similarly to the MSO-2.0 reactions, the addition of a base to the MSO-2.3 reactions compensated for the molecular weight and D_h reductions, leading to molecular weight and D_h values comparable to unreacted starch.

For the MSO-2.0- and MSO-2.3-modified starch products, the decreases in molecular weight or D_h were correlated with the substitution level. Our findings that reactions carried out at high torque led to lower molecular weight products but no increase in substitution level are consistent with previous reports on cross-linked starch prepared under high shear conditions. Deng and coworkers⁴⁸ indeed determined that upon adding a cross-linker to starch in a twin screw extruder, lower molecular weight starch products were obtained as compared with starch

processed under identical conditions but without cross-linker. Upon addition of the cross-linker, increases in torque and temperature were observed as the reaction between GPy units on different starch chains yielded a cross-linked network. When subjected to a high torque and temperature, the starch chains are more easily fragmented, resulting in smaller starch molecules. Gilbert and coworkers⁴⁹ also investigated the fate of starch molecules travelling through a twin screw extruder in the absence of cross-linker, by removing samples at different points along the extruder barrel and measuring their molecular weight. They found that the molecular weight decreased as the starch moved down the barrel. The decrease in molecular weight and size was not instantaneous, but rather time was required for the high molecular weight chains to fragment. Furthermore, chain fragmentation was not evenly distributed across the sample, as longer chains were much more susceptible to degradation. They concluded that fragmentation due to high shear likely occurs near the center of the starch molecules. The resulting products have an intermediate size and, most importantly, the process does not involve random fragmentation, as this would result in a complete shift of the molecular weight distribution to a lower range. The same type of shear-induced degradation was observed for MSO-2.0 and MSO-2.3 melt phase reactions without base. Anhydrides on the same TG should react slowly with different starch chains to form a crossed-linked network under these conditions, as compared with base-promoted reactions. The slow reaction leads to a gradual increase in torque after the addition of the maleated oil, which also promotes starch fragmentation. For reactions with a base the anhydride reacts more quickly with the starch, as reflected in a sharp torque increase. It is also

possible that the reaction produced a rapid increase in temperature, effectively driving off water from the starch melt. Due to the loss of melt integrity early in the reaction, the products obtained with a base did not have enough time to undergo significant fragmentation, similarly to the products removed early in the extruder barrel by Gilbert and coworkers. While the reactions without base and with base ultimately reached similar maximum torque values, the slow reaction of the anhydride without base would have allowed additional fragmentation to take place, resulting in products with a much lower molecular weight and D_h . While MSO-1.1 also had a functionality greater than one, it likely did not form enough intermolecular cross-links to produce significant torque increases and fragmentation, regardless of whether a base was used.

6.4.4 Starch Modification by Reactive Extrusion

Both single and twin screw extruders can be used to produce modified starch in a continuous process on an industrial scale.²² They can mix starch (and other viscous materials) in a homogenous and controlled manner.⁵⁰ Water and other starch plasticizers can be used at low weight loadings under these conditions, which results in a higher starch concentration. The short residence time, low water content and high temperature (in some cases well above the boiling point of water) used in an extruder, along with high shear mixing, have been shown to yield over 10-fold rate enhancements for esterification reactions as compared with dispersed phase reactions.²¹ High temperature and shear enable starch gelatinization early in the extruder barrel. Reactants should be added at a point after full gelatinization is achieved so as to increase the

number of hydroxyls available, maximize the RE, and to yield products with a more homogenous composition.²¹

When DDSA was used to modify starch in a twin screw extruder (Figure 6.12), a trend similar to the reactions in the melt mixer was observed. Without base a RE of 94.8% was obtained at 1.5 wt% loading, decreasing to 59.4% at 5 wt% loading. When NaOH was added, the RE increased to 93.8% at 5 wt% DDSA. Reactive twin screw extrusion of regular maize starch with DDSA has been reported by Wu and coworkers.⁵⁰ The highest RE achieved in that investigation was 78% using 3 wt% DDSA, 110 rpm, 120 °C, 30 wt% water and 0.5% NaOH. The conditions used in the present investigation therefore led to a significant improvement in RE for that system.

For the reactions of starch with TENAX in the twin screw extruder, RE values higher than for DDSA were obtained. Without base, a RE of 93.8% was achieved at 1.6 wt% loading, decreasing to 83.1% at 5.2 wt% loading. The addition of a base to the reaction did not improve on the 86% RE at 3.7 wt% loading, but increased it to 94.4% at 5.2 wt% loading.

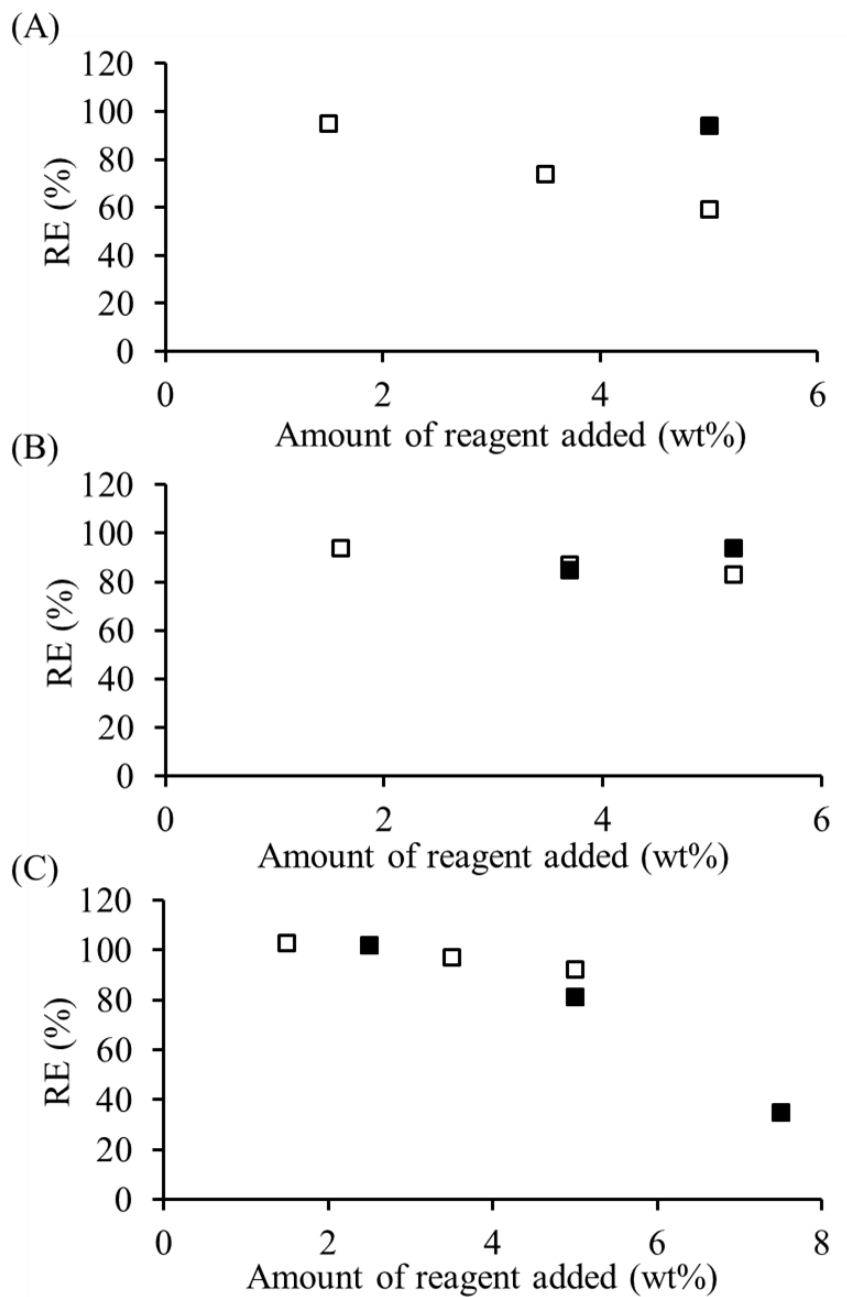


Figure 6.12. Modification of starch in a pilot plant twin screw extruder (□) without base and (■) with 1.1 eq. of NaOH and (A) DDSA, (B) TENAX 2010, and (C) MSO-1.1.

For reactions between starch and MSO-1.1, an apparent RE > 100% was achieved at the lowest weight loading (1.6 wt%), decreasing to 92.2% at a 5 wt% loading. Interestingly, when base was added a drop in RE was observed, in contrast to the melt phase reactions and the previously discussed extrusion reactions: The RE decreased to 81.3% at 5 wt%, and to 34.9% at a loading of 7.5 wt%. A possible explanation for the drop in RE observed is that the addition of base made the starch melt more hydrophilic, such that the hydrophobic anhydride did not have sufficient time to fully react in the extruder. The conversion of maleated vegetable oil achieved in the twin screw extruder without base was higher than in the only previous report on that topic. Narayan and coworkers⁵¹ indeed patented a process on the modification of starch with maleated corn oil in a twin screw extruder. The highest RE reported in the patent was 82%, at 4.5 wt% maleated corn oil loading, using 2,5-bis(*tert*-butylperoxy)-2,5-dimethylhexane (Luperox 101) as catalyst and glycerol as plasticizer, although some water was also present in the starch. A higher conversion was achieved herein without catalyst, and using only water as plasticizer.

The molecular weight and D_h of DDSA-modified starch reactive extrusion products were essentially independent of the DDSA loading (Table 6.7). Previously, reactive extrusion of starch with linear anhydrides²² resulted in degradation of the starch, but that was not seen here. The addition of base did not cause a decrease in molecular weight or D_h , but rather slightly higher molecular weight and D_h values were observed. The use of base is often cited to cause discoloration in the reactive extrusion of starch, which is attributed to degradation, but no decrease in molecular weight has been reported.²¹ The RI peak elution volume for the product

prepared with 5 wt% DDSA slightly decreased, which is consistent with higher molecular weight and D_h values.

Table 6.7. Absolute molecular weight averages and D_h for starch modified with DDSA, TENAX, and maleated soybean oil by reactive extrusion.

Reagent	Loading (wt%)	Base (eq)	M_n (g/mol)	M_w (g/mol)	\bar{D}	D_h (nm)
DDSA	1.5	0	4.3×10^6	7.4×10^6	1.7	64
DDSA	3.5	0	4.7×10^6	8.0×10^6	1.7	66
DDSA	5	0	4.7×10^6	8.2×10^6	1.8	66
DDSA	5	1.1	6.4×10^6	1.5×10^7	2.4	80
Tenax	1.6	0	3.2×10^6	5.1×10^6	1.6	55
Tenax	3.7	0	3.5×10^6	5.8×10^7	1.6	58
Tenax	5.2	0	3.4×10^6	7.2×10^7	2.1	62
Tenax	3.7	1.1	3.7×10^6	7.0×10^7	1.9	61
Tenax	5.2	1.1	3.6×10^6	6.3×10^7	1.7	59
MSO-1.1	1.5	0	2.3×10^6	6.8×10^6	3.0	63
MSO-1.1	3.5	0	1.8×10^6	6.4×10^6	3.5	61
MSO-1.1	5	0	1.8×10^6	6.6×10^6	3.7	59
MSO-1.1	2.5	1.1	3.1×10^6	7.4×10^6	2.4	58
MSO-1.1	5	1.1	1.6×10^6	5.0×10^6	3.1	47
MSO-1.1	7.5	1.1	4.3×10^6	1.2×10^7	2.8	69

The TENAX-modified starch prepared in the extruder, both without and with added base, displayed no significant change in molecular weight or D_h at the different substitution levels. For starch modified with MSO-1.1 without base, there was no change in molecular weight or D_h . Only the 5 wt% MSO-1.1 product obtained with a base had lower molecular weight and D_h values than the corresponding product obtained without base, as well as the other MSO-1.1

products. It is also worth pointing out that since the 5 wt% MSO-1.1 starch without base had a higher RE, the difference in molecular weight and D_h does not seem to be directly related to the substitution level.

In the reactions carried out in the melt mixer, the decrease in molecular weight and D_h observed for MSO-2.0 and MSO-2.3 without base is attributed to increased shear forces imposed on the product. The 7.5 wt% MSO-1.1-modified product had a relatively low (34.9%) RE but noticeably higher molecular weight and D_h than the other MSO-1.1-modified products. A possible explanation for the higher molecular weight and D_h of the 7.5 wt% MSO-1.1 product is that since more NaOH was added to the system due to the higher anhydride loading, the addition of NaOH decreased the torque. The addition of NaOH to starch in the melt mixer resulted in a larger drop in torque as compared to deionized water, and it has indeed been shown before that the addition of NaOH lowers the starch viscosity more than pure water.⁵² The drop in torque and reduced shear forces exerted on the starch would lead to decreased starch chain degradation.

6.5 Conclusions

Hydrophobically modified starch derivatives were successfully prepared by different methods (dispersed phase, melt mixer and extrusion) by reaction with cyclic anhydrides derived from either petroleum products (OSA, DDSA, PA, and TMA) or vegetable oils (TENAX and MSO), through environmentally friendly procedures. The reaction efficiency (RE) was found to depend on the state of the reaction, as well as the structure of the maleated reagent used.

Reactions completed with starch dispersed in water (33 wt% starch) had RE values above 80%, except for DDSA and maleated soybean oil samples. At moderate to high maleated vegetable oil loadings, the reactions were no longer homogeneous. GPC analysis revealed that the molecular weight and hydrodynamic diameter did not increase; therefore the viscosity increases observed are attributed to the hydrophobic modification.

Reactions completed in a heated melt mixer on starch plasticized with water (80 wt% starch) had decreasing REs for increasing anhydride loadings, except for TMA which maintained a high RE at all loadings. Reactions completed with a base had higher REs for all the anhydrides tested, indicating that esterification is favored over hydrolysis. Interestingly, the molecular weight and D_h of the modified starch products were greater than for the products prepared without base, in contrast to previous literature reports.

Reactions with maleated soybean oil in the melt mixer led to a significant increase in the measured torque. The base-promoted reactions, in particular, were no longer plasticized, whereas the reactions without base had a torque increasing throughout the reaction. GPC analysis revealed that the products of the base-promoted reactions had molecular weight and size characteristics similar to unmodified starch, while the products obtained without base had undergone extensive shear-induced chain scission. The decrease in size observed was attributed to the high shear forces experienced by the starch derivatives, due to the increased torque, rather than related to the substitution level.

When comparing the reactive extrusion results with DDSA, TENAX, and MSO-1.1, it should be kept in mind that while the hydrophobicity of the anhydrides increased in the order $\text{DDSA} < \text{TENAX} < \text{MSO-1.1}$, the RE varied in the same order. Noteworthy is the fact that the MSO-1.1-modified product at 1.6 wt% loading reached 100% RE without a base. The addition of a base increased the RE for DDSA and TENAX, while decreasing the RE for MSO-1.1. Reactive extrusion proved to be the most advantageous technique to readily produce hydrophobically modified starch in an environmentally friendly and scalable way. The RE is high enough that the reaction products would not need to be purified before use. A major economic obstacle to the industrial implementation of this modification method is therefore removed.

Chapter 7

Concluding Remarks and Suggestions for Future Work

7.1 Original Contributions to Knowledge

The research described in this Thesis focused primarily on the hydrophobic modification of SNPs or waxy maize starch, as well as the synthesis of new hydrophobic starch modifiers derived from vegetable oils. Hydrophobic modification was first completed on SNPs dispersed in an organic solvent, using either hexanoic or propionic acid anhydride. The hydrophobic modification of waxy maize pregelatinized starch was completed on aqueous dispersions in water (33 wt% starch) with different cyclic anhydrides (either OSA, DDSA, TENAX 2010, PA, TMA, MSO-1.1, MSO-2.0, or MSO-2.3). Native waxy maize starch was also gelatinized *in situ* using water as plasticizer (80 wt% starch), and modified with either castor oil PUPs or cyclic anhydrides in a single process using a melt mixer. Finally, the reactive extrusion of starch was completed (80 wt% starch) using either DDSA, TENAX 2010, or MSO-1.1 as hydrophobic modifying agents.

The HM-SNPs prepared in DMSO with either hexanoic or propionic acid anhydride in the presence of pyridine and DMAP remained water-dispersible and were obtained with a RE of 100% over the entire DS range tested. There was no difference in reactivity observed between hexanoic and propionic acid anhydrides, nor among SNPs of different sizes under these conditions. The integrity of the products was maintained, as the reaction conditions used did not

lead to fragmentation of the starch, and the addition of hydrophobic microdomains did not influence the D_h of the HM-SNPs in DMSO. The synthesized products were transferred to the Duhamel Lab for further characterization by fluorescence spectroscopy.¹

New castor oil PUPs were synthesized using TDI without solvent at an OH:NCO ratio of 1:2, either with 0.1 wt% DBTDL or K-KAT 348, or without catalyst. In spite of the low OH:NCO ratio used, full conversion of the hydroxyl groups was achieved even without catalyst. In the absence of full conversion, the unreacted hydroxyl groups would continue reacting during storage, resulting in lower %NCO contents for the PUPs. A new method to quantify unreacted TDI in the castor oil PUPs using GPC analysis was developed. Previous reports on castor oil PUP syntheses neglected the quantification of unreacted diisocyanate in the PUPs, even though this is the underlying reason for using a low OH:NCO ratio. The castor oil PUPs were used to cross-link starch and to add hydrophobic domains in starch without using organic solvents or catalysts in a melt mixer. The reactions proceeded with high overall RE in less than 15 minutes, such that further purification of the product should not be necessary. The reaction between the starch hydroxyl groups and the isocyanate groups does not form any by-product, hence the reaction has 100% atom economy. The hydrophilic-hydrophobic balance of the modified starch can be predictably tuned for specific applications. Finally, the size of the resulting starch molecules can be controlled through the amount of castor oil PUP added, when the reaction is carried out under high shear.

The maleation of raw linseed oil in a benchtop sealed high pressure reactor led to extensive cross-linking; anti-oxidants and toluene were ineffective at preventing cross-linking in the reaction. In contrast, the maleation of soybean oil could be completed under different conditions without catalysts or solvents, and the products were completely soluble in organic solvents, indicating that extensive cross-linking did not occur in that case. Maleated soybean oil products were synthesized containing up to 2.6 anhydride units on average per triglyceride, which greatly exceeds the maximum value of 1.0 reported in the literature.² The maleation level of soybean oil was controlled by varying the amount of MA in the reaction, using either a benchtop sealed high pressure reactor, a benchtop open glass reactor, or a pilot plant scale open glass reactor. The large scale reaction was most efficient at low and medium MA loadings, while the benchtop open reactor was most efficient at high MA loadings. The type of reactor used influenced the physical properties of the products, as GPC analysis indicated that the sealed high pressure reactor approach led to significant oligomerization of the maleated triglycerides. The maleated soybean oil products from both open reactor methods were predominantly single triglycerides. Finally, a new procedure was developed to determine the weight fraction of unreacted triglycerides remaining in the maleated oil.

Hydrophobic starch esters were successfully prepared by reacting pregelatinized starch dispersions in water (33 wt% starch) with different cyclic anhydrides (OSA, DDSA, TENAX 2010, PA, TMA, MSO-1.1, MSO-2.0, and MSO-2.3). The reaction was completed over 1 h, which represents a large decrease in comparison with previous work in the field.³ The RE was

above 80% irrespective of the anhydride loading, except for high loadings of DDSA and maleated soybean oil. At moderate to high loadings of vegetable oil-derived anhydrides, the reaction mixtures were no longer liquid. GPC analysis revealed that the molecular weight and the D_h did not change for the starch esters. This is the first reported synthesis of starch esters in aqueous media using TENAX 2010 and TMA. While starch esters of PA and maleated soybean oil have been obtained by reactive extrusion, this was not achieved for substitution levels up to 10 wt% nor in aqueous dispersions as reported herein. To reduce the amount of water used and the duration of the reaction, the esterification procedure was transferred to a heated melt mixer, starting from native waxy maize plasticized with water (80 wt% starch), whereby gelatinization occurred *in situ*. For reactions completed without a base, the RE decreased for increasing anhydride loadings, except for TMA which maintained a high RE at all loadings. As expected, reactions completed with a base had higher REs for all the anhydrides tested. The molecular weight and D_h data obtained for the modified starch products prepared with a base were greater than for the products prepared without base. Reactions completed with highly substituted maleated soybean oil in the melt mixer without a base underwent extensive shear-induced chain scission, while the products of the base-promoted reactions did not. For reactive extrusion, the RE increased following the trend DDSA < TENAX < MSO-1.1, i.e. in the same order as the hydrophobicity. The MSO-1.1-modified product at 1.6 wt% loading was obtained with 100% RE without a base. The addition of a base increased the RE for DDSA and TENAX, while decreasing the RE for MSO-1.1. Reactive extrusion proved to be the most advantageous

technique to readily produce hydrophobically modified starch in an environmentally friendly and scalable way. The RE achieved by that method was high enough that the reaction products would not need to be purified before use.

7.2 Suggestions for Future Work

The work presented in this Thesis focused on the synthesis of new hydrophobic starch products, with emphasis on using vegetable oil building blocks as hydrophobic modifying groups. Environmentally friendly procedures were developed to avoid the use of organic solvents. Indeed, the economic viability of modified starch products is often lost due to the need for purification. Consequently, reactions with high atom economy were investigated to produce vegetable oil-based modifying agents as well as hydrophobic starch products.⁴

7.2.1 Measurement of Physical Properties of Synthesized Starch Products

Hydrophobically modified starches have found multiple uses in food and industrial applications. Starch modified with up to 3 wt% OSA has FDA approval for food use.⁵ To the author's best knowledge, maleated soybean oil does not have FDA approval, and the process to receive FDA approval would likely be time-consuming and costly. In the event of FDA approval, maleated soybean oil-modified starch could nevertheless serve as emulsifier or stabilizer in sauces, puddings, and infant formulas.⁶ Maleated soybean oil-modified starch has the potential to replace OSA-modified starch products such as N-Creamer, Purity Gum, CAPSUL, Hi-CAP,

Mira-Cap, DRYFLO, and Clearam.⁷ The ability of maleated soybean oil-modified starch to stabilize Pickering emulsions should be investigated, as it has been done for OSA-modified starch.⁸

Hydrophobic starch esters have numerous applications in materials science, as the hydrophobicity of the products can be tuned by controlling the DS.³ Native and modified starches have been investigated for their film-forming and barrier properties.⁹ Native starch has a high water permeability, however hydrophobic starch esters have been shown to have better water resistance.¹⁰ Changes in hydrophobicity can be measured by water uptake and contact angle measurements.¹¹ Hydrophobic starch products should have a larger contact angle for water droplets as compared to hydrophilic starch products. Finally, hydrophobic starch esters have shown promise in blends with petroleum-based plastics, to increase the degradability of the materials.¹² For this application, starch and the petroleum-based product should form a continuous phase and not experience phase separation to retain mechanical properties comparable to the petroleum-based polymers.¹³ The hydrophobic starch derivatives reported herein should be tested for their tensile strength, Young's modulus, and elongation at break to demonstrate their suitability as replacements for products derived exclusively from petroleum.¹²

7.2.2 Controlled Oligomerization of Maleated Vegetable Oil

The synthesis of maleated linseed oil was completed in a closed reactor, while maleated soybean oil was synthesized in a closed reactor as well as open glass reactors. The use of linseed oil was not explored further due to the extensive occurrence of cross-linking. However the

addition of small amounts of linseed oil (or other drying oils) to less unsaturated vegetable oils (such as soybean oil) in an open glass reactor may be useful to promote the oligomerization of triglycerides. This approach should decrease the amount of unreacted triglycerides in the products. The amount of linseed oil required in the oil mixture would have to be determined experimentally to avoid extensive cross-linking. Another pathway of interest to obtain an oligomerized product could be controlled auto-oxidation of the maleated oil product.¹⁴ The carbon-carbon double bonds in fatty acids can react with atmospheric oxygen, forming a hydroperoxide which subsequently reacts with carbon-carbon double bonds on different fatty acids.¹⁵ The oligomerization process can be accelerated by the addition of driers (metal cations and lipophilic ligands), or a mixture of driers.¹⁴ The drier could be added either before or after the reaction with MA, although if the drier is added before MA, it may interfere with the ene reaction. The maleated oil product could serve in more applications beyond starch modification. It has potential uses in coatings, adhesives, as a plasticizer, or as a monomer in step-growth polymerization.¹⁶ For starch modification, it is expected that a maleated oil with more than one anhydride group per molecule should act as a cross-linker. Finally, a drier (or driers) could be added to maleated soybean oil-modified starch in solution. The hydrophobic domains of the maleated soybean oil-modified starch reported herein contain carbon-carbon double bonds, which could react further with oxygen to form a cross-linked network. Driers added in this scenario would have to be tolerant to water, however. Cross-linking between fatty acid residues in maleated soybean oil-modified starch products would be highly advantageous as air-curable

coatings and adhesives, since the modified starch would form an interpenetrating network and their surface would harden with time.¹⁷

7.2.3 Reactive Extrusion of Starch with Vegetable Oil-based Modifying Agents

The reactive extrusion of waxy maize starch was completed using DDSA, TENAX 2010, and MSO-1.1. The hydrophobic anhydrides used contained predominately one anhydride group per molecule. Maleated vegetable oil with more than one anhydride group would be expected to induce cross-linking of the starch, while also making it more hydrophobic. The increase in torque resulting from cross-linking would favor starch chain scission, yielding hydrophobically modified starch products with decreased molecular weights and D_h .¹⁸ Due to the large molar mass of maleated vegetable oil, a significant decrease in molecular weight and D_h may not be achievable at low weight loadings. A possible solution to this problem could be adding a small molecule cross-linker after the maleated vegetable oil in the extruder barrel. Possible cross-linkers include but are not limited to citric acid, sodium trimetaphosphate, dialdehydes, or malonic acid.^{18,19} For film-forming applications the starch selected should have a higher amylose content, since amylose improves film strength and other functional properties.²⁰

An alternative to maleated vegetable oil to produce cross-linked hydrophobic modified starch could be to use castor oil PUPs. The castor oil PUPs based on TDI indeed reacted with starch in the melt phase with a higher RE than MSO-1.1 at similar weight loadings. It is expected that castor oil PUPs should have a similar, if not higher, RE than MSO-1.1 in twin screw reactive extrusion. In this high shear environment, the addition of castor oil PUPs (not necessarily based

on TDI) should produce an increase in torque, which would lead to starch chain scission and ultimately yield hydrophobically modified starch products with lower molecular weights and D_h . An advantage of using castor oil PUPs is that the resulting urethane bonds with starch have higher hydrolytic stability than ester linkage obtained with maleated soybean oil.²¹ The hydrophobically modified starch products obtained by either method should be further characterized according to the procedures outlined in Section 7.2.1.

7.2.4 Synthesis of Novel Drug Delivery Vehicles derived from Bio-based Materials

The synthesis of water-dispersible HM-SNPs was completed using either hexanoic or propionic acid anhydride. The products will be further characterized by collaborators in the Duhamel lab at UW.¹ The DS of these starch esters is relatively low, up to 0.15 and 0.30 for the hexanoic and propionic acid esters, respectively. HM-SNPs with higher DS, that are still dispersible in water, could be obtained by the addition of hydrophilic polymer chains such as poly(ethylene glycol) (PEG) to the starch. Nanoparticles prepared from either synthetic polymers or metals have previously been shown to illicit inflammatory and toxic responses in cells, and require approval from the FDA for use in the body. In contrast, starch is advantageous because it is cost-effective, non-toxic, renewable, biodegradable, biocompatible, and approved by the FDA for use in the body.²²

For the synthesis of a starch-based drug delivery vehicle, a heterobifunctional PEG chain with an azide chain end and a hydroxyl group at the other end could be modified easily to react

with starch. First, the hydroxyl group could be modified with *p*-toluenesulfonyl chloride in dichloromethane and excess triethylamine. Under these conditions the PEG chains should not degrade, nor would the integrity of the azide at the other chain end be lost. Second, the resulting tosylated PEG chain could be reacted with starch under the same conditions as the linear anhydride in DMSO, using a catalytic amount of DMAP and excess pyridine. It is suggested that the tosylated PEG should be added before the anhydride and be allowed to react completely. The anhydride may otherwise compete to react with hydroxyl groups at the periphery of the starch nanoparticles. High molecular weight PEG may not diffuse deeply into the starch, thereby limiting the number of GPy units with which it can react. The DS of the PEG and anhydride should be optimized to obtain a HM-SNP product stable in water (or buffer solutions). Increasing either the DS or the molecular weight of the PEG chains would increase the hydrophilicity of the product, whereas increasing the DS or chain length of the ester would increase the hydrophobicity of the product. Finally, targeting groups such as small molecules, peptides, or DNA aptamers containing a terminal alkyne or a cell-penetrating agent with a terminal alkyne could be conjugated with the starch particles through copper-catalyzed azide-alkyne Huisgen cycloaddition “click” chemistry.²³

References

Chapter 1

- (1) Bras, J.; Dufresne, A. *Biomacromolecules* **2010**, *11*, 1139–1153.
- (2) Perez, S.; Bertoft, E. *Starch - Stärke* **2010**, *62*, 389–420.
- (3) Ellis, R. P.; Cochrane, M. P.; Dale, M. F. B.; Dupus, C. M.; Andrew, L.; Morrison, I. M.; Prentice, R. D. M.; Swanston, J. S.; Tiller, S. A. *J. Sci. Food Agric.* **1998**, *77*, 289–311.
- (4) Haroon, M.; Wang, L.; Yu, H.; Abbasi, N. M.; Saleem, M.; Khan, R. U.; Ullah, R. S.; Chen, Q. *RSC Adv.* **2016**, *6*, 78264–78285.
- (5) Moad, G. *Prog. Polym. Sci.* **2011**, *36* (2), 218–237.
- (6) Buleon, A.; Colonna, P.; Planchot, V.; Ball, S. *Int. J. Biol. Macromol.* **1998**, *23*, 85–112.
- (7) Wang, S.; Copeland, L. *Crit. Rev. Food Sci. Nutr.* **2015**, *55*, 1081–1097.

Chapter 2

- (1) Marion, P.; Bernela, B.; Piccirilli, A.; Estrine, B.; Patouillard, N.; Guilbot, J.; Jerome, F. *Green Chem.* **2017**, *19*, 4973–4989.
- (2) Clercq, R. De; Dusselier, M.; Sels, B. F. *Green Chem.* **2017**, *19*, 5012–5040.
- (3) Basu, S.; Plucinski, A.; Catchmark, M. *Green Chem.* **2017**, *19*, 4080–4092.

- (4) Hong, M.; Chen, E. Y. *Green Chem.* **2017**, *19*, 3692–3706.
- (5) Hamdy, M. S. *Green Chem.* **2017**, *19*, 5144–5151.
- (6) Ashogbon, A. O.; Akintayo, E. T. *Starch - Stärke* **2014**, *66*, 41–57.
- (7) Kumar, M. N. V. R. *React. Funct. Polym.* **2000**, *46*, 1–27.
- (8) Sullivan, A. C. O. *Cellulose* **1997**, 173–207.
- (9) Brown, R. M. *J. Polym. Sci. Part A Polym. Chem.* **2004**, *42*, 487–494.
- (10) Moon, R. J.; Martini, A.; Nairn, J.; Simonsen, J.; Youngblood, J. *Chem. Soc. Rev.* **2011**, *40*, 3941–3994.
- (11) Manners, D. J. *Carbohydr. Polym.* **1989**, *11*, 87–112.
- (12) Perez, S.; Bertoft, E. *Starch - Stärke* **2010**, *62*, 389–420.
- (13) Le Corre, D.; Bras, J.; Dufresne, A. *Biomacromolecules* **2010**, *11*, 1139–1153.
- (14) Moad, G. *Prog. Polym. Sci.* **2011**, *36* (2), 218–237.
- (15) Pillai, C. K. S.; Paul, W.; Sharma, C. P. *Prog. Polym. Sci.* **2009**, *34*, 641–678.
- (16) Hu, X.; Du, Y.; Tang, Y.; Wang, Q.; Feng, T.; Yang, J.; Kennedy, J. F. *Carbohydr. Polym.* **2007**, *70*, 451–458.
- (17) Beltrame, P. L.; Naggi, A.; Torri, G. *Carbohydr. Polym.* **1990**, *12*, 405–412.
- (18) Buleon, A.; Colonna, P.; Planchot, V.; Ball, S. *Int. J. Biol. Macromol.* **1998**, *23*, 85–112.

- (19) Hoover, R. *Carbohydr. Polym.* **2001**, *45*, 253–267.
- (20) Tester, R. F.; Karkalas, J.; Qi, X. *J. Cereal Sci.* **2004**, *39*, 151–165.
- (21) Wang, S.; Copeland, L. *Crit. Rev. Food Sci. Nutr.* **2015**, *55*, 1081–1097.
- (22) Ellis, R. P.; Cochrane, M. P.; Dale, M. F. B.; Dupus, C. M.; Andrew, L.; Morrison, I. M.; Prentice, R. D. M.; Swanston, J. S.; Tiller, S. A. *J. Sci. Food Agric.* **1998**, *77*, 289–311.
- (23) Li, W.; Corke, H.; Beta, T. *Carbohydr. Polym.* **2007**, *69*, 398–405.
- (24) Ratnayake, W. S.; Jackson, D. S. *Carbohydr. Polym.* **2007**, *67*, 511–529.
- (25) Liu, H.; Xie, F.; Yu, L.; Chen, L.; Li, L. *Prog. Polym. Sci.* **2009**, *34*, 1348–1368.
- (26) Cai, L.; Shi, Y. *Carbohydr. Polym.* **2014**, *105*, 341–350.
- (27) Le Corre, D.; Angellier-Coussy, H. *React. Funct. Polym.* **2014**, *85*, 97–120.
- (28) Carlstedt, J.; Wojtasz, J.; Fyhr, P.; Kocherbitov, V. *Carbohydr. Polym.* **2015**, *129*, 62–69.
- (29) Cai, W.; Diosady, L. L. *J. Food Sci.* **1993**, *58* (4), 872–875.
- (30) Svihus, B.; Uhlen, A. K.; Harstad, O. M. *Anim. Feed Sci. Technol.* **2005**, *122*, 303–320.
- (31) Chen, P.; Yu, L.; Simon, G. P.; Liu, X.; Dean, K.; Chen, L. *Carbohydr. Polym.* **2011**, *83* (4), 1975–1983.
- (32) Vamadevan, V.; Bertoft, E. *Starch - Stärke* **2015**, *67*, 55–68.

- (33) Pushpadass, H. A.; Marx, D. B.; Hanna, M. A. *Starch - Stärke* **2008**, *60*, 527–538.
- (34) Wolf, B. *Curr. Opin. Colloid Interface Sci.* **2010**, *15* (1–2), 50–54.
- (35) Xie, F.; Yu, L.; Liu, H.; Chen, L. *Starch - Stärke* **2006**, *58* (3–4), 131–139.
- (36) Liu, W.; Halley, P. J.; Gilbert, R. G. *Macromolecules* **2010**, *43*, 2855–2864.
- (37) Qiao, D.; Zou, W.; Liu, X.; Yu, L.; Chen, L.; Liu, H.; Zhang, N. *Starch - Stärke* **2012**, *64* (10), 821–825.
- (38) Dias, F. T. G.; Souza, R. C. R.; Andrade, C. T. *Macromol. Symp.* **2011**, *299–300* (1), 139–146.
- (39) Silva, M. C.; Ibezim, E. C.; Ribeiro, T. A. A.; Carvalho, C. W. P.; Andrade, C. T. *Ind. Crops Prod.* **2006**, *24* (1), 46–51.
- (40) Wang, S.; Li, C.; Copeland, L.; Niu, Q.; Wang, S. *Compr. Rev. Food Sci. Food Saf.* **2015**, *14*.
- (41) Kim, H.; Park, S. S.; Lim, S. *Colloids Surfaces B Biointerfaces* **2015**, *126*, 607–620.
- (42) Putaux, J.; Molina-boisseau, S.; Momaur, T.; Dufresne, A. *Biomacromolecules* **2003**, *4*, 1198–1202.
- (43) Song, D.; Thio, Y. S.; Deng, Y. *Carbohydr. Polym.* **2011**, *85* (1), 208–214.
- (44) Sweedman, M. C.; Tizzotti, M. J.; Schäfer, C.; Gilbert, R. G. *Carbohydr. Polym.* **2013**, *92* (1), 905–920.

- (45) Lele, V. V.; Kumari, S.; Niju, H. *Starch - Stärke* **2018**, *1700133*, 1–9.
- (46) Liu, Z.; Li, Y.; Cui, F.; Ping, L.; Song, J.; Ravee, Y.; Jin, L.; Xue, Y.; Xu, J.; Li, G.; Wang, Y.; Zheng, Y. *J. Agric. Food Chem.* **2008**, *56*, 11499–11506.
- (47) Xu, Y.; Miladinov, V.; Hanna, M. A. *Cereal Chem.* **2004**, *81* (6), 735–740.
- (48) Sweedman, M. C.; Hasjim, J.; Tizzotti, M. J.; Schäfer, C.; Gilbert, R. G. *Carbohydr. Polym.* **2013**, *97* (1), 9–17.
- (49) Pal, J.; Singhal, R. S.; Kulkarni, P. R. *Carbohydr. Polym.* **2000**, *43*, 155–162.
- (50) Zheng, B.; Karski, M.; Taylor, S. D. *Carbohydr. Polym.* **2019**, *209* (January), 145–151.
- (51) De Graaf, R. A.; Janssen, L. P. B. M. *Adv. Polym. Technol.* **2003**, *22* (1), 56–68.
- (52) He, G.-Q.; Song, X.-Y.; Ruan, H.; Chen, F. *J. Agric. Food Chem.* **2006**, *54*, 2775–2779.
- (53) Tizzotti, M. J.; Sweedman, M. C.; Tang, D.; Schaefer, C.; Gilbert, R. G. *J. Agric. Food Chem.* **2011**, *59*, 6913–6919.
- (54) Wang, L.; Shogren, R. L.; Willett, J. L. *Starch - Stärke* **1997**, *49* (3), 116–120.
- (55) Bai, Y.; Shi, Y.; Herrera, A.; Prakash, O. *Carbohydr. Polym.* **2011**, *83* (2), 407–413.
- (56) Aburto, J.; Alric, I.; Thiebaud, S.; Borredon, E.; Bikiaris, D.; Prinos, J.; Panayiotou, C. *J. Appl. Polym. Sci.* **1999**, *74*, 1440–1451.
- (57) Bhuniya, S. P.; Rahman, M. S.; Satyanand, A. J.; Gharia, M. M.; Dave, A. M. *J. Polym. Sci. Part A Polym. Chem.* **2003**, *41*, 1650–1658.

- (58) Heinze, T.; Haack, V.; Rensing, S. *Starch - Stärke* **2004**, *56*, 288–296.
- (59) Zhang, Y.; Wang, X.; Zhao, G.; Wang, Y. *Carbohydr. Polym.* **2012**, *87* (4), 2554–2562.
- (60) Fang, J. M.; Fowler, P. A.; Sayers, C.; Williams, P. A. *Carbohydr. Polym.* **2004**, *55*, 283–289.
- (61) Zhang, Y.; Leng, Y.; Zhu, M.; Fan, B.; Yan, R.; Wu, Q. *Carbohydr. Polym.* **2012**, *88* (4), 1208–1213.
- (62) Altuna, L.; Lidia, M.; Laura, M. *Food Hydrocoll.* **2018**, *80*, 97–110.
- (63) Tomasik, P.; Schilling, C. H. *Adv. Carbohydr. Chem. Biochem.* **2004**, *59*, 175–403.
- (64) Aburto, J.; Alric, I.; Borredon, E. *Starch - Stärke* **1999**, *51* (4), 132–135.
- (65) Namazi, H.; Dadkhah, A. *Carbohydr. Polym.* **2010**, *79* (3), 731–737.
- (66) Mullen, J. W.; Pacsu, E. *Ind. Eng. Chem.* **1942**, *34* (10), 1209–1217.
- (67) Jeon, Y.; Viswanathan, A.; Gross, R. A. *Starch - Stärke* **1999**, *51* (2), 90–93.
- (68) Miao, M.; Li, R.; Jiang, B.; Cui, S. W.; Zhang, T.; Jin, Z. *Food Chem.* **2014**, *151*, 154–160.
- (69) Miladinov, V. D.; Hanna, M. A. *Ind. Crop. Prod.* **2000**, *11*, 51–57.
- (70) Tian, Y.; Zhang, X.; Sun, B.; Jin, Z.; Wu, S. *Carbohydr. Polym.* **2015**, *133*, 90–93.
- (71) Chen, Q.; Yu, H.; Wang, L.; Abdin, Z.; Chen, Y.; Wang, J.; Zhou, W.; Yang, X.; Khan, R. U.; Zhang, H.; Chen, X. *RSC Adv.* **2015**, *5*, 67459–67474.

- (72) Masina, N.; Choonara, Y. E.; Kumar, P.; Toit, L. C.; Govender, M.; Indermun, S.; Pillay, V. *Carbohydr. Polym.* **2017**, *157*, 1226–1236.
- (73) Haroon, M.; Wang, L.; Yu, H.; Abbasi, N. M.; Saleem, M.; Khan, R. U.; Ullah, R. S.; Chen, Q. *RSC Adv.* **2016**, *6*, 78264–78285.
- (74) Viswanathan, A. *J. Environ. Polym. Degrad.* **1999**, *7* (4), 191–196.
- (75) Bhattacharyya, D.; Singhal, R. S.; Kulkarni, P. R. *Carbohydr. Polym.* **1995**, *27*, 247–253.
- (76) Volkert, B.; Loth, F.; Lazik, W.; Engelhardt, J. *Starch - Stärke* **2004**, *56*, 307–314.
- (77) Heinze, T.; Liebert, T.; Heinze, U.; Schwikal, K. *Cellulose* **2004**, *11*, 239–245.
- (78) Gimmler, N.; Meuser, F. *Starch - Stärke* **1994**, *47* (7), 268–276.
- (79) Bhandari, P. N.; Hanna, M. A. *Starch - Stärke* **2011**, *63*, 771–779.
- (80) Kuakpetoon, D.; Wang, Y. *Starch - Stärke* **2001**, *53*, 211–218.
- (81) Kato, Y.; Matsuo, R.; Isogai, A. *Carbohydr. Polym.* **2003**, *51*, 69–75.
- (82) Wing, R. E.; Willett, J. L. *Ind. Crops Prod.* **1997**, *7*, 45–52.
- (83) Hirsch, J. B.; Kokini, J. L. *Cereal Chem.* **1997**, *79* (1), 102–107.
- (84) Uslu, M.; Polat, S. *Carbohydr. Polym.* **2012**, *87* (3), 1994–1999.
- (85) Petrovic, Z. S. *Polym. Rev.* **2008**, *48*, 109–155.

- (86) Zhang, C.; Garrison, T. F.; Madbouly, S. A.; Kessler, M. R. *Prog. Polym. Sci.* **2017**, *71*, 91–143.
- (87) Xia, Y.; Larock, R. C. *Green Chem.* **2010**, *12*, 1893–1909.
- (88) Tran, P.; Seybold, K.; Graiver, D.; Narayan, R. *J. Am. Oil Chem. Soc.* **2005**, *82* (3), 189–194.
- (89) Kamal-Eldin, A.; Andersson, R. *J. Am. Oil Chem. Soc.* **1997**, *74* (4), 375–380.
- (90) Sharma, V.; Kundu, P. P. *Prog. Polym. Sci.* **2006**, *31*, 983–1008.
- (91) Stenberg, C.; Svensson, M.; Johansson, M. *Ind. Crops Prod.* **2005**, *21* (2), 263–272.
- (92) Trãn, N. B.; Vialle, J.; Pham, Q. T. *Polymer (Guildf)*. **1997**, *38* (10), 2467–2473.
- (93) Zlatanić, A.; Lava, C.; Zhang, W.; Petrović, Z. S. *J. Polym. Sci. Part B Polym. Phys.* **2004**, *42* (5), 809–819.
- (94) Eren, T.; Küsefoğlu, S. H.; Wool, R. *J. Appl. Polym. Sci.* **2003**, *90* (1), 197–202.
- (95) Dubrulle, L.; Lebeuf, R.; Thomas, L.; Fressancourt-Collinet, M.; Nardello-Rataj, V. *Prog. Org. Coatings* **2017**, *104*, 141–151.
- (96) Kundu, P. P.; Larock, R. C. *Prog. Org. Coatings* **2009**, *65* (1), 10–18.
- (97) Lazzari, M.; Chiantore, O. *Polym. Degrad. Stab.* **1999**, *65* (2), 303–313.
- (98) Petrovic, Z. S.; Zlatanic, A.; Lava, C. C.; Sinadinovic-Fiser, S. *Eur. J. Lipid Sci. Technol.* **2002**, *104*, 293–299.

- (99) Lackinger, E.; Schmid, L.; Sartori, J.; Isogai, A.; Potthast, A.; Rosenau, T. *Holzforschung* **2011**, *65* (1), 3–11.
- (100) Fangrui, M.; Hanna, M. *Bioresour. Technol.* **1999**, *70*, 1–15.
- (101) Math, M. C.; Kumar, S. P.; Chetty, S. V. *Energy Sustain. Dev.* **2010**, *14* (4), 339–345.
- (102) Suppes, G. J.; Dasari, M. A.; Doskocil, E. J.; Mankidy, P. J.; Goff, M. J. *Appl. Catal. A Gen.* **2004**, *257*, 213–223.
- (103) Liu, X.; He, H.; Wang, Y.; Zhu, S.; Piao, X. *Fuel* **2008**, *87*, 216–221.

Chapter 3

- (1) Shogren, R. L.; Biswas, A. *Carbohydr. Polym.* **2006**, *64*, 16–21.
- (2) Zhang, Z.; Macquarrie, D. J.; Clark, J. H.; Matharu, A. S. *RSC Adv.* **2014**, *4*, 41947–41955.
- (3) Enomoto-Rogers, Y.; Iio, N.; Takemura, A.; Iwata, T. *Eur. Polym. J.* **2015**, *66*, 470–477.
- (4) Xie, Q.; Li, F.; Li, J.; Wang, L.; Li, Y.; Zhang, C.; Xu, J. *Carbohydr. Polym.* **2018**, *189*, 56–64.
- (5) Astruc, J.; Nagalakshmaiah, M.; Laroche, G.; Grandbois, M.; Elkoun, S.; Robert, M. *Carbohydr. Polym.* **2017**, *178*, 352–359.
- (6) Gutiérrez, T. J.; Alvarez, V. A. *Carbohydr. Polym.* **2017**, *178*, 260–269.

- (7) You, S.; Fiedorowicz, M.; Lim, S. *Cereal Chem.* **1999**, *76* (1), 116–121.
- (8) Zhu, F.; Corke, H.; Bertoft, E. *Carbohydr. Polym.* **2011**, *84*, 907–918.
- (9) Qin, Y.; Liu, C.; Jiang, S.; Xiong, L.; Sun, Q. *Ind. Crop. Prod.* **2016**, *87*, 182–190.
- (10) Dicke, R. *Cellulose* **2004**, *11*, 255–263.
- (11) Klaochanpong, N.; Pancha-arnon, S.; Uttapap, D. *Food Hydrocoll.* **2017**, *66*, 296–306.
- (12) Singh, J.; Kaur, L.; Mccarthy, O. J. *Food Hydrocoll.* **2007**, *21*, 1–22.
- (13) Altuna, L.; Lidia, M.; Laura, M. *Food Hydrocoll.* **2018**, *80*, 97–110.
- (14) Song, X.; He, G.; Ruan, H.; Chen, Q. *Starch - Stärke* **2006**, *58*, 109–117.
- (15) Bai, Y.; Kaufman, R. C.; Wilson, J. D.; Shi, Y. *Food Chem.* **2014**, *153*, 193–199.
- (16) Jeon, Y.; Viswanathan, A.; Gross, R. A. *Starch - Stärke* **1999**, *51* (2), 90–93.
- (17) Mullen, J. W.; Pacsu, E. *Ind. Eng. Chem.* **1942**, *34* (10), 1209–1217.
- (18) Aburto, J.; Alric, I.; Thiebaud, S.; Borredon, E.; Bikiaris, D.; Prinos, J.; Panayiotou, C. *J. Appl. Polym. Sci.* **1999**, *74*, 1440–1451.
- (19) Sun, R.; Sun, X. F. *Carbohydr. Polym.* **2002**, *47*, 323–330.
- (20) Xu, Y.; Miladinov, V.; Hanna, M. A. *Cereal Chem.* **2004**, *81* (6), 735–740.
- (21) Liu, Z.; Li, Y.; Cui, F.; Ping, L.; Song, J.; Ravee, Y.; Jin, L.; Xue, Y.; Xu, J.; Li, G.; Wang, Y.; Zheng, Y. *J. Agric. Food Chem.* **2008**, *56*, 11499–11506.

- (22) Tizzotti, M. J.; Sweedman, M. C.; Tang, D.; Schaefer, C.; Gilbert, R. G. *J. Agric. Food Chem.* **2011**, *59*, 6913–6919.
- (23) Yang, B. Y.; Montgomery, R. *Starch - Stärke* **2006**, *58*, 520–526.
- (24) Filippo, S. Di; Tupa, M. V; Vázquez, A.; Foresti, M. L. *Carbohydr. Polym.* **2016**, *137*, 198–206.
- (25) Sweedman, M. C.; Tizzotti, M. J.; Schäfer, C.; Gilbert, R. G. *Carbohydr. Polym.* **2013**, *92* (1), 905–920.
- (26) Yokoyama, W.; Renner-Nantz, J. J.; Shoemaker, C. F. *Cereal Chem.* **1998**, *75* (4), 530–535.
- (27) Striegel, A. M.; Haidar, I. A. *Chromatographia* **2018**, *81* (5), 823–827.
- (28) Striegel, A. M. *Chromatographia* **2017**, *80* (6), 989–996.
- (29) Neumann, U.; Wiege, B.; Warwel, S. *Starch - Stärke* **2002**, *54*, 449–453.
- (30) Winkler, H.; Vorweg, W.; Rihm, R. *Carbohydr. Polym.* **2014**, *102*, 941–949.

Chapter 4

- (1) Zhou, X.; Li, Y.; Fang, C.; Li, S.; Cheng, Y.; Lei, W.; Meng, X. *J. Mater. Sci. Technol.* **2015**, *31* (7), 708–722.
- (2) Akindoyo, J. O.; Beg, M. D. H.; Ghazali, S.; Islam, M. R.; Jeyaratnam, N.; Yuvaraj, A. *R. RSC Adv.* **2016**, *6* (115), 114453–114482.

- (3) Noreen, A.; Zia, K. M.; Zuber, M.; Tabasum, S.; Zahoor, A. F. *Prog. Org. Coatings* **2016**, *91*, 25–32.
- (4) Yang, H.; Wang, X.; Yu, B.; Yuan, H.; Song, L.; Hu, Y.; Yuen, R. K. K.; Yeoh, G. H. *J. Appl. Polym. Sci.* **2013**, *128* (5), 2720–2728.
- (5) He, Y.; Zhang, X.; Zhang, X.; Huang, H.; Chang, J.; Chen, H. *J. Ind. Eng. Chem.* **2012**, *18* (5), 1620–1627.
- (6) Gurunathan, T.; Mohanty, S.; Nayak, S. K. *Prog. Org. Coatings* **2015**, *80*, 39–48.
- (7) Heintz, A. M.; Duffy, D. J.; Hsu, S. L.; Suen, W.; Chu, W.; Paul, C. W. *Macromolecules* **2003**, *36* (8), 2695–2704.
- (8) Eschig, S.; Schirp, C.; Salthammer, T. *Eur. J. Lipid Sci. Technol.* **2014**, *116* (8), 943–951.
- (9) Lackinger, E.; Schmid, L.; Sartori, J.; Isogai, A.; Potthast, A.; Rosenau, T. *Holzforschung* **2011**, *65* (1), 3–11.
- (10) Eren, T.; Küsefoğlu, S. H.; Wool, R. *J. Appl. Polym. Sci.* **2003**, *90* (1), 197–202.
- (11) Kamal-Eldin, A.; Andersson, R. *J. Am. Oil Chem. Soc.* **1997**, *74* (4), 375–380.
- (12) Quesada, J.; Morard, M.; Vaca-García, C.; Borredon, E. *J. Am. Oil Chem. Soc.* **2003**, *80* (3), 281–286.
- (13) Lava, C.; Zhang, W. E. I.; Petrovic, Z. S. *J. Polym. Sci. Part B Polym. Phys.* **2004**, *42*, 809–819.
- (14) Trân, N. B.; Vialle, J.; Pham, Q. T. *Polymer (Guildf)*. **1997**, *38* (10), 2467–2473.

- (15) Zia, F.; Zia, K. M.; Zuber, M.; Kamal, S.; Aslam, N. *Carbohydr. Polym.* **2015**, *134*, 784–798.
- (16) Moad, G. *Prog. Polym. Sci.* **2011**, *36* (2), 218–237.
- (17) O'Brien, S.; Wang, Y. J. *Carbohydr. Polym.* **2009**, *77* (3), 464–471.
- (18) Shi, M.; Gu, F.; Wu, J.; Yu, S.; Gao, Q. *Starch - Stärke* **2013**, *65* (11–12), 947–953.
- (19) Nabar, Y. U.; Draybuck, D.; Narayan, R. *J. Appl. Polym. Sci.* **2006**, *102* (1), 58–68.
- (20) Altuna, L.; Lidia, M.; Laura, M. *Food Hydrocoll.* **2018**, *80*, 97–110.
- (21) Xu, Y.; Miladinov, V.; Hanna, M. A. *Cereal Chem.* **2004**, *81* (6), 735–740.
- (22) Kim, M.; Lee, S. J. *Carbohydr. Polym.* **2002**, *50* (4), 331–337.
- (23) Barikani, M.; Mohammadi, M. *Carbohydr. Polym.* **2007**, *68* (4), 773–780.
- (24) Qiao, D.; Zou, W.; Liu, X.; Yu, L.; Chen, L.; Liu, H.; Zhang, N. *Starch - Stärke* **2012**, *64* (10), 821–825.
- (25) Silva, A. L.; Bordado, J. C. *Catal. Rev. - Sci. Eng.* **2004**, *46* (1), 31–51.
- (26) Blank, W. J.; He, Z. A.; Hessell, E. T. *Prog. Org. Coatings* **1999**, *35* (1–4), 19–29.
- (27) Tran, N. B.; Pham, Q. T. *Polymer (Guildf)*. **1997**, *38* (13), 3307–3314.
- (28) Striegel, A. M.; Haidar, I. A. *Chromatographia* **2018**, *81* (5), 823–827.
- (29) Ajithkumar, S.; Kansara, S. S.; Patel, N. K. *Eur. Polym. J.* **1998**, *34* (9), 1273–1276.
- (30) Zhang, Y.; Huang, Y.; Chen, X.; Wu, Z.; Wu, Q. *Ind. Eng. Chem. Res.* **2011**, *50*, 11906–11911.
- (31) Lehmann, A.; Volkert, B.; Hassan-Nejad, M.; Greco, T.; Fink, H. P. *Green Chem.* **2010**,

12 (12), 2164–2171.

- (32) McPherson, A. E.; Bailey, T. B.; Jane, J. *Cereal Chem.* **2000**, 77 (3), 320–325.
- (33) Liu, W.; Halley, P. J.; Gilbert, R. G. *Macromolecules* **2010**, 43, 2855–2864.
- (34) Song, D.; Thio, Y. S.; Deng, Y. *Carbohydr. Polym.* **2011**, 85 (1), 208–214.
- (35) Bras, J.; Dufresne, A. *Biomacromolecules* **2010**, 11, 1139–1153.
- (36) Leng, Y.; Zhang, Y.; Chen, X.; Yi, C.; Fan, B.; Wu, Q. *Ind. Eng. Chem. Res.* **2011**, 50 (19), 11130–11135.
- (37) Chen, X.; Zhang, Y.; Zhang, P.; Fan, B.; Wu, Q. *Starch - Stärke* **2012**, 64 (4), 255–262.
- (38) Wu, Q.; Chen, X.; Zhang, Y.; Wu, Z.; Huang, Y. *Ind. Eng. Chem. Res.* **2014**, 50, 2008–2014.
- (39) Zhang, Y.; Zhang, P.; Chen, X.; Wu, Z.; Wu, Q. *Ind. Eng. Chem. Res.* **2011**, 50, 2111–2116.
- (40) Zhang, Y.; Leng, Y.; Zhu, M.; Fan, B.; Yan, R.; Wu, Q. *Carbohydr. Polym.* **2012**, 88 (4), 1208–1213.
- (41) Willett, J. L.; Millardt, M. M.; Jasberg, B. K. *Polymer (Guildf)*. **1997**, 38 (24), 5983–5989.

Chapter 5

- (1) Quesada, J.; Morard, M.; Vaca-García, C.; Borredon, E. *J. Am. Oil Chem. Soc.* **2003**, 80 (3), 281–286.
- (2) Tran, P.; Seybold, K.; Graiver, D.; Narayan, R. *JAOCS, J. Am. Oil Chem. Soc.* **2005**, 82

- (3), 189–194.
- (3) Kamal-Eldin, A.; Andersson, R. *J. Am. Oil Chem. Soc.* **1997**, *74* (4), 375–380.
- (4) Zlatanić, A.; Lava, C.; Zhang, W.; Petrović, Z. S. *J. Polym. Sci. Part B Polym. Phys.* **2004**, *42* (5), 809–819.
- (5) Eren, T.; Küsefoğlu, S. H.; Wool, R. *J. Appl. Polym. Sci.* **2003**, *90* (1), 197–202.
- (6) Bickford, W. G.; Krauczunas, P.; Wheeler, D. H. *Oil Soap* **1942**, *19* (2), 23–27.
- (7) Lackinger, E.; Schmid, L.; Sartori, J.; Isogai, A.; Potthast, A.; Rosenau, T. *Holzforschung* **2011**, *65* (1), 3–11.
- (8) Lackinger, E.; Schmid, L.; Sartori, J.; Isogai, A.; Potthast, A.; Rosenau, T. *Holzforschung* **2011**, *65* (1), 13–19.
- (9) Lackinger, E.; Isogai, A.; Schmid, L.; Sartori, J.; Potthast, A.; Rosenau, T. *Holzforschung* **2011**, *65* (1), 21–27.
- (10) Lackinger, E.; Schmid, L.; Sartori, J.; Potthast, A.; Rosenau, T. *Holzforschung* **2011**, *65* (2), 171–176.
- (11) ASTM D94-07 (Reapproved 2012). *Standard Test Methods for Saponification Number of Petroleum Products*; ASTM International: West Conshohocken, PA, 2012;
www.astm.org.
- (12) Ionescu, A.; Piétri, N.; Hillebrand, M.; Monnier, M.; Aycard, J. P. *Can. J. Chem.* **2002**, *80* (5), 455–461.

Chapter 6

- (1) Zhou, J.; Ren, L.; Tong, J.; Xie, L.; Liu, Z. *Carbohydr. Polym.* **2009**, 78 (4), 888–893.
- (2) Bai, Y.; Shi, Y.; Herrera, A.; Prakash, O. *Carbohydr. Polym.* **2011**, 83 (2), 407–413.
- (3) Ma, Z.; Zhao, S.; Cheng, K.; Zhang, X.; Xu, X.; Zhang, L. *J. Appl. Polym. Sci.* **2007**, 104, 3124–3128.
- (4) You, S.; Fiedorowicz, M.; Lim, S. *Cereal Chem.* **1999**, 76 (1), 116–121.
- (5) Miao, M.; Li, R.; Jiang, B.; Cui, S. W.; Zhang, T.; Jin, Z. *Food Chem.* **2014**, 151, 154–160.
- (6) Sweedman, M. C.; Tizzotti, M. J.; Schäfer, C.; Gilbert, R. G. *Carbohydr. Polym.* **2013**, 92 (1), 905–920.
- (7) Vaidya, U. R.; Bhattacharya, M. *J. Appl. Polym. Sci.* **1994**, 52 (5), 617–628.
- (8) Vamadevan, V.; Bertoft, E. *Starch - Stärke* **2015**, 67, 55–68.
- (9) Klavons, J. A.; Dintzis, F. R.; Millard, M. M. *Cereal Chem.* **1997**, 74 (6), 832–836.
- (10) Chen, P.; Yu, L.; Simon, G. P.; Liu, X.; Dean, K.; Chen, L. *Carbohydr. Polym.* **2011**, 83 (4), 1975–1983.
- (11) Buleon, A.; Colonna, P.; Planchot, V.; Ball, S. *Int. J. Biol. Macromol.* **1998**, 23, 85–112.
- (12) Li, W.; Corke, H.; Beta, T. *Carbohydr. Polym.* **2007**, 69, 398–405.
- (13) Bras, J.; Dufresne, A. *Biomacromolecules* **2010**, 11, 1139–1153.
- (14) He, G.-Q.; Song, X.-Y.; Ruan, H.; Chen, F. *J. Agric. Food Chem.* **2006**, 54, 2775–2779.
- (15) Shogren, R. L. *Carbohydr. Polym.* **1996**, 29 (I), 57–62.

- (16) Chi, H.; Xu, K.; Xue, D.; Song, C.; Zhang, W.; Wang, P. **2007**, *40*, 232–238.
- (17) Li, D.; Zhang, X.; Tian, Y. *Int. J. Biol. Macromol.* **2016**, *86* (3), 119–125.
- (18) Shogren, R. L.; Viswanathan, A.; Felker, F.; Gross, R. A. *Starch - Stärke* **2000**, *52*, 196–204.
- (19) Li, G.; Zhu, F. *Int. J. Biol. Macromol.* **2018**, *114*, 767–775.
- (20) Xue, T.; Yu, L.; Xie, F.; Chen, L.; Li, L. *Food Hydrocoll.* **2008**, *22*, 973–978.
- (21) Moad, G. *Prog. Polym. Sci.* **2011**, *36* (2), 218–237.
- (22) Miladinov, V. D.; Hanna, M. A. *Ind. Crop. Prod.* **2000**, *11*, 51–57.
- (23) Quesada, J.; Morard, M.; Vaca-García, C.; Borredon, E. *J. Am. Oil Chem. Soc.* **2003**, *80* (3), 281–286.
- (24) Eren, T.; Küsefoğlu, S. H.; Wool, R. *J. Appl. Polym. Sci.* **2003**, *90* (1), 197–202.
- (25) Lackinger, E.; Schmid, L.; Sartori, J.; Isogai, A.; Potthast, A.; Rosenau, T. *Holzforschung* **2011**, *65* (1), 3–11.
- (26) Ren, L.; Jiang, M.; Tong, J.; Bai, X.; Dong, X.; Zhou, J. *Carbohydr. Polym.* **2010**, *82* (3), 1010–1013.
- (27) Tran, P.; Seybold, K.; Graiver, D.; Narayan, R. *J. Am. Oil Chem. Soc.* **2005**, *82* (3), 189–194.
- (28) Wildi, R. H.; Van Egdome, E.; Bloembergen, S. Process for Producing Biopolymer Nanoparticles. U.S. Patent 9,662,824, 2017.
- (29) Wildi, R. H.; Van Egdome, E.; Bloembergen, S. Process for producing Biopolymer

- Nanoparticles. U.S. Patent 9,011,741, 2015.
- (30) Caldwell, C. G.; Wurzburg, O. B. Polysaccharide Derivatives of Substituted Dicarboxylic Acids. U.S. Patent 2,661,349, 1953.
- (31) Jeon, Y.; Viswanathan, A.; Gross, R. A. *Starch - Stärke* **1999**, *51* (2), 90–93.
- (32) Bhosale, R.; Singhal, R. *Carbohydr. Polym.* **2006**, *66*, 521–527.
- (33) Raquez, J.; Nabar, Y.; Srinivasan, M. *Carbohydr. Polym.* **2008**, *74* (2), 159–169.
- (34) Xie, F.; Yu, L.; Liu, H.; Chen, L. *Starch - Stärke* **2006**, *58* (3–4), 131–139.
- (35) Dias, F. T. G.; Souza, R. C. R.; Andrade, C. T. *Macromol. Symp.* **2011**, *299–300* (1), 139–146.
- (36) Whitney, K.; Reuhs, B. L.; Ovando, M.; Simsek, S. *Food Chem.* **2016**, *211*, 608–615.
- (37) Bai, Y.; Shi, Y. C. *Carbohydr. Polym.* **2011**, *83* (2), 520–527.
- (38) Hui, R.; Qi-he, C.; Ming-liang, F.; Qiong, X.; Guo-qing, H. *Food Chem.* **2009**, *114* (1), 81–86.
- (39) Song, X.; Zhu, W.; Li, Z.; Zhu, J. *Starch - Stärke* **2010**, *62* (12), 629–636.
- (40) Qiao, D.; Zou, W.; Liu, X.; Yu, L.; Chen, L.; Liu, H.; Zhang, N. *Starch - Stärke* **2012**, *64* (10), 821–825.
- (41) Xu, Z.; Wan, H.; Miao, J.; Han, M.; Yang, C.; Guan, G. *J. Mol. Catal. A Chem.* **2010**, *332* (1–2), 152–157.
- (42) Doane, M.; Wing, R. E.; Farag, S.; Reinhardt, R. M.; Farag, S. *Starch - Stärke* **1996**, *79* (1975), 275–279.

- (43) Ghosh Dastidar, T.; Netravali, A. N. *Carbohydr. Polym.* **2012**, *90* (4), 1620–1628.
- (44) Tomasik, P.; Wang, Y. J.; Jane, J. *Starch - Stärke* **1995**, *47* (3), 96–99.
- (45) Fischer, E. R.; Boyd, P. G. Water Soluble Corrosion Inhibitors. U.S. Patent 5,759,485, 1998.
- (46) Lazzari, M.; Chiantore, O. *Polym. Degrad. Stab.* **1999**, *65* (2), 303–313.
- (47) Lu, X.; Huang, J.; He, G.; Yang, L.; Zhang, N.; Zhao, Y.; Qu, J. *Ind. Eng. Chem. Res.* **2013**, *52* (38), 13677–13684.
- (48) Song, D.; Thio, Y. S.; Deng, Y. *Carbohydr. Polym.* **2011**, *85* (1), 208–214.
- (49) Liu, W.; Halley, P. J.; Gilbert, R. G. *Macromolecules* **2010**, *43*, 2855–2864.
- (50) Tian, Y.; Zhang, X.; Sun, B.; Jin, Z.; Wu, S. *Carbohydr. Polym.* **2015**, *133*, 90–93.
- (51) Narayan, R.; Balakrishnan, S.; Shin, B.-Y. Starch-Vegetable Oil Graft Copolymers and their Biofiber Composites, and a Process for their Manufacture. U.S. Patent 7,553,919, 2006.
- (52) Lai, L. N.; Karim, A. A.; Norziah, M. H.; Seow, C. C. *J. Food Sci.* **2004**, *69* (4), 249-256.

Chapter 7

- (1) Kim, D.; Amos, R.; Gauthier, M.; Duhamel, J. *Langmuir* **2018**, *34*, 8611–8621.
- (2) Lackinger, E.; Schmid, L.; Sartori, J.; Isogai, A.; Potthast, A.; Rosenau, T. *Holzforschung* **2011**, *65* (1), 3–11.

- (3) Jeon, Y.; Viswanathan, A.; Gross, R. A. *Starch - Stärke* **1999**, *51* (2), 90–93.
- (4) Moad, G. *Prog. Polym. Sci.* **2011**, *36* (2), 218–237.
- (5) Liu, Z.; Li, Y.; Cui, F.; Ping, L.; Song, J.; Ravee, Y.; Jin, L.; Xue, Y.; Xu, J.; Li, G.; Wang, Y.; Zheng, Y. *J. Agric. Food Chem.* **2008**, *56*, 11499–11506.
- (6) He, J.; Liu, J.; Zhang, G. *Biomacromolecules* **2008**, *9*, 175–184.
- (7) Sweedman, M. C.; Tizzotti, M. J.; Schäfer, C.; Gilbert, R. G. *Carbohydr. Polym.* **2013**, *92* (1), 905–920.
- (8) Ettelaie, R.; Holmes, M.; Chen, J.; Farshchi, A. *Food Hydrocoll.* **2016**, *58*, 364–377.
- (9) Belhassen, R.; Vilaseca, F.; Mutjé, P.; Boufi, S. *Ind. Crops Prod.* **2014**, *53*, 261–267.
- (10) Shogren, R. L. *Carbohydr. Polym.* **1996**, *29* (I), 57–62.
- (11) Zhou, J.; Ren, L.; Tong, J.; Xie, L.; Liu, Z. *Carbohydr. Polym.* **2009**, *78* (4), 888–893.
- (12) Thakore, I. M.; Desai, S.; Sarawade, B. D.; Devi, S. *Eur. Polym. J.* **2001**, *37*, 151–160.
- (13) Ma, X.; Chang, P. R.; Yu, J.; Wang, N. *Carbohydr. Polym.* **2008**, *71* (2), 229–234.
- (14) Stenberg, C.; Svensson, M.; Johansson, M. *Ind. Crops Prod.* **2005**, *21* (2), 263–272.
- (15) Kundu, P. P.; Larock, R. C. *Prog. Org. Coatings* **2009**, *65* (1), 10–18.
- (16) Eren, T.; Küsefoğlu, S. H.; Wool, R. *J. Appl. Polym. Sci.* **2003**, *90* (1), 197–202.

- (17) Sharma, V.; Kundu, P. P. *Prog. Polym. Sci.* **2006**, *31*, 983–1008.
- (18) Song, D.; Thio, Y. S.; Deng, Y. *Carbohydr. Polym.* **2011**, *85* (1), 208–214.
- (19) Ghosh Dastidar, T.; Netravali, A. N. *Carbohydr. Polym.* **2012**, *90* (4), 1620–1628.
- (20) Pushpadass, H. A.; Marx, D. B.; Hanna, M. A. *Starch - Stärke* **2008**, *60*, 527–538.
- (21) Pegoretti, A.; Fambri, L.; Penati, A.; Kolarik, J. *J. Appl. Polym. Sci.* **1998**, *70*, 577–586.
- (22) Rodrigues, A.; Emeje, M. *Carbohydr. Polym.* **2012**, *87*, 987–994.
- (23) Dag, A.; Durmaz, H.; Demir, E.; Hizal, G.; Tunca, U. *J. Polym. Sci. Part A Polym. Chem.* **2008**, *46*, 6969–6977.